Development of Polymer Gel Systems to Improve Volumetric Sweep and Reduce Producing Water/Oil Ratios

Annual Report

for the reporting period
7/01/2002 – 6/30/2003

by

G. Paul Willhite, Stan McCool, Don W. Green
Min Cheng, Rajeev Jain, Tuan Nguyen

November 2003

Contract Number DE-FC26-02NT15363
Contract Dates 7/01/2002 - 6/30/2005

The University of Kansas Center for Research, Inc.
Tertiary Oil Recovery Project
Lawrence, KS 66045

This report was prepared as an account of work sponsored by an agency of the United States Government. Neither the United States Government nor any agency thereof, nor any of their employees, makes any warranty, express or implied, or assumes any legal liability or responsibility for the accuracy, completeness, or usefulness of any information, apparatus, product, or process disclosed, or represents that its use would not infringe privately owned rights. Reference herein to any specific commercial product, process, or service by trade name, trademark, manufacturer, or otherwise does not necessarily constitute or imply its endorsement, recommendation, or favoring by the United States Government or any agency thereof. The views and opinions of authors expressed herein do not necessarily state or reflect those of the United States Government or any agency thereof.

Abstract

Gelled polymer treatments are applied to oil reservoirs to increase oil production and to reduce water production by altering the fluid movement within the reservoir. This report describes the results of the first year of a three-year research program that is aimed at the understanding of the chemistry of gelation and the fundamental mechanisms that alter the flows of oil and water in reservoir rocks after a gel treatment. Work has focused on a widely-applied system in field applications, the partially hydrolyzed polyacrylamide-chromium acetate gel. Gelation occurs by network formation through the crosslinking of polyacrylamide molecules as a result of reaction with chromium acetate. The initial reaction between chromium acetate and one polymer is referred to as the uptake reaction. The uptake reaction was studied as functions of chromium and polymer concentrations and pH values. Experimental data were regressed to determine a rate equation that describes the uptake reaction of chromium by polyacrylamide. Pre-gel aggregates form and grow as the reactions between chromium acetate and polyacrylamide proceed. A statistical model that describes the growth of pre-gel aggregates was developed using the theory of branching processes. The model gives molecular weight averages that are expressed as functions of the conversion of the reactive sites on chromium acetate or on the polymer molecule. Results of the application of the model correlate well with experimental data of viscosity and weight-average molecular weight and gives insights into the gelation process.

A third study addresses the flow of water and oil in rock material after a gel treatment. Previous works have shown that gel treatments usually reduce the permeability to water to a greater extent than the permeability to oil is reduced. This phenomenon is referred to as disproportionate permeability reduction (DPR). Flow experiments were conducted to determine the effect of polymer and chromium concentrations on DPR. All gels studied reduced the permeability to water by a greater factor than the factor by which the oil permeability was reduced. Greater DPR was observed as the concentrations of polymer and chromium were increased. Increased pressure gradients during oil flow decreased the oil permeability and the water permeability that was measured afterward. Lower pressure gradients that were applied subsequently moderately affected water permeabilities but did not affect oil permeabilities. A conceptual model of the mechanisms responsible for DPR is presented. Primary features of the model are (1) the development of flow channels through the gel by dehydration of the gel and by re-connection of pre-treatment, residual oil volume and (2) high flow resistance in the channels during water flow is caused by significant saturations of oil remaining in the channels.

Table of Contents

		Page No.
	Abstract	iii
	List of Figures	v
	List of Tables and Exhibits	ix
Chapter 1	Introduction	1-1
Chapter 2	Modeling of Molecular Weight Averages of Crosslinked Polyacrylamide-Chromium(III) Pre-Gel Aggregates Using the Theory of Branching Processes	2-1
Chapter 3	Kinetic Study of the Chromium(III) Acetate- Hydrolyzed Polyacrylamide Uptake Reaction	3-1
Chapter 4	Effects of Composition of a Polyacrylamide-Chromium Acetate Gel System and the Applied Pressure Gradient on Gel Dehydration and Disproportionate Permeability Reduction in Sandpacks	4-1
Chapter 5	Technology Transfer	5-1

List of Figures

Fig. No.	Title	Page No.
2.1	Four reacted states of a tri-functional precursor.	2-3
2.2	Molecular weight averages of pre-gel aggregates for system containing 5000 ppm AlcoFlood 935 (Lot7158V) and 100 ppm chromium trimer.	2-19
2.3	Viscosity vs. reaction time, weight-average molecular weight vs. conversion of chromium functionalities for a gel system containing 5000 ppm AlcoFlood 935, Lot 7158V and 100 ppm chromium trimer).	2-19
2.4	Molecular weight averages of pre-gel aggregates for system containing 5000 ppm AlcoFlood 935 (Lot 7158V) and 20 ppm chromium trimer.	2-20
2.5	Molecular weight averages of pre-gel aggregates for system containing 5000 ppm AlcoFlood 935 (Lot A2247BOV) and 100 ppm chromium trimer.	2-20
2.6	Molecular weight averages of pre-gel aggregates for system containing 5000 ppm AlcoFlood 935 (Lot A2247BOV) and 20 ppm chromium trimer.	2-21
2.7	Comparison of experimental and modeled chromium uptake data (AlcoFlood 935, A2247 BOV, 5000 ppm and various initial chromium concentrations).	2-23
3.1	Structures of chromium acetate trimers given by Tackett [1990].	3-5
3.2	Data and curve fit to unreacted chromium trimer concentration as a function of time for different initial chromium concentrations; ~5000 mg/kg polymer conc. and a pH of ~4.9.	3-11
3.3	Data and curve fit of unreacted chromium trimer concentration as a function of time for different initial polymer concentrations; ~200 mg/kg chromium conc. and a pH of 4.9.	3-11
3.4	Data and curve fit of unreacted chromium trimer concentration as a function of time for different initial pH values; ~200 mg/kg chromium conc. and a pH of 4.9.	3-12

Fig. No.	Title	Page No.
3.5	Comparison of the results of the integration of the rate equation with data of the unreacted chromium trimer concentration as a function of time at different initial chromium concentrations; ~5000 mg/kg polymer conc. and a pH of ~4.9.	3-12
3.6	Comparison of the results of the integration of the rate equation with data of the unreacted chromium trimer concentration as a function of time at different initial polymer concentrations; ~200 mg/kg chromium conc. and a pH of 4.9.	3-13
3.7	Comparison of the results of the integration of the rate equation with data of the unreacted chromium trimer concentration as a function of time at different initial pH values; ~200 mg/kg chromium conc. and a pH of 4.9.	3-13
3.8	Concentration of reacted chromium at the gel time as a function of the chromium concentration in the gelant; ~5000 mg/kg polymer conc. and a pH of ~4.9.	3-14
3.9	Correlation of the reciprocal of the gel time with concentration of reacted chromium at the gel time; ~5000 mg/kg polymer conc. and a pH of ~4.9.	3-14
3.10	Variables used in mass balances on the centrifugal filter device.	3-17
4.1	Schematic of equipment for flow experiments.	4-2
4.2	Bulk gel times as a function of polymer concentration and polymer-to-chromium mass ratios.	4-7
4.3	Volume fraction of gel dehydrated as a function of time; oil flood at pressure gradient of 20 psi/ft..	4-10
4.4	Volume fraction of gel dehydrated as a function of time for weak gels (polymer concentrations of 3000 ppm or less).	4-10
4.5	Permeability to oil as a function of polymer concentration after gel dehydration at a pressure gradient of 20 psi/ft.	4-11
4.6	Permeability to water as a function of polymer concentration after gel dehydration at a pressure gradient of 20 psi/ft.	4-11

Fig. No.	Title	Page No.
4.7	Permeability to oil for strong gels as a function of pressure gradient after gel dehydration at a pressure gradient of 20 psi/ft; polymer concentrations of 3000 ppm and higher.	4-13
4.8	Permeability to oil for weak gels as a function of pressure gradient after gel dehydration at a pressure gradient of 20 psi/ft; polymer concentrations of 2500 ppm and lower.	4-13
4.9	Permeability to water for strong gels as a function of pressure gradient after gel dehydration at a pressure gradient of 20 psi/ft; polymer concentrations of 3000 ppm and higher.	4-14
4.10	Permeability to water for weak gels as a function of pressure gradient after gel dehydration at a pressure gradient of 20 psi/ft; polymer concentrations of 2500 ppm and lower.	4-14
4.11	Residual resistance factors for oil as a function of polymer concentration at two applied pressure gradients after dehydration at a pressure gradient of 20 psi/ft.	4-15
4.12	Residual resistance factors for water as a function of polymer concentration at two applied pressure gradients after dehydration at a pressure gradient of 20 psi/ft.	4-15
4.13	Residual resistance factors for oil as a function of applied pressure gradient for strong gels (polymer concentrations of 3000 ppm or higher) after dehydration at a pressure gradient of 20 psi/ft.	4-16
4.14	Residual resistance factors for oil as a function of applied pressure gradient for weak gels (polymer concentrations of 2500 ppm or lower) after dehydration at a pressure gradient of 20 psi/ft.	4-16
4.15	Residual resistance factors for water as a function of applied pressure gradient for strong gels (polymer concentrations of 3000 ppm or higher) after dehydration at a pressure gradient of 20 psi/ft.	4-17
4.16	Residual resistance factors for water as a function of applied pressure gradient for weak gels (polymer concentrations of 2500 ppm or lower) after dehydration at a pressure gradient of 20 psi/ft.	4-17

Fig. No.	Title	Page No.
4.17	Residual resistance factors for oil as a function of applied pressure gradient for strong gels (polymer concentrations of 3000 ppm or higher) after dehydration at a pressure gradient of 50 psi/ft.	4-18
4.18	Residual resistance factors for water as a function of applied pressure gradient for strong gels (polymer concentrations of 3000 ppm or higher) after dehydration at a pressure gradient of 50 psi/ft.	4-18
4.19	Selectivity as a function of polymer concentration at two applied pressure gradients after dehydration at a pressure gradient of 20 psi/ft.	4-20
4.20	Selectivity as a function of applied pressure gradient for strong gels (polymer concentrations of 3000 ppm or higher) after dehydration at a pressure gradients of 20 and 50 psi/ft.	4-20
4.21	Selectivity as a function of applied pressure gradient for weak gels (polymer concentrations of 2500 ppm or lower) after dehydration at a pressure gradient of 20 and 50 psi/ft.	4-21
4.22	Residual oil and water saturations in the new pore space after brine and oil floods, respectively, at pressure gradients of 20 psi/ft.	4-27

List of Tables

Table No.	Title	Page No.
2.1	Functionality of polymer (average number of carboxylate groups per polymer molecule), f_A.	2-16
2.2	Initial number and weight fractions of polymer and chromium trimer.	2-17
2.3	Comparison of molecular weight averages for the gel system and the pre-gel aggregates.	2-17
2.4	Experimental and theoretical data of gel time for different gel systems.	2-21
2.5	Reaction states of chromium trimer at gel time/conversion for gel systems prepared from 5000 ppm AlcoFlood 935, A2247BOV and various initial chromium concentrations; degree of hydrolysis of 10% was assumed.	2-22
3.1	Cr(III) and carboxyl source and experimental conditions.	3-3
3.2	Comparison of reaction orders for Cr(III), carboxyl and H^+.	3-4
3.3	Gelant composition, gel time and amount of chromium reacted at gel time.	3-9
4.1	Proposed mechanisms for disproportionate permeability reductions.	4-2
4.2	Sequence of experiments in each sandpack.	4-3
4.3	Summary sandpack properties. Permeability values were determined for the internal 8-inch long section of the sandpack. Porosity and saturations were determined for the entire sandpack.	4-4
4.4	Volume of gel dehydrated and dehydration time of different gel compositions.	4-8
4.5	Fraction of gel dehydrated and material balances for polymer during and after dehydration at 20 psi/ft.	4-22
4.6	Fraction of gel dehydrated and material balances for polymer after all displacement runs.	4.23
4.7	Results of material balances on chromium.	4.23

Table No.	Title	Page No.
4.8	Saturation values and permeability data after each flow experiment in TN003; Gel contained 4000 ppm polyacrylamide.	4-25
4. 9	Saturation values and permeability data after each flow experiment in TN011; Gel contained 3500 ppm polyacrylamide.	4-25
4.10	Saturation values and permeability data after each flow experiment in TN007; Gel contained 3000 ppm polyacrylamide.	4-26
4.11	Saturation values and permeability data after each flow experiment in TN004; Gel contained 2500 ppm polyacrylamide.	4-26
4.12	Saturation values and permeability data after each flow experiment in TN009; Gel contained 2500 ppm polyacrylamide.	4-27

Chapter 1

Introduction

The research goals are to improve the effectiveness of polymer gels to increase volumetric sweep efficiency of fluid displacement processes and reduce water production in production wells. Improvements in these areas have the potential to slow the rate of decline in oil production from existing wells and increase the ultimate oil recovery from existing reservoirs. The research is based on laboratory experiments and conceptual models developed from interpretation of these data. The program is organized into two major tasks: (1) In-depth Treatment of Matrix Rock from Injection Wells, and (2) Treatment of Production Wells to Control Water Production.

Task 1 seeks to develop design tools to enable the evaluation of gelled polymer systems to treat high-permeability layers that are distant from injection wells when there is crossflow between layers. A component of this task is a fundamental study of the formation and characterization of pre-gel aggregates in commonly used commercial systems. We intend to obtain experimental data and, based on these data, develop a mathematical/empirical model to predict the placement behavior of polymer systems that form pre-gel aggregates in matrix rock. Results related to Task 1 are presented in Chapters 2 and 3. Task 2 consists of fundamental studies of disproportionate permeability reduction of porous media by dehydration of gels after placement. These studies will lead to an understanding of the mechanisms of water control in production wells and aid in development of methods for designing these treatments. Chapter 4 describes results from Task 2. Task 3 covers technology transfer. Presentations and technical papers that present results from this work and work conducted in a previous DOE contract are documented in Chapter 5.

Work described in this report focused on a gel system containing partially hydrolyzed polyacrylamide and chromium acetate, which is commonly applied in field treatments. Gels are formed by building a network by crosslinking the polymer molecules. A crosslink is formed when two HPAM molecules react with one Cr(III) complex ion. These reactions are described by:

$$\text{Cr} + \text{P1} \rightarrow \text{Cr-P1} \qquad \text{(uptake)} \qquad \text{Eq. 1.1}$$

$$\text{Cr-P1} + \text{P2} \rightarrow \text{P2-Cr-P1} \qquad \text{(crosslink)} \qquad \text{Eq. 1.2}$$

P1 and P2 represent different polymer molecules. The first reaction of polymer P1 with the chromium complex ion is commonly called the uptake reaction. The reaction with the second polymer P2 creates a crosslink between the polymers and is termed the crosslink reaction. As additional crosslinks occur, pre-gel aggregates form and grow in size. A model was derived and is presented in Chapter 2 that describes the uptake and crosslinking reactions. The model is probability based and provides molecular weight averages of the pre-gel aggregates as a function of conversion of reaction sites. Results from the model are correlated with previously obtained experimental data of viscosity and weight average molecular weights. The model offers an explanation to why the viscosity of these gel systems remains fairly constant for a time period followed by a rapid increase in viscosity. We intend to pursue this type of modeling.

A kinetic study of the uptake reaction between chromium acetate and polyacrylamide (Eq. 1.1) is presented in Chapter 3. The reaction was followed by determining the concentration of chromium in the solvent as a function of time. Solvent was removed from the gelant using a centrifugal filtration device. The experimental data were regressed to derive a reaction rate equation for chromium as a function of chromium concentration, polymer concentration and pH value.

Results of a study on the effect of gelant composition on disproportionate permeability reduction (DPR) is presented in Chapter 4. DPR refers to the phenomenon whereby a gel treatment in a porous medium reduces the brine permeability by a greater factor than the oil permeability is reduced. Gelants with polymer concentrations between 2100 and 4000 ppm were placed and allowed to gel in foot-long sandpacks. Flow channels through the gels were formed during the injection of oil that dehydrated a significant portion of the gel and re-connected most of the pre-treatment residual oil. Water permeabilities were reduced by greater factors than oil permeabilities for all compositions. This was attributed to high oil saturations in the channels during water flow. Gels with higher polymer concentrations reduced the permeability to water by a greater factor than the factor by which the oil permeability was reduced. Rate tests were conducted to determine the effect of pressure gradient on permeability reduction.

Chapter 2

Modeling of Molecular Weight Averages of Crosslinked Polyacrylamide-Chromium(III) Pre-Gel Aggregates Using the Theory of Branching Processes

Graduate Research Assistant: Min Cheng

Introduction

Aqueous gel systems formed by crosslinking of partially hydrolyzed polyacrylamide (HPAM) with chromium(III) ions are used to improve volumetric sweep efficiency and reduce water production in oil reservoirs. During injection of gelants through reservoir rocks, pre-gel aggregates filter from the solution resulting in high flow resistance and impeding flow.

The formation and growth of pre-gel aggregates in quiescent gelants has been examined by our organization using multi-angle laser light scattering (MALLS), flow field-flow fractionation (FFFF) and equilibrium dialysis (EqD). The weight-average molecular weights, z-average root-mean-square (rms) radii and hydrodynamic size of pre-gel aggregates were determined as a function of reaction time [Willhite *et al*., 2003].

The objective of this work is to develop a kinetic model that describes the growth of pre-gel aggregates in bulk gelation. The model should predict: (1) gel time; (2) molecular weight and size averages; (3) molecular weight and size distributions of pre-gel aggregates, as a function of reaction time, polymer and chromium(III) concentrations, and other parameters (pH value, acetate-chromium ratio, *etc.).* This fundamental study of the crosslinking process will serve as a basis for modeling the filtration of pre-gel aggregates during flow through porous rocks.

In this chapter, a simplified model is derived for calculating molecular weight averages of pre-gel aggregates using the theory of branching processes (TBP). The molecular weight averages are expressed as functions of the conversion of the reactive sites (functional groups) on the polymer and chromium crosslinker. Model results are compared to experimental data and future work is proposed.

Network Formation Theories

Network formation theories are divided into three major categories according to Dusek [1985, 1986]:

A. Statistical methods. The reacting molecules are first described as a system of reacting precursors (units) with appropriate functionalities (reaction sites). The reactions are followed by determining the fraction of each precursor with different number of reacted functionalities using statistical methods. At a given total conversion of the functionalities, the composition (molar mass averages or distribution of molar masses) can be determined by the proper combination of the precursors. This method was selected for this study.

B. Kinetic methods. Reactions between any pair of molecules existing in the system are considered. Every molecule is treated as a component and the time dependence of their fractions

is described by a series (up to infinity) of differential equations. An advantage of the kinetic method is its adherence to kinetically controlled chemical process. Statistical methods do not consider time dependence. Mathematical complexity is a disadvantage of the kinetic method.

C. Network models generated in space. These models are based on 2D or 3D simulations. Monomer units are placed on a lattice and bonds are introduced between them either at random or according to given rules.

The process of network formation is sub-divided into three stages according to their characteristic features:
(1) Pre-gel stage: Molecular weight and polydispersity of aggregates increase. The sol (finite molecules which can be extracted) fraction, w_s , is unity and the gel (infinite, insoluble structures) fraction, w_g , is zero. The characteristic parameters are: molecular weight averages, molecular weight distribution; rms radius, hydrodynamic radius; and viscosity.
(2) Gel point: A structure (molecule) with infinite molecular weight appears for the first time at gel point. The weight average molecular weight diverges to infinity while the number-average molecular weight is still finite. The sol fraction is unity. The characteristic parameters are gel time and gel conversion (or critical conversion).
(3) Post-gel stage: Sol and gel exist simultaneously. w_s decreases from unity to zero, while w_g increases from zero to unity.
This work will initially focus on stages 1 and 2 of network formation.

A procedure for the development of a kinetic model using statistical methods is proposed: First, theoretical models will be developed to predict the averages and distributions of molecular weight and size of pre-gel aggregates as a function of conversion of functional groups using statistical methods. The time dependence of molecular weight and size of pre-gel aggregates will be determined experimentally using multi-angle laser light scattering and other methods. Previous experimental data will be analyzed and additional data will be taken. Relationships between conversion and reaction time will be determined by correlating experimental data with the theoretical models, providing the time-dependence feature to the theoretical model.

Example of the Application of the TBP

The statistical method is based on Flory-Stockmayer model [Flory, 1953] and was generalized by M. Gordon [1962], resulting in what is now called the theory of branching processes (TBP) or cascade theory. The TBP uses probability generating functions (pgf) and cascade substitution as mathematical tools. The methods are introduced by describing the application of the TBP to a single-component system [Dusek, 1986, 2002].

Figure 2.1 describes a simple case of the crosslinking reaction for a system composed of one type of *precursor* unit that has three *functional groups*. After some reaction, the precursor can be in four reaction states depending on conversion, or extent of reaction. That is, none, one, two or three of the functionalities have reacted and the number fraction of the precursors in each of these reaction states is defined as a0, a1, a2 and a3, respectively, where the subscript represents

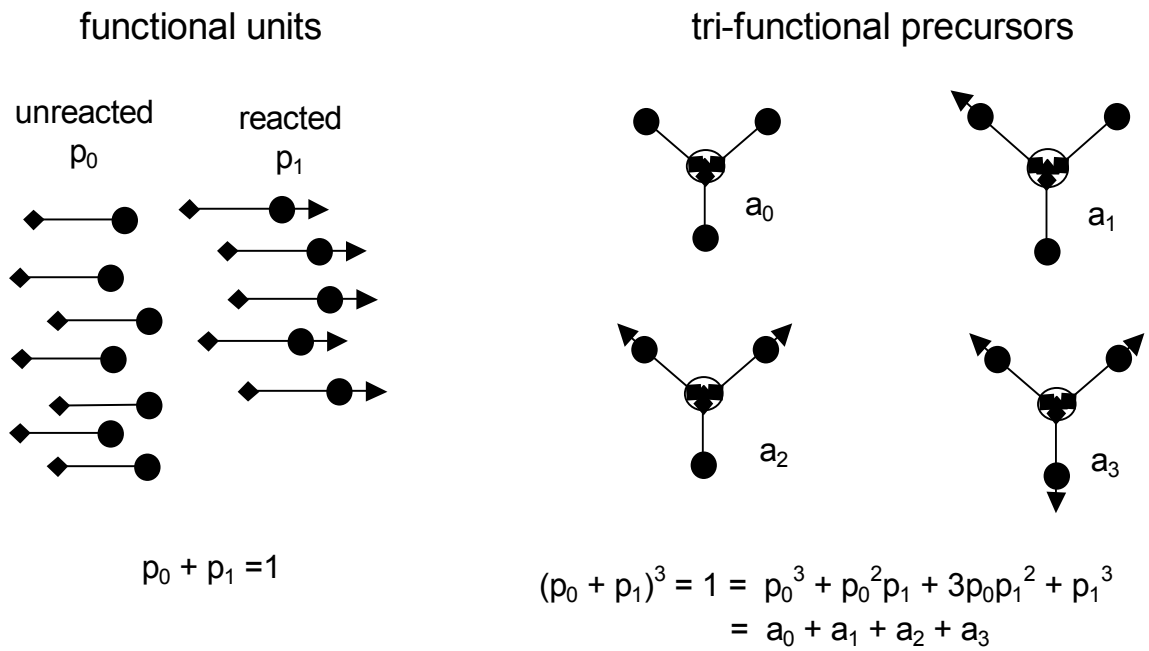

Figure 2.1 – Four reacted states of a tri-functional precursor.

the number of reacted functional groups. a_i is also the probability of finding a *precursor* with *i* reacted groups. The summation of the a_i(s) is unity. Initially, all functionalities (reaction sites) are unreacted and a_0 is unity and a_1, a_2 and a_3 are zero.

The probabilities of finding an unreacted or a reacted *functional group* in the system are defined as p_0 and p_1, respectively. Since the functional groups must be reacted or unreacted, $p_1 + p_0 = 1$, or $p_1 = 1 - p_0$. Molar conversion of the functional groups is defined as α. For this system, $\alpha = p_1$.

Two rules are applied for reaction of the functional groups: (1) the functional groups have equal and independent reactivity, (2) there is no intra-molecular crosslinking (cyclization), that is , unreacted functional groups on a connected structure may not react.

Building a tri-functional precursor unit from three functional groups using probability concepts results in Equation 2.1which is the relationship between the probabilities (or fractions) of finding the two states of the functional groups (p_0 and p_1)and the probabilities (or fractions) of finding the four reaction states of the precursor (a_i(s)).

$$1 = (p_0 + p_1)^3 = p_0^3 + p_0^2 p_1 + 3 p_0 p_1^2 + p_1^3 = a_0 + a_1 + a_2 + a_3 \qquad \text{Eq. 2.1}$$

where $a_0 = p_0^3$ $\quad a_1 = 3p_0^2 p_1$ $\quad$ Eqs. 2.2a,b

$a_2 = 3p_0 p_1^2$ $\quad a_3 = p_1^3$ $\quad$ Eqs. 2.2c,d

For a given conversion of functional groups, α, p_0 and p_1 are determined and the fraction of each reactive state of the precursor can be calculated from Equations 2.2a,b,c,d. The analysis to this point gives no information on how the four types of precursors are connected to form larger structures. This type of information is provided through the application of probability generating functions, pgf(s), and the procedure of cascade substitution.

Crosslinked structures are generated by combining the precursor units, one unit at a time in successive generations. The number-fraction distribution of precursor units in the 0th generation (one precursor unit in size) is given by Equation 2.1 as $a_0 : a_1 : a_2 : a_3$. This distribution is expressed in the form of a pgf, $F_0(z)$, in Equation 2.3.

$$F_0(z) = a_0 + a_1 z + a_2 z^2 + a_3 z^3 = \sum_{i=0}^{3} a_i z^i \qquad \text{Eq.2.3}$$

In Equation 2.3, z is an auxiliary (dummy) variable through which the operations with the pgf are performed and the subscript on F represents the generation. Specifically, $F_0(z)$ is the pgf for the number of bonds issuing from the precursor units in Generation 0 to Generation 1. $F_0(z)$ can also be written in terms of the conversion, α, as shown in Equation 2.4.

$$F_0(z) = (1-\alpha)^3 + 3(1-\alpha)^2 \alpha z + 3(1-\alpha)\alpha^2 z^2 + \alpha^3 z^3 = (1-\alpha+\alpha z)^3 \qquad \text{Eq 2.4}$$

An example of how pgf(s) can be used to determine information about the reactive system is to determine the expectation, or mean, of the distribution. The expectation is obtained by differentiation of $F_0(z)$ with respect to z at z = 1 and the relationship is given in Equation 2.6. The quantity calculated by Eq. 2.6 is the average number of reacted functional groups per precursor unit.

$$\frac{\partial F_0(z)}{\partial z} = F_0'(z) = \sum_{i=1}^{3} i a_i z^{i-1} = a_1 + 2a_2 z + 3a_3 z^2 = 3\alpha(1-\alpha+\alpha z)^2 \qquad \text{Eq. 2.5}$$

$$\left(\frac{\partial F_0(z)}{\partial z}\right)_{z=1} = F_0'(1) = \sum_{i=1}^{3} i a_i = a_1 + 2a_2 + 3a_3 = 3\alpha \qquad \text{Eq. 2.6}$$

Structures are built, one precursor unit at a time, in successive generations. For the next generation, namely 1, a pgf is derived that describes the number of additional bonds issuing from units in Generation 1, *i.e.,* for the number of bonds issuing from units in Generation 1 to units in Generation 2. In Generation 1, the probability of a precursor unit to combined with a reacted functional group in Generation 2 is proportional to the product of its molar fraction and the number of reacted groups ($i \cdot a_i$), because one precursor unit with i reacted groups can be combined with a reacted group in Generation 2 in i ways. The total number of bonds would be:

Total # of bonds between
Generations 1 and 2 $= a_1 + 2\,a_2 + 3\,a_3$

The fraction, or probability, of bonds for the precursor with one, two and three reacted functionality(s) would equal, respectively,

$$a_1 \;/\; (\, a_1 + 2\, a_2 + 3\, a_3 \,) \qquad [\text{defined as } a_0^*] \qquad \text{Eq. 2.7}$$

$$2\, a_2 \;/\; (\, a_1 + 2\, a_2 + 3\, a_3 \,) \qquad [\text{defined as } a_1^*] \qquad \text{Eq. 2.8}$$

$$3\, a_3 \;/\; (\, a_1 + 2\, a_2 + 3\, a_3 \,) \qquad [\text{defined as } a_2^*] \qquad \text{Eq. 2.9}$$

The pgf for Generation 1 would then be

$$F_1(z) = \frac{a_1}{a_1 + 2a_2 + 3a_3} + \frac{2a_2}{a_1 + 2a_2 + 3a_3} z + \frac{3a_3}{a_1 + 2a_2 + 3a_3} z^2 \qquad \text{Eq. 2.10}$$

or

$$F_1(z) = a_1^* + 2a_2^* z + 3a_3^* z^2 = \sum_{i=1}^{3} a_i^* z^{i-1} \qquad \text{Eq 2.11}$$

a_i^* is the probability of finding in Generation 1 a unit with *i* reacted functional groups which issues (*i-1)* bonds to Generation 2. Note that the precursor with no reacted functionalities *(i=0)* is in Generation 0 and does not appear in Generations greater than 0.

The analysis described above for Generation 1 holds for all generations greater than 0. The general pgf(s) for generations greater than 0 is:

$$F(z) = F_1(z) = F_2(z) = F_{G>0}(z) = a_1^* + 2a_2^* z + 3a_3^* z^2 = \sum_{i=1}^{3} a_i^* z^{i-1} \qquad \text{Eq. 2.12}$$

Inspection of preceding equations reveals the following important relationship between F(z) and $F_0(z)$.

$$F(z) = \frac{\partial F_0(z)}{\partial z} \Bigg/ \left(\frac{\partial F_0(z)}{\partial z} \right)_{z=1} \qquad \text{Eq. 2.13}$$

The analysis to this point was conduct for a tri-functional precursor. The analysis can also be conducted for a precursor that has a functionality *f* [Dusek, 1986]. Relationships for a precursor with *f* functionality are presented here and are used in the following section to describe the crosslinking of HPAM by a chromium crosslinker.

The pgf for Generation 0 of an *f*-functional precursor is:

$$F_0(z) = \sum_{i=0}^{f} a_i z^i = (1 - \alpha + \alpha z)^f \qquad \text{Eq. 2.14}$$

where the coefficients are given by the binomial expansion.

$$a_i = \binom{f}{i} p_0^{\,f-i} p_1^{\,i} \quad = \binom{f}{i} (1-\alpha)^{f-i} \alpha^i \qquad \text{Eq. 2.15}$$

It is noted that $\sum a_i = 1$ and

$$F_0(1) = 1 \qquad \text{Eq. 2.16}$$

The derivative of the Generation 0 pgf with respect to z have the following relationships:

$$\frac{\partial F_0(z)}{\partial z} = F_0'(z) = \sum_{i=1}^{f} i a_i z^{i-1} = \alpha f (1-\alpha+\alpha z)^{f-1} \qquad \text{Eq. 2.17}$$

and

$$\left(\frac{\partial F_0(z)}{\partial z}\right)_{z=1} = F_0'(1) = \sum_{i=1}^{f} i a_i = f\alpha \qquad \text{Eq. 2.18}$$

The pgf(s) for generations greater than 0 is:

$$F(z) = \frac{\partial F_0(z)}{\partial z} \Bigg/ \left(\frac{\partial F_0(z)}{\partial z}\right)_{z=1} = \frac{F_0'(z)}{F_0'(1)} = \frac{\sum_{i=1}^{f} i a_i z^{i-1}}{\sum_{i=1}^{f} i a_i} = \sum_{i=1}^{f} \frac{i a_i}{\sum_{i=1}^{f} i a_i} z^{i-1} = \sum_{i=1}^{f} a_i^* z^{i-1} \qquad \text{Eq. 2.19}$$

F(z) also can be expressed in the form of conversion α and functionality *f*:

$$F(z) = \frac{F_0'(z)}{F_0'(1)} = (1-\alpha+\alpha z)^{f-1} \qquad \text{Eq. 2.20}$$

It is noted that:

$$F'(z) = (f-1)\alpha(1-\alpha+\alpha z)^{f-2} \qquad \text{Eq. 2.21}$$

and

$$F'(1) = (f-1)\alpha \qquad \text{Eq. 2.22}$$

In order to extract more information from this type of analysis, another generating function is derived through the use of cascade substitution. In particular, the distribution of molecules according to their degree of polymerization is sought. The weight-fraction generating function (wfgf), *W(z)* [Good, 1955] provides this information and is defined as:

$$W(z) = \sum_{i=1}^{\infty} w_i z^i \qquad \text{Eq. 2.23}$$

where w_i is the weight fraction of the *i-mer* and is equal to the probability that a repeat unit chosen at random in the system is found to be a part of an *i-mer*. *W(z)* is also a function of $F_0(z)$ and *F(z)* by noting that $zF_0(z)$ counts the units in a molecule up to Generation 1 and $zF_0(zF(z))$ counts the units in a molecule up to Generation 2, and so on. Continuing the cascade substitution to infinity counts the units in molecules of all sizes and gives the weight-fraction distribution as:

$$W(z) = zF_0(zF(zF(zF...))) = zF_0(u(z)) \qquad \text{Eq. 2.24}$$

where

$$u(z) = zF(u(z)) \qquad \text{Eq. 2.25}$$

In terms of the conversion, α, *W(z)* and *u(z)* become:

$$W(z) = z(1-\alpha+\alpha u(z))^f \qquad \text{Eq. 2.26}$$

$$u(z) = zF(u(z)) = z(1-\alpha+\alpha u(z))^{f-1} \qquad \text{Eq. 2.27}$$

It can be shown [Dusek, 1986] that the weight-average degree of polymerization P_w is given by Equation 2.28.

$$P_w = \sum_{i=1}^{\infty} i w_i = \left(\frac{\partial W(z)}{\partial z}\right)_{z=1} = 1 + \frac{F_0'(1)}{1-F'(1)} = \frac{1+\alpha}{1-(f-1)\alpha} \qquad \text{Eq. 2.28}$$

The gel point is defined as point at which P_w diverges to infinity, that is, there is a molecule with an infinite molecular weight. At the gel point, $\lim_{\alpha\to\alpha_c} P_w(\alpha) = \infty$, so that $1-(f-1)\alpha = 0$, and the critical conversion (conversion at the gel point) is given by Equation 2.29.

$$\alpha_c = \frac{1}{f-1} \qquad \text{Eq. 2.29}$$

The number-average degree of polymerization, P_n, is given by the ratio of number of units to the number of molecules. Since the formation of one bond will cause the number of molecules to decrease by one, the number of molecules = initial number of units – number of bonds. Because the number of bonds is equal to one half of the number of reacted functional groups, thus,

$$P_n = \frac{1}{1-F_0'(1)/2} = \frac{1}{1-f\alpha/2} \qquad \text{Eq. 2.30}$$

The use of pgf(s) makes the procedures for derivation of various statistical averages (of molecular weight, degree of polymerization, *etc*.) highly economical and routine, because this method does not depend on getting an explicit algebraic expression for the molecular weight distribution. The weight-fraction of *i-mer*, w_i, is expressed implicitly in the wfgf, W(z) (cf. Eq.

2.23) and can be extracted by advanced mathematical procedures. It is planned to determine molecular weight distributions in future work.

Model Describing the Crosslinking of HPAM by Chromium(III) Acetate

The Theory of Branching Processes was applied to the crosslinking of hydrolyzed polyacrylamide (HPAM) by chromium(III) acetate. A model is developed that describes the molecular weight averages of pre-gel aggregates as a function of the conversion of functional groups on the HPAM and chromium(III).

Gel System. The gel system is composed of HPAM molecules and chromium(III) complex ions. HPAM is polydisperse with weight-average molecular weight of about 6 million. Carboxylate groups along the polymer chain are the functional groups that react with the chromium complexes. One polymer molecule contains many carboxylate groups depending on the degree of hydrolysis. HPAM is crosslinked by chromium acetate. The reactions are described by two ligand exchange reactions in Equations 2.31 and 2.32.

$$Cr(L)_n + P1\text{-}CO_2^- \rightarrow Cr(L)_{n-1}(P1\text{-}CO_2^-) + L \qquad \text{(uptake)} \qquad \text{Eq. 2.31}$$

$$Cr(L)_{n-1}(P1\text{-}CO_2^-) + P2\text{-}CO_2^- \rightarrow (P2\text{-}CO_2^-)Cr(L)_{n-2}(P1\text{-}CO_2^-) + L \qquad \text{(crosslink)} \qquad \text{Eq. 2.32}$$

P1 and P2 represent different polymer molecules and the $-CO_2^-$ represents one functional group on each of the polymers in these equations. The first reaction of a polymer (P1) with the chromium complex is commonly called the uptake reaction. The reaction of a second polymer (P2) with the chromium complex creates a crosslink between the polymers and is termed the crosslink reaction.

Tackett [1989] characterized the structures in chromium acetate solutions and found the dominant species is cyclic chromium trimer with associated ligands for solutions at pH values typical of the gelant systems ($4 < pH < 5.5$). Replacement of acetate groups by hydroxyl groups causes ring opening and the formation of linear chromium trimer at pH values above 5.5. Generally, the chromium complex ion is thought to be a trimer and that it reacts with only two carboxylate groups. Steric hindrance reduces the possibility of reaction to a third carboxylate group.

Model and Assumptions. An initial, simplified model of the HPAM-chromium acetate gelant was developed using the Theory of Branching Processes. The model system was a two-component system, HPAM units and chromium trimer units. HPAM was designated Unit A. The model is simplified by assuming the HPAM (Unit A) is monodisperse, that is , all the polymer chains have the same degree of polymerization resulting in the initial equality of the weight-average and number-average molecular weights. The model is further simplified by assuming the functionalities of Unit A are distributed evenly. The functionality of Unit A, f_A, is a constant (the number of carboxyl groups on each polymer molecule is the same.) Chromium acetate trimer (3Cr) was designated Unit B. The functionality of Unit B was 2 ($f_B = 2$). That is, one chromium trimer can react with, at most, two polymer molecules.

The following three rules for the reaction between Units A and B were assumed.

(1) Equal and independent reactivity of each functional group;
(2) No intra-molecular crosslinking (cyclization) in the pre-gel stage. The two functionalities on Unit B (chromium trimer) can not react with two functionalities (carboxyl groups) on one Unit A;
(3) Alternating reactions only, which means only Unit A can react with Unit B; no polymer-polymer or trimer-trimer reactions.

The modeling procedure consist of deriving relationships for the weight-average and number-average molecular weights as functions of the initial conditions and conversions of the precursor units. Relationships for the conversions of the functional groups at the gel point (critical conversions) as functions of the initial conditions were also derived. The general principles applied to the single-component system in the example shown above were applied to the two-component system in the following sections.

Weight-average molecular weight. The pgf for Generation 0 of a two-component system [Dusek, 1986; Huybrechts and Dusek, 1998] is

$$\begin{aligned} F_0(z) &= n_A F_{0A}(z_B) + n_B F_{0B}(z_A) \\ &= n_A(1-\alpha_A+\alpha_A z_B)^{f_A} + n_B(1-\alpha_B+\alpha_B z_A)^{f_B} \end{aligned} \qquad \text{Eq. 2.33}$$

where

n_A, n_B	–	initial number (molar) fractions of polymer and chromium trimer, respectively,
z	–	a vector, **z** = (z_A, z_B), auxiliary variables in pgf,
f_A, f_B	–	functionalities of polymer and chromium trimer, respectively. In this model the functionality of polymer, f_A, is the average number of carboxylate groups per polymer molecule,
α_A, α_B	–	conversions of functional group A (carboxylate group) and B (chromium functionalities), respectively,

and the components of $F_0(\mathbf{z})$ are

$$F_{0A}(z_B) = (1-\alpha_A+\alpha_A z_B)^{f_A} = \sum_{i=0}^{f_A} a_i z_B^i \qquad \text{Eq. 2.34}$$

$$F_{0B}(z_A) = (1-\alpha_B+\alpha_B z_A)^{f_B} = \sum_{i=0}^{f_B} b_i z_A^i \qquad \text{Eq. 2.35}$$

The subscript B on *z* indicates the bond extends to group B. Similarly, the subscript A indicates the bond extends to group A (alternating reaction). Coeffiecients a_i and b_i represent the number fraction of precursors A and B, respectively, with *i* reacted functional groups. The pgfs for the number of bonds issuing from units in Generations > 0 were obtained by differentiation of Eqs. 2.34 and 2.35.

$$F_A(z_B) = \frac{\partial F_{0A}(z_B)}{\partial z_B} \Bigg/ \left(\frac{\partial F_{0A}(z_B)}{\partial z_B} \right)_{z_B=1} = (1-\alpha_A + \alpha_A z_B)^{f_A - 1} \qquad \text{Eq. 2.36}$$

$$F_B(z_A) = \frac{\partial F_{0B}(z_A)}{\partial z_A} \Bigg/ \left(\frac{\partial F_{0B}(z_A)}{\partial z_A} \right)_{z_A=1} = (1-\alpha_B + \alpha_B z_A)^{f_B - 1} \qquad \text{Eq. 2.37}$$

The weight fraction generating function (wfgf), W(**z**), for the two-component system [Dusek, 1986; Huybrechts and Dusek, 1998]is

$$W(z) = w_A W_A(z) + w_B W_B(z) \qquad \text{Eq. 2.38}$$

where w_A, w_B are the initial weight fractions of polymer and chromium trimer, respectively. The components of the wfgf, $W_A(z)$ and $W_B(z)$, are:

$$W_A(z) = z_A^{M_A} F_{0A}(u_B) = z_A^{M_A}(1-\alpha_A + \alpha_A u_B)^{f_A} \qquad \text{Eq. 2.39}$$

$$W_B(z) = z_B^{M_B} F_{0B}(u_A) = z_B^{M_B}(1-\alpha_B + \alpha_B u_A)^{f_B} \qquad \text{Eq. 2.40}$$

with $$u_A = z_A^{M_A} F_A(u_B) = z_A^{M_A}(1-\alpha_A + \alpha_A u_B)^{f_A - 1} \qquad \text{Eq. 2.41}$$

$$u_B = z_B^{M_B} F_B(u_A) = z_B^{M_B}(1-\alpha_B + \alpha_B u_A)^{f_B - 1} \qquad \text{Eq. 2.42}$$

M_A and M_B are molecular weights of the polymer and chromium trimer, respectively. The z(s) in the above equations are raised to the powers of the molecular weights, M_A and M_B, to weigh the units and give the weight-average. (This formulation is different than in the example for the single component system where the weight-average degree of polymerization, P_w, was sought).

The weight-average molecular weight of the entire gel system, which includes polymer and chromium trimer precursors and combinations thereof, is:

$$M_w = \left(\frac{\partial W(z)}{\partial z_A} + \frac{\partial W(z)}{\partial z_B} \right)_{z_A = z_B = 1} \qquad \text{Eq. 2.43}$$

M_w is obtained by differentiation of Eqs. 2.39 and 2.40 and by substitution of the results into Eq. 2.43. For compactness, $z = z_A = z_B$ (= 1) and $F_Y^X = \left[\frac{\partial F_Y(z)}{\partial z_X} \right]_{z=1}$.

$$\begin{aligned} \left. \frac{\partial W(z)}{\partial z_A} \right|_{z=1} &= \left[w_A \frac{\partial W_A(z)}{\partial z_A} + w_B \frac{\partial W_B(z)}{\partial z_A} \right]_{z=1} \\ &= \left[w_A \left(M_A z_A^{M_A - 1} F_{0A}(u_B) + z_A^{M_A} F_{0A}^B u_B^A \right) + w_B z_B^{M_B} F_{0B}^A u_A^A \right]_{z=1} \\ &= w_A \left(M_A + F_{0A}^B u_B^A \right) + w_B F_{0B}^A u_A^A \end{aligned} \qquad \text{Eq. 2.44}$$

$$\left.\frac{\partial W(z)}{\partial z_B}\right|_{z=1} = \left[w_A \frac{\partial W_A(z)}{\partial z_B} + w_B \frac{\partial W_B(z)}{\partial z_B} \right]_{z=1}$$
$$= \left[w_A z_A^{M_A} F_{0A}^B u_B^B + w_B \left(M_B z_B^{M_B - 1} F_{0B}(u_A) + z_B^{M_B} F_{0B}^A u_A^B \right) \right]_{z=1} \qquad \text{Eq. 2.45}$$
$$= w_A F_{0A}^B u_B^B + w_B \left(M_B + F_{0B}^A u_A^B \right)$$

Equations 2.44 and 2.45 were simplified by noting that when **z** = 1, u = u(**z**) = 1, $F_{0A}(1) = F_{0B}(1) = 1$, $F_A(1) = F_B(1) = 1$.

The derivatives of u_A and u_B at $z = 1$ are obtained from Eqs. 2.41 and 2.42.

$$u_A^A = \left[M_A z_A^{M_A - 1} F_A(u_B) + z_A^{M_A} F_A^B u_B^A \right]_{z=1} = M_A + F_A^B u_B^A \qquad \text{Eq. 2.46}$$
$$u_A^B = \left(z_A^{M_A} F_A^B u_B^B \right)_{z=1} = F_A^B u_B^B \qquad \text{Eq. 2.47}$$
$$u_B^A = \left(z_B^{M_B} F_B^A u_A^A \right)_{z=1} = F_B^A u_A^A \qquad \text{Eq. 2.48}$$
$$u_B^B = \left[M_B z_B^{M_B - 1} F_B(u_A) + z_B^{M_B} F_B^A u_A^B \right]_{z=1} = M_B + F_B^A u_A^B \qquad \text{Eq. 2.49}$$

Substitution of Eq. 2.48 into Eq. 2.46 yields

$$u_A^A = M_A + F_A^B F_B^A u_A^A \qquad \text{Eq 2.50}$$

Solving for u_A^A gives

$$u_A^A = \frac{M_A}{1 - F_A^B F_B^A} \qquad \text{Eq. 2.51}$$

By similar substitutions and rearrangements:

$$u_B^B = \frac{M_B}{1 - F_A^B F_B^A} \qquad \text{Eq. 2.52}$$
$$u_A^B = \frac{F_A^B \cdot M_B}{1 - F_A^B F_B^A} \qquad \text{Eq. 2.53}$$
$$u_B^A = \frac{F_B^A \cdot M_A}{1 - F_A^B F_B^A} \qquad \text{Eq. 2.54}$$

Substitutions of Eqs. 2.51 – 2.54 into Eqs. 2.44 -2.45 and then Eq. 2.44 and 2.45 into Eq. 2.43 gives

$$M_w = \left(\frac{\partial W(z)}{\partial z_A} + \frac{\partial W(z)}{\partial z_B} \right)_{z=1}$$

$$= w_A \left(M_A + F_{0A}^B u_B^A \right) + w_B F_{0B}^A u_A^A + w_A F_{0A}^B u_B^B + w_B \left(M_B + F_{0B}^A u_A^B \right)$$

$$= w_A \left(M_A + \frac{F_{0A}^B F_B^A \cdot M_A}{1 - F_A^B F_B^A} \right) + w_B \left(\frac{F_{0B}^A \cdot M_A}{1 - F_A^B F_B^A} \right)$$

$$+ w_A \left(\frac{F_{0A}^B \cdot M_B}{1 - F_A^B F_B^A} \right) + w_B \left(M_B + \frac{F_{0B}^A F_A^B \cdot M_B}{1 - F_A^B F_B^A} \right)$$

$$M_w = w_A M_A + w_B M_B + \frac{1}{1 - F_A^B F_B^A} \cdot \left[w_A \left(M_A F_{0A}^B F_B^A + M_B F_{0A}^B \right) + w_B \left(M_A F_{0B}^A + M_B F_{0B}^A F_A^B \right) \right]$$

Eq. 2.55

From Eqs. 2.34 through 2.37, the derivatives of $F_{0A}(z_B)$, $F_{0B}(z_A)$, $F_A(z_B)$ and $F_B(z_A)$ at **z** = 1 are obtained:

$$F_{0A}^B = f_A \alpha_A \qquad F_{0B}^A = f_B \alpha_B$$

$$F_A^B = (f_A - 1)\alpha_A \qquad F_B^A = (f_B - 1)\alpha_B$$

Substitution of these derivatives into Eq. 2.55 gives

$$M_w = w_A M_A + w_B M_B + \frac{1}{D} \{ w_A \left[M_A f_A \alpha_A (f_B - 1)\alpha_B + M_B f_A \alpha_A \right] + w_B \left[M_B f_B \alpha_B (f_A - 1)\alpha_A + M_A f_B \alpha_B \right] \}$$

Eq. 2.56

where $D = 1 - F_A^B F_B^A = 1 - (f_A - 1)(f_B - 1) \cdot \alpha_A \alpha_B$ Eq. 2.57

The conversions of functional groups on precursor A (carboxyl groups) and on precursor B (chromium functionalities) are related by the following equations which equates the number of converted functionalities of each precursor since only alternating reactions are allowed. That is, the number of A functionalities that are converted equals the number of B functionalities converted.

$$n_A f_A \alpha_A = n_B f_B \alpha_B$$ Eq. 2.58

$$\alpha_B = \frac{n_A f_A}{n_B f_B} \cdot \alpha_A = r_A \alpha_A$$ Eq. 2.59

where $r_A = \frac{n_A f_A}{n_B f_B}$, the initial molar ratio of carboxylate groups to chromium functionalities.

Substitution of Eq. 2.59 into Eq. 2.56 gives the weight-average molecular weight in terms of the conversion of A (α_A).

$$M_w = w_A M_A + w_B M_B + \frac{1}{D}\{w_A\left[M_A f_A (f_B - 1) r_A \alpha_A^2 + M_B f_A \alpha_A\right] + w_B\left[M_B f_B (f_A - 1) r_A \alpha_A^2 + M_A f_B r_A \alpha_A\right]\} \quad \text{Eq. 2.60}$$

A similar relationship is derived for M_w as a function of the conversion of B (α_B).

$$M_w = w_A M_A + w_B M_B + \frac{1}{D}\{w_A\left[M_A f_A (f_B - 1)\frac{\alpha_B^2}{r_A} + M_B f_A \frac{\alpha_B}{r_A}\right] + w_B\left[M_B f_B (f_A - 1)\frac{\alpha_B^2}{r_A} + M_A f_B \alpha_B\right]\} \quad \text{Eq. 2.61}$$

The weight-average molecular weight of the *entire* gel system is then expressed as a function of the conversions of the carboxylate groups or chromium functionalities. To calculate the weight-average molecular weight of pre-gel aggregates (structures containing one or more polymer molecules), the first term is separated from the summation in the definition of the weight-average molecular weight.

$$M_w = \sum_{i=1}^{\infty} w_i M_i = w_1 M_1 + \sum_{i=2}^{\infty} w_i M_i = w_1 M_1 + \sum_{i=2}^{\infty} w_i \left(\frac{\sum_{i=2}^{\infty} w_i M_i}{\sum_{i=2}^{\infty} w_i} \right) \quad \text{Eq. 2.62}$$

Let i=1 be the unreacted chromium trimer, then the molecules of i =2→ ∞ represent molecules that contain one or more polymer precursors (or pre-gel aggregates). The molecular weight of the unreacted trimer is M_B (= M_1), the summation of w_i equals one (or 1- w_1 = $\sum_{i=2}^{\infty} w_i$), and the term in brackets is the weight-average molecular weight of the pre-gel aggregates, defined as $M_{w\text{-}agg}$. Substitution of these relations into Eq. 2.62 and rearrangement gives

$$M_{w-agg} = \frac{M_w - w_1 M_B}{1 - w_1} \quad \text{Eq. 2.63}$$

w_1 is the weight fraction of unreacted trimer in the entire system (or weight of unreacted trimer divided by the total weight of trimer and polymer) and is the product of b_0 and w_B (the initial weight fraction of trimer in the entire system). b_0 is the coefficient of the first term in the expansion of F_{0B} (z_A) in Eq. 2.35 and is the number of chromium trimers that have no reacted functionalities divided by the total number of trimers. b_0 also equals the weight of unreacted chromium trimer divided by the total weight of trimer. b_0 is given as a function of the conversion of B according to Eq. 2.15.

$$b_0 = \binom{f_B}{0}(1-\alpha_B)^{f_B}\alpha_B{}^0 = (1-\alpha_B)^{f_B}$$

Substitution gives w_1 in terms of the initial weight fraction, functionality and conversion of trimer.

$$w_1 = w_B b_0 = w_B (1-\alpha_B)^{f_B} \qquad \text{Eq. 2.64}$$

The weight-average molecular weight of pre-gel aggregates is

$$M_{w-agg} = \frac{M_w - w_1 M_B}{1-w_1} = \frac{M_w - w_B M_B (1-\alpha_B)^{f_B}}{1-w_B(1-\alpha_B)^{f_B}} \qquad \text{Eq. 2.65}$$

Critical conversion at the gel point. The weight-average molecular weight of the entire gel system diverges to infinity at the gel point. This occurs when $D = 0$ in Eq. 2.56. The critical conversions are determined from Eq. 2.57, setting $D = 0$.

$$D = 0 = 1-(f_A-1)(f_B-1)\cdot\alpha_A\alpha_B \qquad \text{Eq.2.66}$$

Rearrangement gives the critical conversions as

$$\alpha_{crit,A} = \left[\frac{1}{(f_A-1)(f_B-1)\cdot r_A}\right]^{1/2} \qquad \text{Eq. 2.67}$$

$$\alpha_{crit,B} = \left[\frac{r_A}{(f_A-1)(f_B-1)}\right]^{1/2} \qquad \text{Eq. 2.68}$$

Number-average molecular weight. The number-average molecular weight of the gel system is the total weight of system (grams of chromium trimer and polymer) divided by the total gram-moles of molecules. For each reaction, or bond formed, the number of molecules is reduced by one.

$$M_n = \frac{Total\ mass\ (grams)}{Total\ \#\ of\ molecules\ (moles)}$$

$$M_n = \frac{Total\ mass\ (grams)}{Initial\ moles\ of\ molecules\ -\ moles\ of\ bonds\ formed}$$

Division of each quantity in the above equation by *the initial moles of molecules* gives:

$$M_n = \frac{Total\ mass\ (grams)\ /\ Initial\ moles\ of\ molecules}{1-\ (Moles\ of\ bonds\ formed\ /\ Initial\ moles\ of\ molecules)}$$

The *Total mass (grams)/ Initial moles of molecules* is equivalent to $n_A M_A + n_B M_B$. The *Moles of bonds formed/Initial moles of molecules* is equivalent to $n_A f_A \alpha_A$ or $n_B f_B \alpha_B$. Substitution of these quantities gives the number-average molecular weight as

$$M_n = \frac{n_A M_A + n_B M_B}{1 - n_A f_A \alpha_A} = \frac{n_A M_A + n_B M_B}{1 - n_B f_B \alpha_B} \qquad \text{Eq. 2.69}$$

The number-average molecular weight of pre-gel aggregates (structures containing one or more polymer molecules) is determined by a procedure similar to that for finding the weight-average molecular weight above. The first tem is separated from the summation in the definition of the number-average molecular weight.

$$M_n = \sum_{i=1}^{\infty} n_i M_i = n_1 M_1 + \sum_{i=2}^{\infty} n_i M_i = n_1 M_1 + \sum_{i=2}^{\infty} n_i \left(\frac{\sum_{i=2}^{\infty} n_i M_i}{\sum_{i=2}^{\infty} n_i} \right) \qquad \text{Eq. 2.70}$$

Let i=1 be the unreacted chromium trimer, then the molecules of i =2→ ∞ represent molecules that contain one or more polymer precursors (or pre-gel aggregates). The molecular weight of the unreacted trimer is M_B (= M_1), the summation of n_i equals one (or 1- n_1 = $\sum_{i=2}^{\infty} n_i$), and the term in brackets is the number-average molecular weight of the pre-gel aggregates, defined as $M_{n\text{-}agg}$. Substitution of these relations into Eq. 2.70 and rearrangement gives

$$M_{n-agg} = \frac{M_n - n_1 M_B}{1 - n_1} \qquad \text{Eq. 2.71}$$

n_1 is the number fraction of unreacted trimer in the entire system (or number of unreacted trimers divided by the total number of molecules). Noting that the *total number of molecules / initial number of molecules* is equal to $1\text{-}n_B f_B \alpha_B$, b_0 [= $(1\text{-}\alpha_B)^{f_B}$] is equal to the *number of unreacted trimers / initial number of trimers*, and n_B is equal to the *initial number of trimers / sum of initital number of trimers and polymers*, n_1 is given by

$$n_1 = \frac{n_B b_0}{1 - n_B f_B \alpha_B} = \frac{n_B (1 - \alpha_B)^{f_B}}{1 - n_B f_B \alpha_B} \qquad \text{Eq. 2.72}$$

Substitution of Eqs. 2.72 and 2.69 into Eq. 2.71 gives the number-average molecular weight of the pre-gel aggregates in terms of initial conditions and the conversion of the chromium trimer (α_B).

$$M_{n-agg} = \frac{M_n - \dfrac{M_B n_B (1 - \alpha_B)^{f_B}}{1 - n_B f_B \alpha_B}}{1 - \dfrac{n_B (1 - \alpha_B)^{f_B}}{1 - n_B f_B \alpha_B}} = \frac{n_A M_A + n_B M_B [1 - (1 - \alpha_B)^{f_B}]}{1 - n_B f_B \alpha_B - n_B (1 - \alpha_B)^{f_B}} \qquad \text{Eq. 2.72}$$

Comparison of the Model to Experimental Data

The mathematical model was compared to experimental data that were measured on polyacrylamide-chromium acetate gel systems. The experimental data were taken from Willhite *et al.* [2003] and from Jain, which are presented in Chapter 3 of this report. Input parameters required for the model, which are the initial conditions for the experimental system were determined as follows.

The values of initial parameters for the gel system used by Willhite et al. [2003] were:

- Degree of hydrolysis of polymer: 8%
- Molecular weight of polymer measured by MALLS, M_A:
  - 5.26×10^6 g/mol for polyacrylamide, AlcoFlood 935, Lot No. 7158V
  - 6.64×10^6 g/mol for polyacrylamide, AlcoFlood 935, Lot No. A2247BOV
- Active polymer content in weighed samples: 90 wt%
- Concentration of polymer (active content not considered): 5000 ppm
- Molecular weight of chromium trimer, M_B: $3 \times 52 = 156$ g/mol
  (Molar masses of the atoms associated with the chromium trimer are neglected.)
- Functionality of chromium trimer: $f_B = 2$
- Concentration of chromium trimer: 100 ppm; 20 ppm

The functionality of A and initial fractions of A and B are given in Tables 2.1 and 2.2, respectively, for a gel system prepared with 5000 ppm AlcoFlood 935, Lot 7158V and 100 ppm chromium trimer as an example.

Table 2.1 – Functionality of polymer (average number of carboxylate groups per polymer molecule), f_A.

	Polymer, AlcoFlood935, 7158V
Molecular weight, M_A, g/mol	5.26×10^6
Degree of hydrolysis	8 %
Number of monomers per polymer molecule*	72137
Functionality, f_A	$72137 \times 8\% = 5771$

* Since 8% of monomer is hydrolyzed to carboxylate which is present as sodium salt, there are two types of monomers in a polymer molecule:

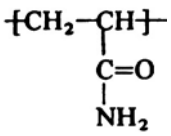

molecular weight = 71.1 g/mol

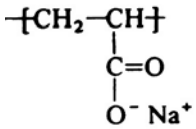

molecular weight = 94.0 g/mol

So the number of monomers per polymer molecule (degree of polymerization)

$$= \frac{5.26 \times 10^6}{71.1 \times (1 - 0.08) + 94.0 \times 0.08} = 72137$$

Table 2.2 – Initial number and weight fractions of polymer and chromium trimer.

i = A, B	A Polymer	B Chromium trimer
Molecular weight, M_i, g/mol	5.26×10^6	156
Functionality, f_i	5771	2
Concentration, ppm	5000	100
Active concentration, c_i, ppm	4500	100
Number of moles per gram gelant, $N_i = c_i/M_i$, 10^{-6} moles/g	8.56×10^{-4}	0.64
Number fraction, $n_i = N_i/\Sigma N_i$	1.33×10^{-3}	0.999
Weight fraction, $w_i = c_i/\Sigma c_i$	0.98	0.02
$r_A = n_A f_A / n_B f_B$	3.85	

The various molecular weight averages were determined from the model as a function of the conversion of chromium functionalities, α_B. The weight-average molecular weights of gel system and pre-gel aggregates were calculated using Eqs. 2.61 and 2.65. The number-average molecular weights of gel system and pre-gel aggregates were calculated using Eqs. 2.69 and 2.72, respectively. The critical conversion of the chromium trimer, α_B, was obtained by Eq. 2.68.

The various average molecular weights for the gel system with input parameters described above are given in Table 2.3 as a function of the conversion of B. The critical conversion of B for this system is 0.0258. The weight-average molecular weight of the pre-gel aggregates is very close to that of the gel system due to the low weight fraction and low molecular weight of the chromium trimer. However, due to its high molar fraction, the contribution of chromium trimer to number-average molecular weight of the gel system is dominant, resulting in M_n having a much lower value than $M_{n\text{-}agg}$. It is also noted that the initial weight average and number average molecular weights for the pre-gel aggregates are the same (zero conversion) since the polymer was assumed to be mono-dispersed.

Table 2.3 – Comparison of molecular weight averages for the gel system and the pre-gel aggregates.

Conversion	M_w (g/ mole)	$M_{w\text{-}agg}$ (g/ mole)	M_n (g/mole)	$M_{n\text{-}agg}$ (g/ mole)
α_B	Gel system	Pre-gel aggregates	Gel system	Pre-gel aggregates
0	5.15×10^6	5.26×10^6	7166	5.26×10^6
0.005	5.35×10^6	5.47×10^6	7239	5.36×10^6
0.01	6.06×10^6	6.19×10^6	7312	5.69×10^6
0.015	7.77×10^6	7.94×10^6	7388	6.33×10^6
0.02	1.29×10^7	1.31×10^7	7465	7.52×10^6
0.025	8.12×10^7	8.29×10^7	7543	9.90×10^6

The calculated weight-average molecular weight of pre-gel aggregates was compared with experimental data of the weight-average molecular weight determined by a multi-angle laser

light scattering (MALLS) detector [Willhite *et al.*, 2003] in Figure 2.2 for a gel system prepared from 5000 ppm AlcoFlood935, 7158V and 100 ppm chromium trimer. The model calculations were fitted to the MALLS data by adjusting the scale of reaction time axis in relation to the conversion axis. The calculated number-average molecular weight of pre-gel aggregates is also shown in Figure 2.2. Both the weight-average and the number-average molecular weights increase slowly during the low conversion range or initial stage of the gelation process. As the reactions continue, the weight-average molecular weight increases at a faster rate indicating an increase of the polydispersity of the pre-gel aggregates. As the critical conversion of 0.0258 is approached, the weight-average molecular weight increases dramatically and diverges to infinity, while the number-average molecular weight only about doubles in value.

Viscosity as a function of time for the same gel system is shown in Figure 2.3 along with the modeled weight-average molecular weight vs. conversion of chromium functionalities. Adjustment of the reaction time in relation to the conversion of B is the same as in the previous figure. The development of the viscosity and the weight-average molecular weight are similar, increasing slowly in the initial stage, then increasing sharply near the gel time or critical conversion. During the gelation process, the larger the molecules become, the higher their expectancy for participation in further crosslinking by virtue of their high number of functionalities. That is, larger pre-gel aggregates are increasing in size faster than the small aggregates since the larger aggregates have more reaction sites. The rapid development and growth of large molecules as the critical conversion is approached results in an abrupt increase in the viscosity of the gelant (Note the log scale for viscosity in the figure). A relationship between viscosity and the weight-average molecular weight may provide a method to explain the viscosity behavior of gel system quantitatively in future work.

Molecular weight averages of the pre-gel aggregates determined from the model and experimentally determined weight average molecular weights for different gel systems (two polymer lots and two chromium concentrations) are shown in Figures 2.4 – 2.6. The initial conditions (model parameters) were different for each of these systems. The reaction-time scale was adjusted in each figure to match the experimental data with the model results. The adjustment was somewhat arbitrary. The results of the model show a rapid increase in weight average molecular weight that was not observed for the experiment results. The experimental measurements were terminated at about the gel time (determined by viscosity measurements) due to large uncertainty of the results. Large uncertainties in the experimental data are consistent with the presence of very large molecules which would translate to increased values of the weight average molecular weight.

Gel times are compared for each of the gel systems in Table 2.4. The experimental gel time was defined as the time when the viscosity of the gel system abruptly increased to a value greater than 1000 cp. This was determined by periodically removing an aliquot from the gel system and measuring the viscosity. A theoretical gel time was defined as the time that corresponded to the critical conversion (from Figures 2.2 – 2.6) and was dependent on fitting the experimental

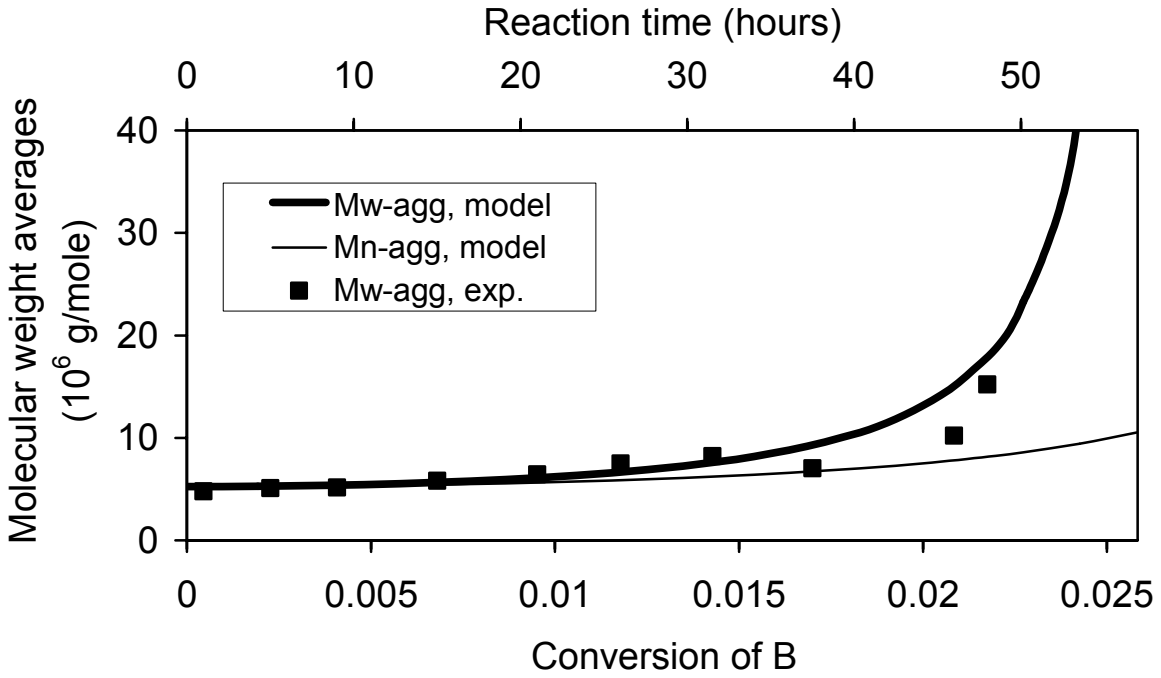

Figure 2.2 – Molecular weight averages of pre-gel aggregates for system containing 5000 ppm AlcoFlood 935 (Lot7158V) and 100 ppm chromium trimer.

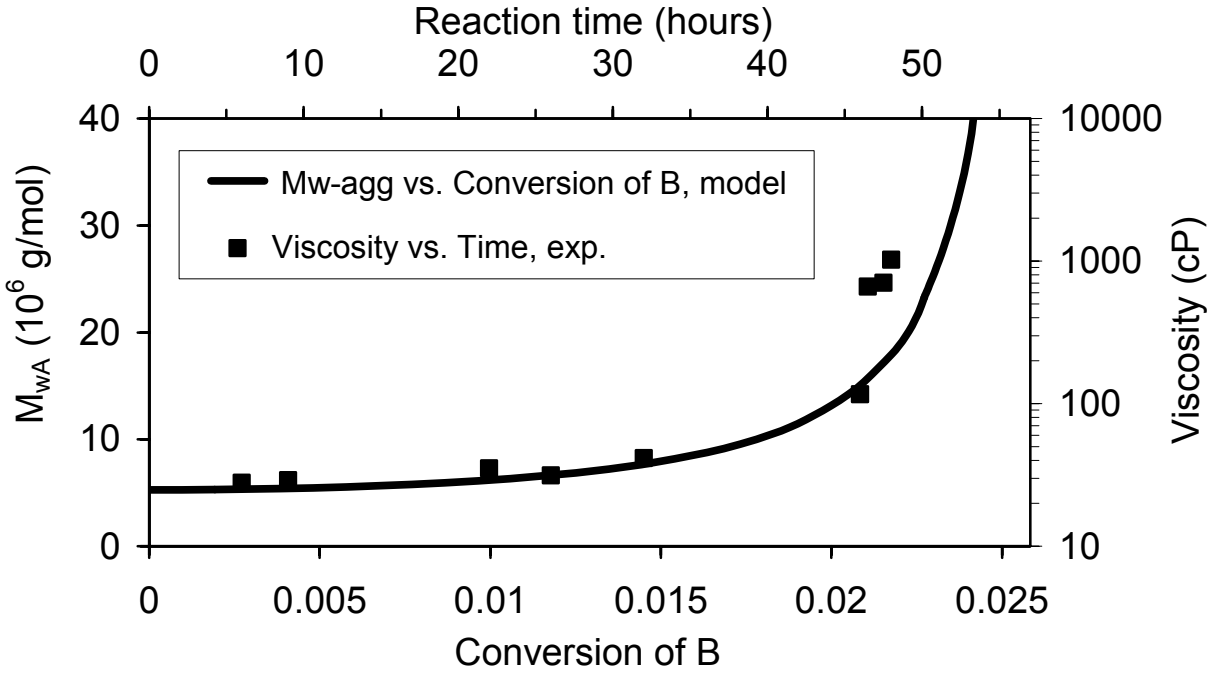

Figure 2.3 – Viscosity vs. reaction time, weight-average molecular weight vs. conversion of chromium functionalities for a gel system containing 5000 ppm AlcoFlood 935, Lot 7158V and 100 ppm chromium trimer).

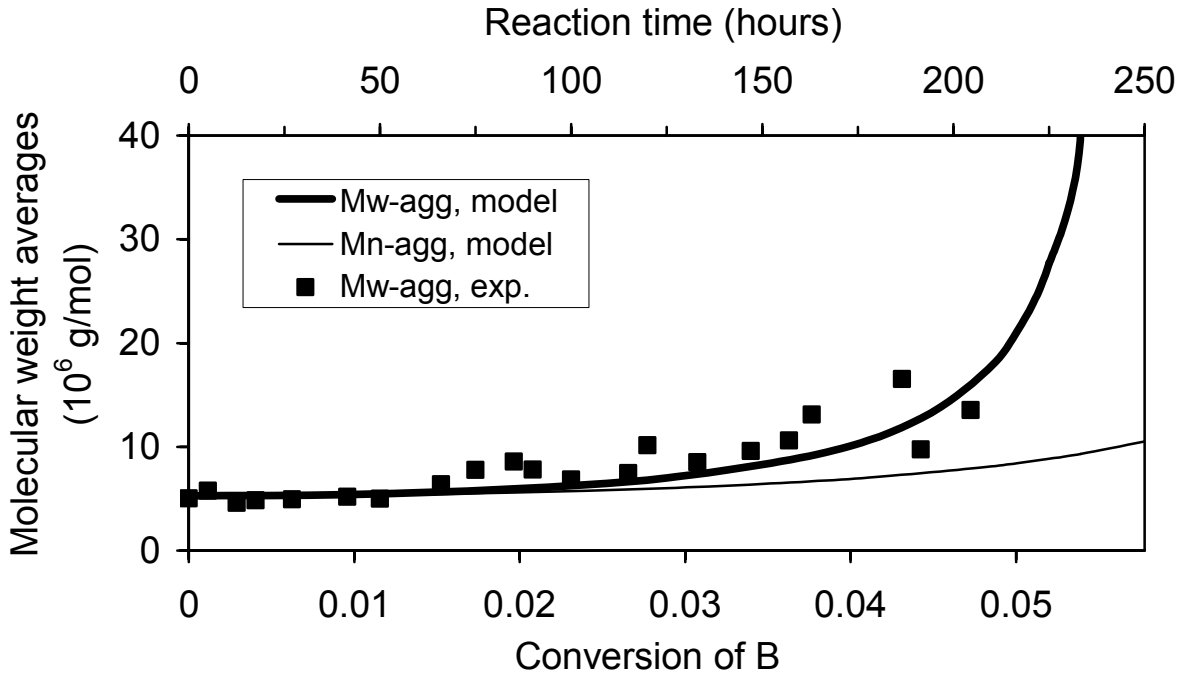

Figure 2.4 – Molecular weight averages of pre-gel aggregates for system containing 5000 ppm AlcoFlood 935 (Lot 7158V) and 20 ppm chromium trimer.

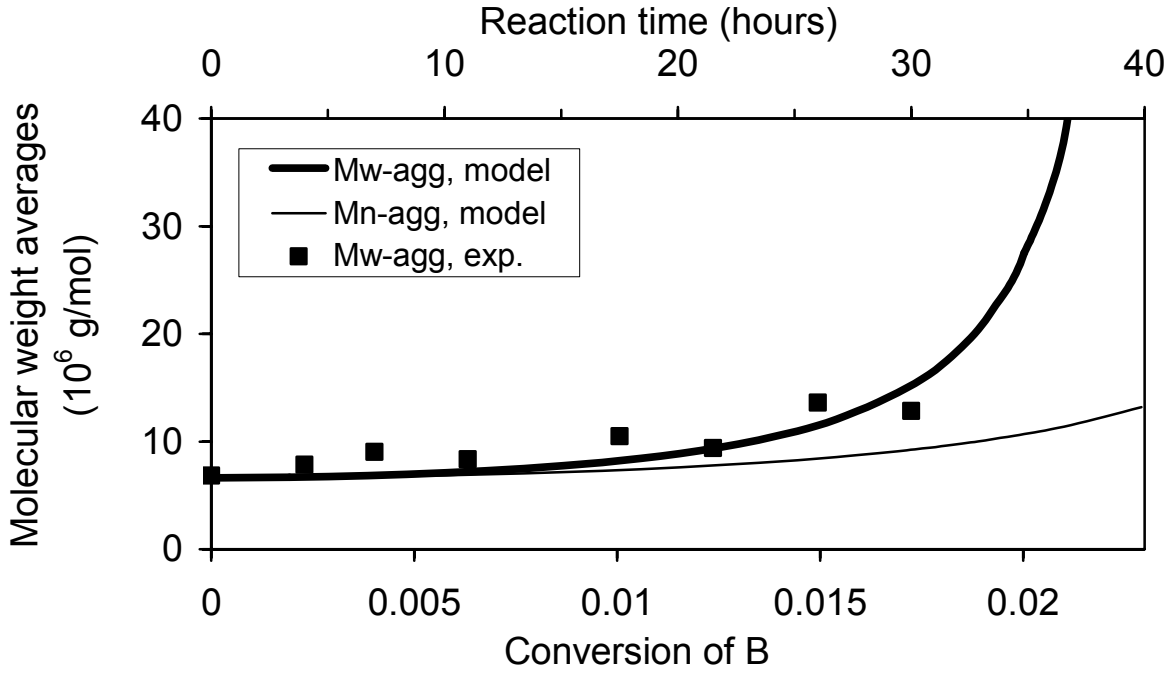

Figure 2.5 – Molecular weight averages of pre-gel aggregates for system containing 5000 ppm AlcoFlood 935 (Lot A2247BOV) and 100 ppm chromium trimer.

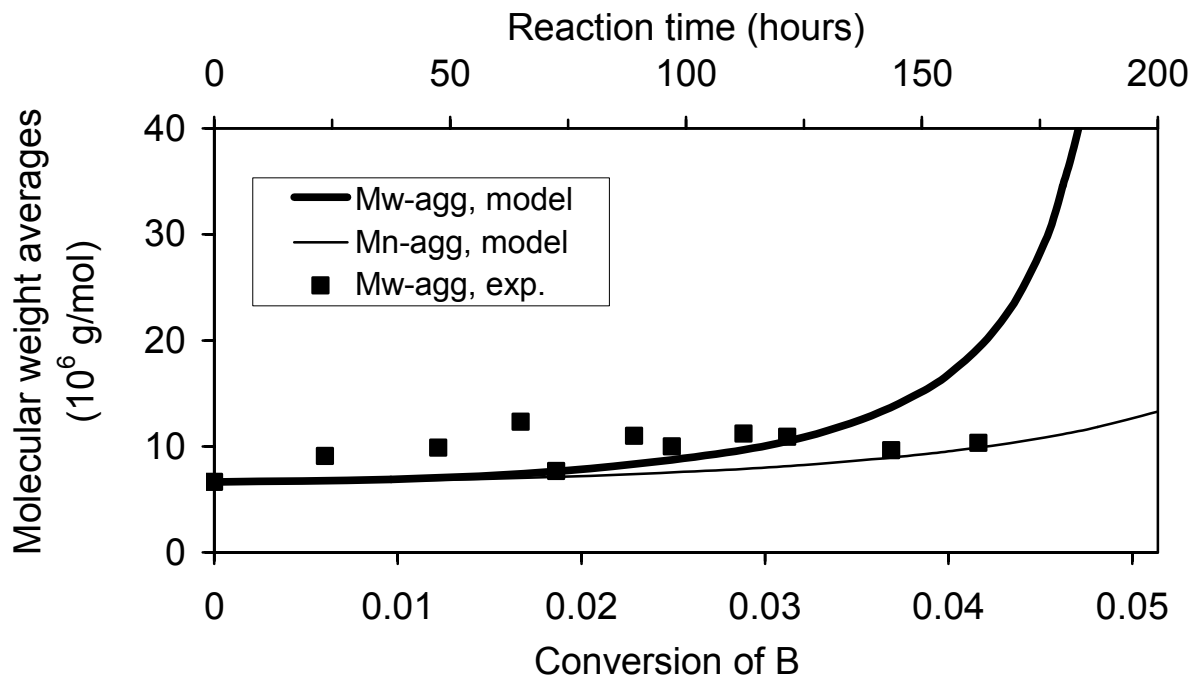

Figure 2.6 – Molecular weight averages of pre-gel aggregates for system containing 5000 ppm AlcoFlood 935 (Lot A2247BOV) and 20 ppm chromium trimer.

MALLS data to the model results. The experimental gel time was approximately 80% of the theoretical gel time for all four gel systems. The theoretical gel time is the time required for the first molecule in the system to attain an *infinite* molecular weight and this condition is suspected to occur sometime after the abrupt increase in viscosity. This might explain why the weight-average molecular weight of pre-gel aggregates determined by MALLS does not show an abrupt increase like the model results, since the MALLS measurements were terminated at the experimental (viscosity) gel time.

Table 2.4 – Experimental and theoretical data of gel time for different gel systems.

Polymer Conc. (ppm)	Cr trimer Conc. (ppm)	Gel time by viscosity (hours)	$\alpha_{crit,\,A}$	$\alpha_{crit,\,B}$	Theoretical gel time corresponding to α_{crit} (hours)
AlcoFlood 935, 7158V					
5000	100	48	0.00671	0.0258	57
	20	200	0.00300	0.0578	250
AlcoFlood 935, A2247BOV					
5000	100	30	0.00597	0.0230	40
	20	160	0.00267	0.0514	200

A kinetic study of the uptake reaction of the chromium acetate trimer with polyacrylamide is presented in Chapter 3 of this report. Chromium uptake was determined by measuring the unreacted chromium concentration in the gel system as a function of time. Results from that study for Series I runs that were conducted at different initial chromium concentrations are given in Table 2.5. The percentage of chromium that had reacted with the polymer (uptake) for each run at different initial chromium concentration is listed. All of the runs were conducted with polymer concentrations of about 5,000 ppm. These experimental results are compared to results of the mathematical model. In the model, the fraction of chromium that has reacted with polymer is given by the sum of b_1 and b_2, which are the coefficients in the pgf of Equation 2.35. b_1 and b_2 are the fractions that have 1 and 2 reacted functional groups, respectively. The values of b_i are given in terms of conversion by Equation 2.15. The critical conversion of B (chromium trimer, Equation 2.68) and the values of b_i at the critical conversion are given in Table 2.5 for each of the experimental runs. A comparison of the value of $(b_1 + b_2)$ % to the experimental uptake data is shown in Figure 2.7. The comparison indicates a proportional relationship with the experimental data about 4 times greater than the values calculated by the model. The difference between the experimental and calculated values is in part due to the assumption of no intra-molecular crosslinking (cyclization) in model. Intra-molecular crosslinking consumes carboxylate groups and unreacted chromium trimer without increasing the molecular weight.

Table 2.5 – Reaction states of chromium trimer at gel time/conversion for gel systems prepared from 5000 ppm AlcoFlood 935, A2247BOV and various initial chromium concentrations; degree of hydrolysis of 10% was assumed.

Chromium Conc. (ppm)	Chromium uptake at gel time (Exp) (%)	$\alpha_{crit,\,B}$ (model)	$b_0 = (1-\alpha)^2$ (%)	$b_1 = 2(1-\alpha)\alpha$ (%)	$b_2 = \alpha^2$ (%)	Chromium uptake at $\alpha_{crit,\,B}$ b_1+b_2 (%)
252	16	0.0145	97.11	2.87	0.02	2.89
201	18	0.0163	96.77	3.20	0.03	3.23
150	20	0.0188	96.28	3.68	0.04	3.72
101	22	0.0230	95.45	4.49	0.05	4.55
75	26	0.0266	94.76	5.17	0.07	5.24
51	36	0.0325	93.60	6.29	0.11	6.40
21	49	0.0514	89.98	9.75	0.26	10.02

Future Work

The model developed here with simplifying assumptions of mono-dispersed polymer and no intra-molecular crosslinking generally describes some of the features of the crosslinking process of polyacrylamide by chromium acetate and warrants further exploitation. It is planned to incorporate in the model distributions for molecular weight and functionality of the polymer precursor and to take into account intra-molecular crosslinking which is expected to be an important feature. It is also planned to develop mathematical procedures to determine molecular

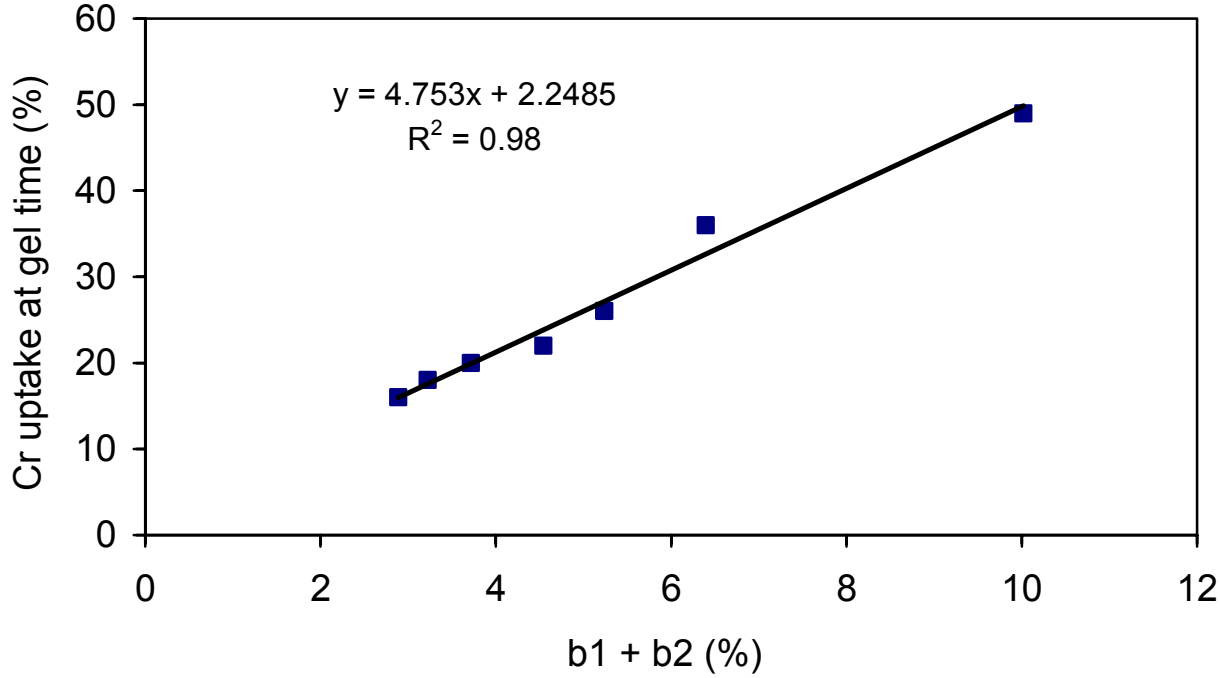

Figure 2.7 – Comparison of experimental and modeled chromium uptake data (AlcoFlood 935, A2247 BOV, 5000 ppm and various initial chromium concentrations).

weight distributions, in addition to molecular weight averages, as a function of conversion. Relationships between conversion and time will be developed by matching/correlating the model to experimental data. Types of experimental data that will be determined include molecular weight distributions, gel times by viscosity measurements and rheological parameters such as the storage and loss moduli. These data will also be used to verify the mathematical model(s).

Nomenclature

a_i, b_i	–	Number (or molar) fraction of precursor A with i reacted functional groups, $i = 0 \sim f_A$. Fraction based on total (or initial) number of units of precursor A only. This number fraction is equivalent to the weight fraction for precursor A. Similar definitions for b_i.
f_A, f_B	–	Functionalities of precursor A (polymer) and precursor B (chromium trimer), respectively.
n_A, n_B	–	Initial number (or molar) fractions of precursor A (polymer) and precursor B (chromium trimer), respectively. Fractions based on the initial number (or moles) of precursor A and of precursor B.
n_i	–	Number (or molar) fraction of molecules with molecular weight of M_i at a given conversion. Fraction based on total number of molecules of the entire gel system at the same conversion.
n_1	–	Number fraction of unreacted chromium trimers at a given conversion. Fraction based on the total number of molecules at the same conversion.
p_0, p_1	–	Probabilities of finding an unreacted and a reacted functional group in the system, respectively. Also equals the number fraction of unreacted

and reacted functional groups, respectively.

r_A	–	Initial number (or molar) ratio of A functionalities (carboxylate groups) to B functionalities (chromium functionalities).
w_A, w_B	–	Initial weight fractions of precursor A (polymer) and precursor B (chromium trimer), respectively. Fraction based on total weight of precursor A (polymer) and precursor B (chromium trimer).
w_i	–	Weight fraction of molecules with molecular weight of M_i. Fraction based on total weight of molecules of the entire gel system (total weight of polymer and chromium trimer).
w_1	–	Weight fraction of unreacted chromium trimer at a given conversion. Fraction based on total weight of molecules of the entire gel system (total weight of polymer and chromium trimer).
z	–	A vector, $\mathbf{z} = (z_A, z_B)$, auxiliary variables in pgf.
M_A, M_B	–	Molecular weight of precursor A (polymer) and precursor B (chromium trimer), respectively.
M_i	–	Molecular weight of molecules with weight fraction w_i or number fraction n_i.
M_n	–	Number-average molecular weight of the entire gel system.
$M_{n\text{-}agg}$	–	Number-average molecular weight of pre-gel aggregates.
M_w	–	Weight-average molecular weight of the entire gel system.
$M_{w\text{-}agg}$	–	Weight-average molecular weight of pre-gel aggregates.
P_n	–	Number-average degree of polymerization.
P_w	–	Weight-average degree of polymerization.
α_A, α_B	–	Conversions of functionalities on precursor A (carboxylate groups on polymer) and functionalities on precursor B (chromium functionalities), respectively.

References

1. Dusek, K.: "Formation-Structure Relationships in Polymer Networks", *Br. Polym. J.*, 17 (1985), 185-189.
2. Dusek, K.: "Network formation in curing of epoxy resins", *Adv. Polym. Sci.,* 78 (1986), 1-57.
3. Dusek K. and Duskova-Smrckova, M.: *Crosslinking and Polymer Networks*, DTW Associates Course (2002).
4. Flory, P.J.: *Principles of polymer Chemistry*, Cornell University Press, Ithaca, New York (1953).
5. Good, I. J.: "The Joint Distribution for the Sizes of the Generations in a Cascade Process," *Proc. Camb. Phil. Soc.,* 51 (1955), 240-242.
6. Gordon, M. "Good's Theory of Cascade Processes Applied to the Statistics of Polymer Distributions," *Proc. Roy. Soc., London,* A268 (1962), 240-256.
7. Huybrechts, J. and Dusek, K.: "Star oligomers with different reactivity in low VOC polyurethane coatings: Part III", *Surface Coating International*, 5(1998), 234-239.
8. Tackett, J. E.: "Characterization of Chromium(III) Acetate in Aqueous Solution", *Applied Spectroscopy*, 43 (1989), No. 3, 490-499
9. Willhite, G. P., Green, D.W. and McCool, C.S.: "Increased oil recovery from Mature Oil Fields using Gelled Polymer Treatments," Annual Report for June, 1999 - June 2002, Report No. 99BC15209-5, Contract No. DE-AC26-99BC15209, US DOE (2003).

Chapter 3

Kinetic Study of the Chromium(III) Acetate – Hydrolyzed Polyacrylamide Uptake Reaction

Graduate Research Assistant: Rajeev Jain

Introduction

The application of crosslinked-polymers gels for permeability modification of petroleum reservoirs has been effective to improve displacement efficiency, increased crude oil production and to reduce water production. The treatment of an injection well consists of injecting an aqueous solution containing polymer and a crosslinker into the high permeability zones or fractures of the reservoir which have been previously swept by displacing fluid. The polymer reacts with the crosslinker in situ to form a three dimensional gel network, reducing the effective permeability of these zones. The displacing fluid injected after the treatment is diverted into the low permeability, oil-bearing zones resulting in additional oil recovery. Gels are also applied in production well to reduce water production.

One widely used gel system is an aqueous solution of partially hydrolyzed polyacrylamide and a chromium(III) salt . Chromium(III) forms a complex ion in solution and reacts with polymer molecules to form crosslinks resulting in a network or gel. Chromium acetate is a preferred crosslinker due to its relative inertness to reservoir conditions and relatively long gel times as compared to inorganic chromium salts.

The rates of the reactions between chromium and the polymer control the development of the network structure which, in turn, controls the injection time or distance that a gelant/gel can be place from a wellbore. Kinetic models of the reactions involved provide a basis for treatment design and placement strategies. The objective of this study was to determine the rate of the reaction between Cr(III) and polyacrylamide when the chromium is supplied as the acetate salt. This reaction, often referred to as the uptake reaction, is known to be a function of reactant concentrations, salinity, temperature, and solution pH. An experimental approach was based on the use of a centrifugal filter device to separate solvent from the gelant. The solvent was analyzed for unreacted chromium. A reaction rate model for chromium uptake was developed.

Background

Partially hydrolyzed polyacrylamides (HPAM) are crosslinked by chromium(III) to form gels. HPAM is a linear polymer with amide and carboxylate side groups. The fraction of carboxylate side groups is described as the degree of hydrolysis, usually stated as a percentage value. The degree of hydrolysis for HPAMs used to form gels ranges between 5 and 20 %. Gel times are shorter (faster reaction rates) with increased carboxylate content of the HPAM. The general consensus of several investigations is that chromium(III) reacts with the carboxylate group on the polymer. Chromium(III) forms complex ions in solution often with several structures of varied complexity depending on the ligands existing in the solution. Generally, the reaction between the Cr(III) complex ion and HPAM is a ligand exchange reaction. A description of this reaction is given by Equation 3.1 [Albonico et al., 1993].

$$Cr(L)_n + m\ P\text{-}CO_2^- \Leftrightarrow Cr\ (P\text{-}CO_2^-)_m\ (L)_{n-m} + m\ L \qquad \text{Eq. 3.1}$$

In Equation 3.1, L represents a ligand forming a coordinate bond with chromium, such as an acetate ion, a water molecule or a hydroxyl group. $P\text{-}CO_2^-$ represents one carboxyl group on a polyacrylamide molecule. The ligand exchange reaction occurs through associative interchange where the bond between the Cr(III) complex and the entering ligand is partially formed before the bond with the leaving ligand is broken. The extent to which ligand exchange occurs depends on the relative replacement tendencies of the entering and leaving ligand, the relative concentration of reactants, and the length of time [Hunt, 1987]. Several authors have rated the replacement power of anions. Udy [1956] gives the following list of anions where the relative replacement power for nitrate is lowest and power increases through the list to oxylate. (Anions to the right will replace those to the left.)

$$NO_3^- < Cl^- < SO_4^{2-} < HCOO^- < CH_3COO^- < SO_3^- < C_2O_4^-$$

weakest Strongest

Rollinson [1956] placed glycolate, tartarate, and citrate, between acetate and oxolate, in that order. A study of effective gelation delaying ligands for Cr(III)-HPAM gels by Burrafato et al. [1990] indicated that replacement power of carboxyl group on polyacrylamide is between that of acetate and citrate.

Gels are formed by building a 3D network that is accomplished by crosslinking the polymer molecules. A crosslink is formed when carboxylate groups from two HPAM molecules react with one Cr(III) complex ion. These reactions are described by Equations 3.2 and 3.3.

$$Cr(L)_n + P1\text{-}CO_2^- \rightarrow Cr(L)_{n-1}(P1\text{-}CO_2^-) + L \qquad \text{(uptake)} \qquad \text{Eq. 3.2}$$

$$Cr(L)_{n-1}(P1\text{-}CO_2^-) + P2\text{-}CO_2^- \rightarrow (P2\text{-}CO_2^-)Cr(L)_{n-2}(P1\text{-}CO_2^-) + L \qquad \text{(crosslink)} \qquad \text{Eq. 3.3}$$

P1 and P2 represent different polymer molecules in these equations. The first reaction of a polymer (P1) with the chromium complex is commonly called the uptake reaction. The reaction of a second polymer (P2) with the chromium complex creates a crosslink between the polymers and is termed the crosslink reaction.

Several investigations have been conducted on the gelation reactions when using inorganic salts of Cr(III), such as $CrCl_3$ or $Cr(NO_3)_3$. Hunt [1987] reported that gelation occurred up to a pH value of 5.8. Visible precipitation of Cr(III) was observed at higher pH values. Lockhart [1991] in his chemical and structural studies on Cr(III)-HPAM gels concluded that gelation occur at pH ≤ 5.3 where Cr(III) was present in soluble molecular form and that at pH values greater than 7, Cr(III) forms insoluble colloids and the polymer solution remains fluid indicating no gelation. For the pH interval between 6.1 and 6.6, gelation occurred but the solution was turbid indicating presence of some colloidal Cr(III). These results showed that Cr(III) precipitation is a competitive reaction to the uptake and crosslink reactions when the pH of the solution is above about 5.5 and the solutions contains typical chromium concentrations of about 150 ppm.

Precipitation is relatively rapid in solutions prepared with inorganic chromium salts. The precipitation of chromium is described by Equation 3.4.

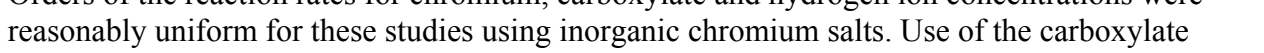

$$Cr^{+3} + 3\ OH^{-} \rightarrow Cr(OH)_3\ (\text{precipitate}\downarrow) \qquad \text{Eq. 3.4}$$

Kinetics of Cr(III)-carboxyl uptake reaction using inorganic chromium salts has been investigated. Experimental conditions and results of these studies are summarized in Tables 3.1 and 3.2 [Dona, 1993]. Several techniques to follow the Cr(III)-carboxyl reaction were used. Hamm et al. used polarography to characterize the reactions of Cr(III). Banarjea and Chaudhuri, and Montanari et al. employed UV spectroscopy. Hunt [1987] and Dona [1993] used the method of equilibrium dialysis to separate unreacted chromium from diluted gel sample and measured chromium concentration by either atomic absorption spectrophotometry or UV absorption. Orders of the reaction rates for chromium, carboxylate and hydrogen ion concentrations were reasonably uniform for these studies using inorganic chromium salts. Use of the carboxylate concentration in the rate equations implied or assumed that the carboxylate group is the reactive site on HPAM.

Table 3.1 - Cr(III) and carboxyl source and experimental conditions.

Study	Cr(III) source	Carboxyl source	Brine salt	pH	T ^{o}C
Hamm et al.	$Cr(NO_3)_3$	glycolic acid ($HOCH_2CO_2H$)	$KClO_4$ or KNO_3	3.5 – 6.0	25
Banerjea and Chaudhuri	$Cr(ClO_4)_3$	Glycine ($H_2NCH_2CO_2H$)	$NaClO_4$	3.0 – 3.8	40
Khan and Kabir-Ud-Din	$Cr(NO_3)_3$	Glycine	KNO_3	3.4 – 4.5	45
Hartley	$CrCl_3$	Carboxyl group on wool protein	KNO_3	1.7 – 2.5	93
Hunt	$Cr(NO_3)_3$	PAAm(2.3 mole% carboxyl)	KNO_3	4.0 – 5.5	25
Montanari et al.	$Cr(NO_3)_3$	PAAm(7.5 mole% carboxyl)	$NaClO_4$	4.2 – 4.9	20
Dona	$Cr(NO_3)_3$	PAAm(2.3 mole% carboxyl)	$NaClO_4$	4.0	25

Gelation behavior of HPAM with organic salts of chromium is different than with inorganic chromium salts. Gel times for HPAM with organic and inorganic chromium salts were determined as a function of pH by Lockhart [1991]. Gel times for the inorganic salt (hydrated Cr^{+3}) decreased sharply with increase in pH of the solution. The influence of pH on the gel times for the organic salt (chromium acetate) was much less. Additionally, the gel times for the chromium acetate system in the pH range between 4 and 6, typical application values, are significantly longer than for the inorganic chromium salt. The longer gel times for the acetate system allow for longer injection times in field applications.

Table 3.2 - Comparison of reaction orders for Cr(III), carboxyl and H^+.

Study	Cr(III) reaction Order	Carboxyl reaction order	H^+ reaction order
Hamm et al.	+1	0	-1
Banerjea and Chaudhuri	+1	+1	-1
Khan and Kabir-Ud-Din	Cr(III) held constant	+1	-1
Hartley	+1	+1	not determined
Hunt	+1.32	+0.8	-1
Montanari et al.	+1	+0.8	-0.8
Dona	+1	+1	-1

Acetate delays gelation due to its stronger affinity as a ligand in the chromium complex ion as compared to systems prepared with inorganic salts of chromium where the ligands are inorganic anions or water molecules. The structure of chromium acetate also affects its reactivity with the carboxylate groups on HPAM. The structure of chromium acetate in solution is affected by the pH, the age of the solution and the ratio of acetate to chromium. Tackett [1990] used several techniques to characterize chromium acetate in solution under variety of conditions. Tackett found that at pH values below 4.5, an acetate-to-chromium ratio of 3:1 and after sufficient time, green cyclic chromium trimer (shown in Figure 3.1a) was the dominant species in a solution. As the pH of the solution is increased using a base, hydroxyl groups starts replacing the bridging acetate group. The cyclic structure is retained up to pH 5.5. Further increase in pH converts the cyclic trimer to linear trimer (Figure 3.1b) with two bridging acetate groups, four bridging hydroxyl group and a bidentate acetate group on each end. Depending on pH, there exists an equilibrium between the cyclic trimer and linear trimer with different degrees of hydroxyl substitution. Additional increase in pH causes the precipitation of the complex. The trimer species were the dominant structures. However, other structures were indicated including chromium oxylate in the commercial product from McGean-Rohco, the source of chromium acetate used in this work.

Experimental Materials and Procedures

Experiments were conducted to determine the effect of chromium concentration, polymer concentration and pH on the reaction of chromium acetate and HPAM (uptake reaction) in aqueous 1.0% KCl solvent at a temperature of 25°C. The reaction was followed by determining the concentration of unreacted chromium in the solvent as a function of time. Solvent was separated from an aliquot of the reacting gelant using a centrifugal filtration device. A reaction rate model of HPAM-Cr(III) uptake reaction was developed through regression of the experimental data.

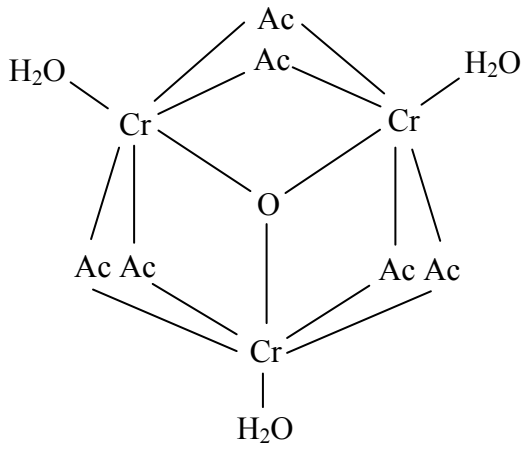

(a) Cyclic form.

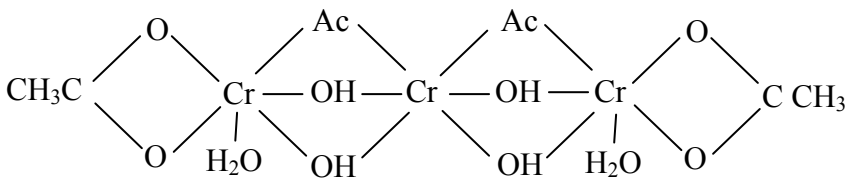

(b) Linear form.

Figure 3.1 - Structures of chromium acetate trimers given by Tackett [1990].

Gelants were prepared by mixing water and stock solutions of HPAM, chromium acetate and sodium azide. Sodium azide was used as a bactericide at a concentration of 10 mg/kg in the gelant. The pH was measured and sometimes adjusted with drops of solutions of HCl or KOH. Gelants were kept at 25°C by a temperature-controlled water bath. Samples were removed periodically for viscosity and pH measurements and for analyses of unreacted chromium. For chromium analysis, solvent was removed from the sample with a Centricon® Plus-20 Centrifugal Filter Device (Millipore Corp.) rated at a 5,000 nominal molecular weight cutoff (MWCO). The centrifugal filters were cleaned (spun with water) before use to remove trace amounts of glycerine that is used as a humectant. The samples were rotated in a swinging bucket (radius of 9 cm) at 2700 rpm for 15 minutes. The filtration force was approximately 730 g. The volume of filtrate decrease with longer reaction times. The mass of filtrate and retentate were measured. Chromium concentrations were determined for the filtrate, retentate and for the original gelant charged to the filter device. Chromium material balances showed that the amount of chromium removed after the centrifugation was usually within 2% of the chromium initially charged. TOC measurements were conducted on the filtrate to estimate the amount of polymer that passed through the centrifugal filter devices.

Chromium concentrations were determined by oxidizing Cr(III) to Cr(VI) and measuring the absorbance with a UV-VIS spectrometer at a wavelength of 373nm and applying a calibration curve. Oxidation of the chromium was accomplished by combining equal portions of the sample, 3% hydrogen peroxide and 1N KOH solutions and heating the mixture for an hour at 87°C. The oxidized samples were diluted to chromium concentrations between 5 and 10 ppm for absorption measurement. Relative standard deviations of less than 0.1% were typical for eleven measurements.

Polymer concentrations were determined in the polymer stock solutions and in the filtrate from the centrifugal devices by determining the concentration of the total organic carbon (TOC). A Shimadzu-5000(A) TOC analyzer was used and calibrated with potassium hydrogen phthalate standards of known carbon concentrations and then calibrated with polymer standards that were prepared from the solid polymer. No provision was made for the active amount of polymer in the weighed solid samples. The determination of polymer concentrations in samples containing chromium (e.g. filtrates from the centrifugal filter devices) was complicated by the presence of additional carbon from acetate that was introduced with the chromium. In those cases, it was assumed that the molar concentration of acetate was 3.0 times the molar concentration of chromium (measured values) and the TOC measurements were adjusted to account for the acetate for the determination of polymer concentrations. The molar ratio of acetate to chromium was verified by TOC measurements on chromium acetate solutions.

A Brookfield digital viscometer (Model DV- I +) was used to monitor the viscosity and determine the gel time of the gelants. The gel time was defined as the time when the viscosity of the gel solution increases abruptly to a value greater than 1,000 cP at a shear rate of 2.25 s^{-1}. The temperature of the viscometer was controlled at 25°C.

Stock Solutions. Polymer stock solutions were prepared at concentrations of 10,000 mg/kg polyacrylamide (Alcoflood 935, Lot # A2247 BOV) and 2.00 wt.% KCl in water. (Polymer stocks with alternate KCl concentrations were prepared for gelants with polymer concentrations other than 5,000 mg/kg.) Solid polymer beads were added gradually to the vortex shoulder of the stirred, cold 2.0 % KCl solvent. The container was sealed and the mixture stirred for 3 days for complete dissolution of the polymer. The polymer solution was slightly cloudy after dissolution. The polymer solution was then pressure filtered through a glass fiber filter (1 micron pore size) at 10 psi. The filtered polymer solution was clear. The solution was then dialyzed exhaustively in 12,000-14,000 MWCO pore size regenerated cellulose membrane tubing against KCl solvent of the same KCl concentration. The dialysis removed the low molecular-weight polymers in order to minimize the amount of polymer that would pass through the centrifugal filter device. The solvent-to-polymer solution ratio for the dialysis was approximately 30:1 by volume. The solvent was stirred continuously at low speed and was changed each day for three days. Carbon concentration was measured in each solvent batch. No carbon was detected in the solvent (dialysate) removed from the second and third batch. The polymer concentration in the dialyzed solution was determined as described above.

Chromium stock solutions at concentrations of 500 mg/kg or 1000 mg/kg were prepared by diluting an aqueous solution of 50% chromium(III) acetate (McGean Rohco, Inc.; Lot # 40086816) with water. Aqueous stock solutions of sodium azide were prepared at a

concentration of 1,000 mg/kg. Water purified by reversed-osmosis, filtration, and deionization (> 18 MΩ-cm) was used in all solutions.

Solution preparation was conducted on a weight basis. Concentration units of mg/kg, or ppm, represent the mass of a component per mass of the solution. Density of a gelant containing 5,000 mg/kg HPAM, 200 mg/kg chromium (acetate salt) and 1.0 wt.% KCl was 1.0054 g/mL at 25°C.

The Kinetic Model and Data Processing

The uptake reaction of chromium by HPAM was followed by determining and mathematically modeling the concentration of unreacted chromium in the gelant. The uptake reaction was assumed to be a reaction between a chromium trimer complex (cyclic or linear form) with the carboxylate group on the HPAM. Stoichiometry of the reaction was represented by Equation 3.5.

$$Cr_3 \quad + \quad CO_2^-\text{-P} \quad \rightarrow \quad Cr_3\text{-}CO_2^-\text{-P} \qquad \text{Eq. 3.5}$$

chromium trimer ion — *carboxylate group on HPAM* — *product*

Based on Equation 3.5, the rate expression for the disappearance of the unreacted Cr(III) trimer in the gelant is given by Equation 3.6.

$$r_{Cr3} = -\frac{dC_{Cr3}}{dt} = k\,\frac{C_{Cr3}^{a}\;[(C_{carb})_0 - ((C_{Cr3})_0 - C_{Cr3})]^b}{C_H^c} \qquad \text{Eq. 3.6}$$

where,

- C_{cr3} = concentration of unreacted chromium trimer, moles/kg,
- C_{carb} = concentration of unreacted carboxylate groups, moles/kg,
- C_H = concentration of hydrogen ion, moles/kg,
- k = reaction rate constant,
- a,b,c = reaction orders with respect to chromium trimer, carboxylate groups and hydrogen ion,
- 0 = subscript denoting initial concentration.

Data from the series of experimental runs were processed and applied in Equation 3.6 to regress values of the reaction rate constant, k, and the reaction orders, a,b and c. Data was processed by the following procedures and assumptions.

The pH of the gelant was measured and the chromium concentration in the filtrate from the centrifugal device was determined at selected reaction times during a gelation experiment. Polymer concentration in the filtrate was also determined since it was found that small amounts of polymer passed through the filter. Chromium concentrations measured in the filtrate were corrected for the amount of chromium that was attached, or reacted with, the polymer. Measured chromium concentrations were converted to unreacted chromium trimer concentration by Equation 3.7.

$$C_{cr3} = (6.41\times10^{-6} \text{ moles trimer/mg chromium})\, C_{Cr\,S}\, \{1-[1-(C_{Cr\,F}/C_{Cr\,S})]/[1-(C_{P\,F}/C_{P\,S})]\} \quad \text{Eq. 3.7}$$

where C_{Cr3} = concentration of un-reacted chromium trimer, moles/kg,
$C_{Cr\,S}$ = concentration of chromium in gelant, mg/kg,
$C_{Cr\,F}$ = concentration of chromium in filtrate, mg/kg,
$C_{P\,F}$ = concentration of polymer in filtrate, mg/kg,
$C_{P\,S}$ = concentration of polymer in gelant, mg/kg.

Equation 3.7 was derived from a material balance on chromium and polymer in the centrifugal filter device due to the chromium that passed through the filter by being attached/reacted with the polymer that passed through the filter. Assumptions used in the material balance were (1) the concentrations of unreacted chromium in the filtrate and gelant were equal, and (2) the mass ratio of reacted chromium to polymer was equal in the filtrate and gelant. Derivation of the material balance is given in the appendix.

The derivative term in Eq. 3.6, $d\,C_{cr3}/dt$, was determined by curve-fitting Eq. 3.8 to the C_{Cr3} – time data using the Levenberg-Marquardt method (Polymath software). The regressed coefficients, A and B, were use to calculate the derivative by Equation 3.9.

$$C_{cr3} = A\, e^{Bt} \quad \text{Eq. 3.8}$$

$$d\,C_{cr3}/dt = A\,B\,e^{Bt} \quad \text{Eq. 3.9}$$

Hydrogen ion concentrations, C_H, were calculated from the measured pH values according to Equation 3.10.

$$C_H = 10^{-pH} \quad \text{Eq 3.10}$$

Equation 3.6 gives the carboxylate concentration, C_{carb}, as $[(C_{carb})_0 - ((C_{Cr3})_0 - C_{Cr3})]$, where the C_{carb} decreases with reaction with the chromium trimer on a mole-to mole basis. No provision was provided for reduction of C_{carb} due to the crosslinking reaction. The initial carboxylate concentration, $(C_{carb})_0$, was determined from the initial polymer concentration (measured by the TOC method described above), a degree of hydrolysis of 10% (measured in-house by a titration method [Michnick, 2003]) and assuming sodium was the cation of the carboxylate group in the solid polymer.

Processed data at each measurement time for all of the runs were regressed to determine the rate constant and the reaction orders of Equation 3.6. The regression was performed with Polymath software using the Levenberg-Marquardt method.

The kinetic model, Equation 3.6 with the regressed parameters, was integrated numerically to give unreacted chromium trimer concentrations as a function of time for each run. The model values were plotted with the data to assess the model fit. To accomplish the numerical integration, the pH data of each run were curve fitted to various functions of time to provide hydrogen ion concentrations at each time step of the integration. The RK-56 method in Polymath was used for the integration.

Results and Discussion

Three series of runs were conducted to determine the effects of initial concentration of chromium (acetate salt), initial concentration of HPAM and initial pH on the rate of reaction between chromium acetate and HPAM. Gelant compositions and the gel time determined by viscosity measurements are show in Table 3.3. Concentrations in the table are given by the commonly used weight/weight units. Wide ranges of chromium and HPAM concentrations were studied in Series I and II. The pH range in Series III was limited to an upper value of 5.5 due to difficulty in maintaining a stable pH at higher values.

Table 3.3 – Gelant composition, gel time and amount of chromium reacted at gel time.

Series	Gelant Compostion*			Gel Time (h)	Cr Uptake at gel time (mg/kg)	pH at gel time
	Cr (mg/kg)	Polymer (mg/kg)	Initial pH			
I Cr Conc.	252	5410	4.82	18	41	4.75
	201	5010	4.93	19	36	4.86
	150	4900	4.91	25	30	4.84
	100	5040	4.87	31	22	4.85
	101	4860	4.87	31	22	4.84
	102	4980	4.89	33	23	4.87
	75.5	5520	4.88	41	20	4.84
	50.6	5040	4.94	61	18	4.93
	20.7	5000	4.91	140	10.2	4.96
II Polymer Conc.	201	7530	4.92	12	30	4.86
	202	6330	4.92	16	30	4.88
	202	3550	4.90	42	40	4.81
	201	2010	4.94	No gel in 17 days.		4.81
III pH	201	4800	5.51	16	34	5.39
	200	4940	5.22	16	35.5	5.13
	202	4870	4.62	25	34	4.62
	200	4890	4.32	28	31	4.34
	202	4800	4.02	34	33	4.08

* All gelants contained 1.00 wt % KCl.

Gel times for the runs decreased with increased chromium concentration, polymer concentration and initial pH values. Small changes in pH values occurred during gelation as shown by the initial and final values given in Table 3.3. The values of chromium uptake and pH at the gel time (Table 3.3) were determined from lines regressed through the data. Chromium uptake and pH measurements were conducted up to the vicinity of the gel time.

Unreacted chromium trimer concentrations, C_{Cr3} in units of moles/kg, for Series I runs that were conducted with different initial chromium concentrations are shown in Figure 3.2 as a function of time. Regressed lines (Equation 3.8) for each initial chromium concentration are also shown in the figure. Three runs were conducted at an initial chromium concentration of 100 ppm. (C_{Cr3} = 0.641×10^3 g-moles/kg) and one line was regressed using the combined data. The regressed lines were extrapolated and the values of the chromium concentration at zero time were always about 5% lower than the measure chromium concentration in the gelant. No reason was determined for this observation.

Unreacted chromium trimer concentrations, C_{Cr3}, for Series II and III Runs that were conducted with different initial polymer concentrations and initial pH values are shown as functions of time in Figures 3.3 and 3.4 along with the regressed lines. The extrapolated values of chromium concentration at zero time for Series II and III were also about 5% lower than the measure chromium concentration in the gelant.

The rate constant and reaction orders for the equation of the reaction rate were regressed from the data for all the runs in Series I , II and III. The results are given by Equation 3.11.

$$r_{Cr3} = -\frac{\mathrm{d}C_{Cr3}}{\mathrm{d}t} = k\,\frac{C_{Cr3}^{1.01}\;[(C_{carb})_0 - ((C_{Cr3})_0 - C_{Cr3})]^{0.84}}{C_H^{0.39}} \qquad \text{Eq. 3.11}$$

where $k = 6.2 \times 10^{-3}\ \mathrm{h}^{-1}\ (\mathrm{mol/kg})^{-0.46}$

The regression yielded an R^2 of 0.979. Reaction orders for chromium trimer (acetate salt) and polymer (carboxyl group) were approximately one, similar to the reaction orders determined for the reaction of *inorganic* chromium salts with carboxylates (Table 3.2). The reaction order for the hydrogen ion was -0.39. This value was significantly different than the values for systems with inorganic chromium salts (about -1) and corresponded to the weaker dependence pH has on the gelation of systems prepared with chromium acetate (organic salts). This is consistent with the observations made by Lockhart [1991].

Equation 3.11 was integrated numerically for all the runs using the initial conditions except the initial chromium concentrations were reduced by 5% to reflect the observation that the extrapolation of the data to zero time yielded an initial concentration that was about 95% of the measured value. Comparisons of the integration of Equation 3.11 and the data are shown in Figures 3.5 to 3.7.

The amount of chromium reacted at the gel time for each run is listed in Table 3.3 and is plotted in Figure 3.8 for Series I runs as a function of the initial chromium concentration. Less chromium was reacted at the gel time for lower initial chromium concentrations. Only 10 mg/kg of chromium reacted with the polymer at the gel time for the run with the lowest initial chromium concentration of 20 mg/kg showing that less than 10 mg/kg of chromium is required to gel a typical 5,000 mg/kg polymer solution. Data from Series I runs were also correlated in Figure 3.9 where the reciprocal of the gel time is plotted as a function the amount of chromium reacted at the gel time. Extrapolation of the data to an infinite gel time (1/[gel time] = 0) gave a value of chromium reacted of about 5.5 mg/kg, a value indicative of the minimum amount required for gelation.

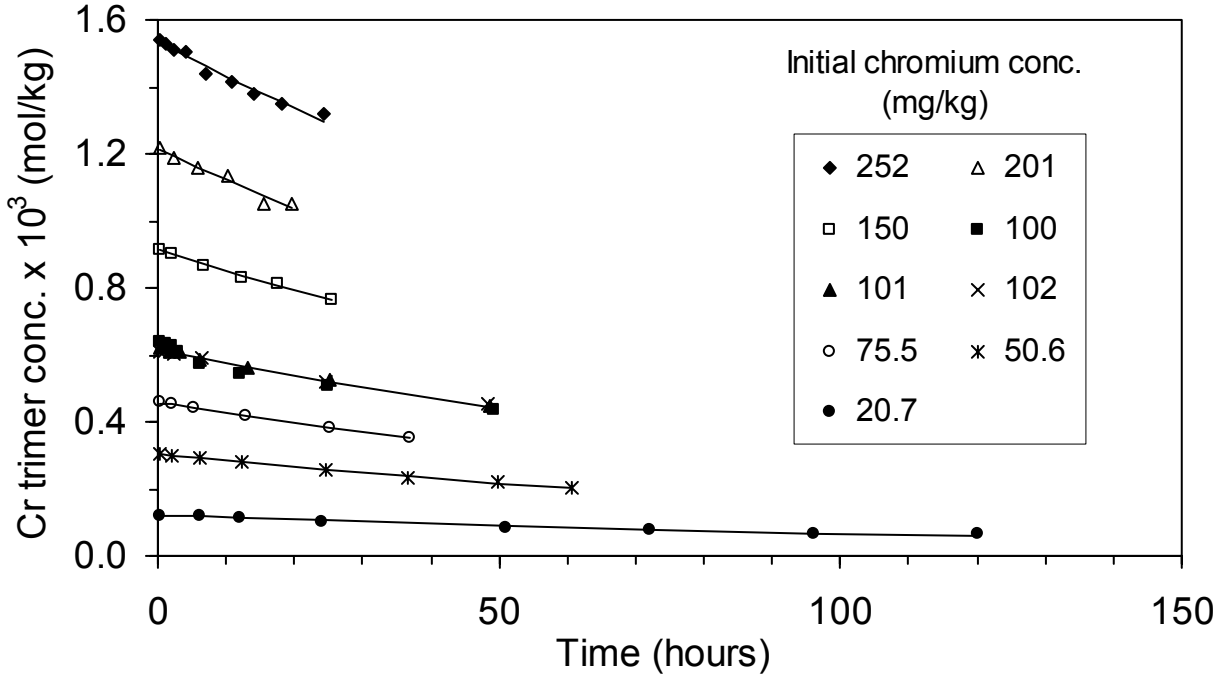

Figure 3.2 – Data and curve fit to unreacted chromium trimer concentration as a function of time for different initial chromium concentrations; ~5000 mg/kg polymer conc. and a pH of ~4.9.

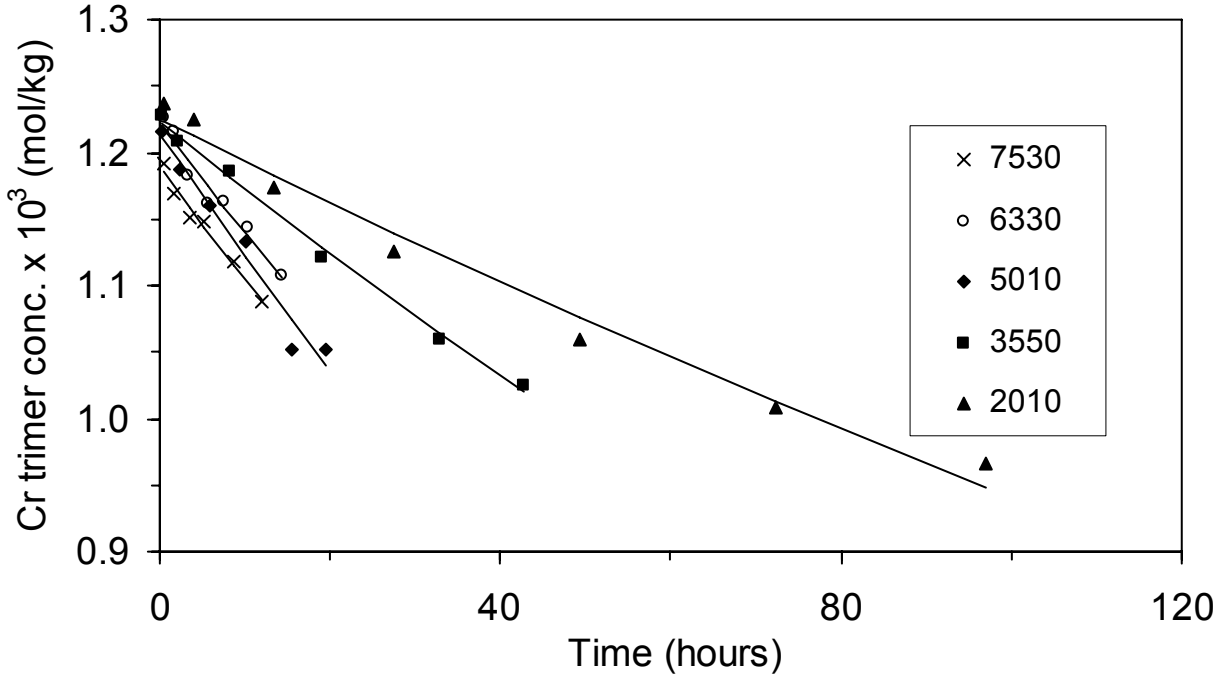

Figure 3.3 – Data and curve fit of unreacted chromium trimer concentration as a function of time for different initial polymer concentrations; ~200 mg/kg chromium conc. and a pH of 4.9.

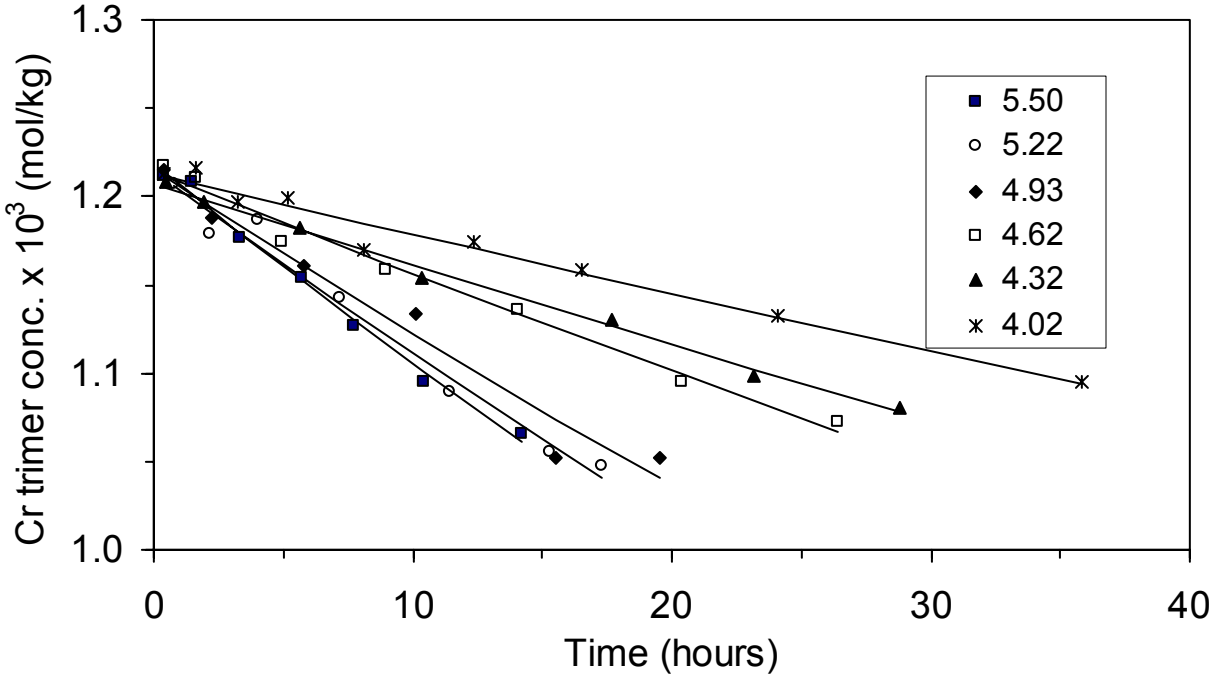

Figure 3.4 - Data and curve fit of unreacted chromium trimer concentration as a function of time for different initial pH values; ~200 mg/kg chromium conc. and a pH of 4.9.

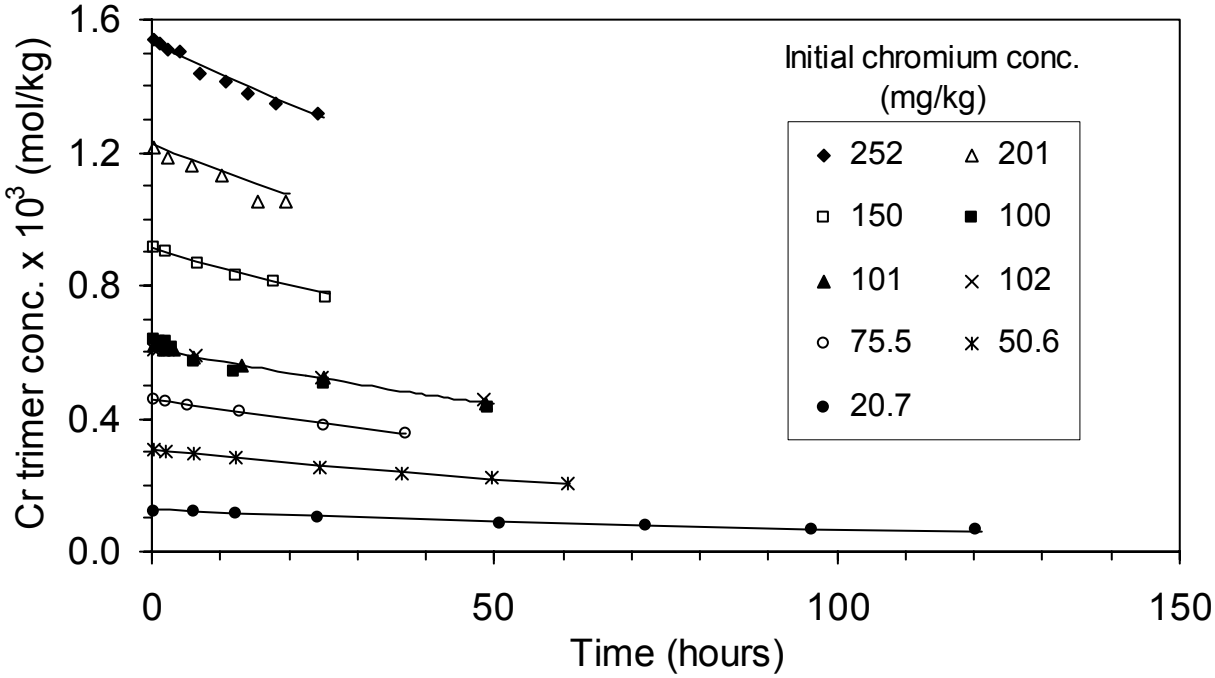

Figure 3.5 – Comparison of the results of the integration of the rate equation with data of the unreacted chromium trimer concentration as a function of time at different initial chromium concentrations; ~5000 mg/kg polymer conc. and a pH of ~4.9.

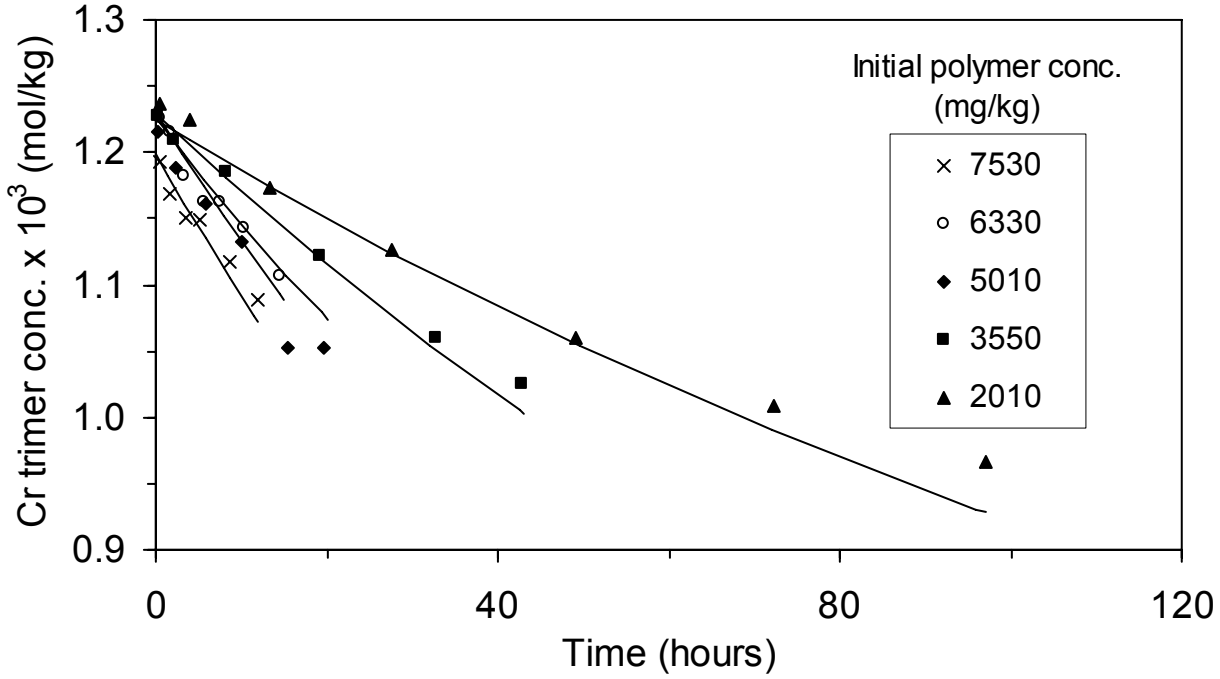

Figure 3.6 – Comparison of the results of the integration of the rate equation with data of the unreacted chromium trimer concentration as a function of time at different initial polymer concentrations; ~200 mg/kg chromium conc. and a pH of 4.9.

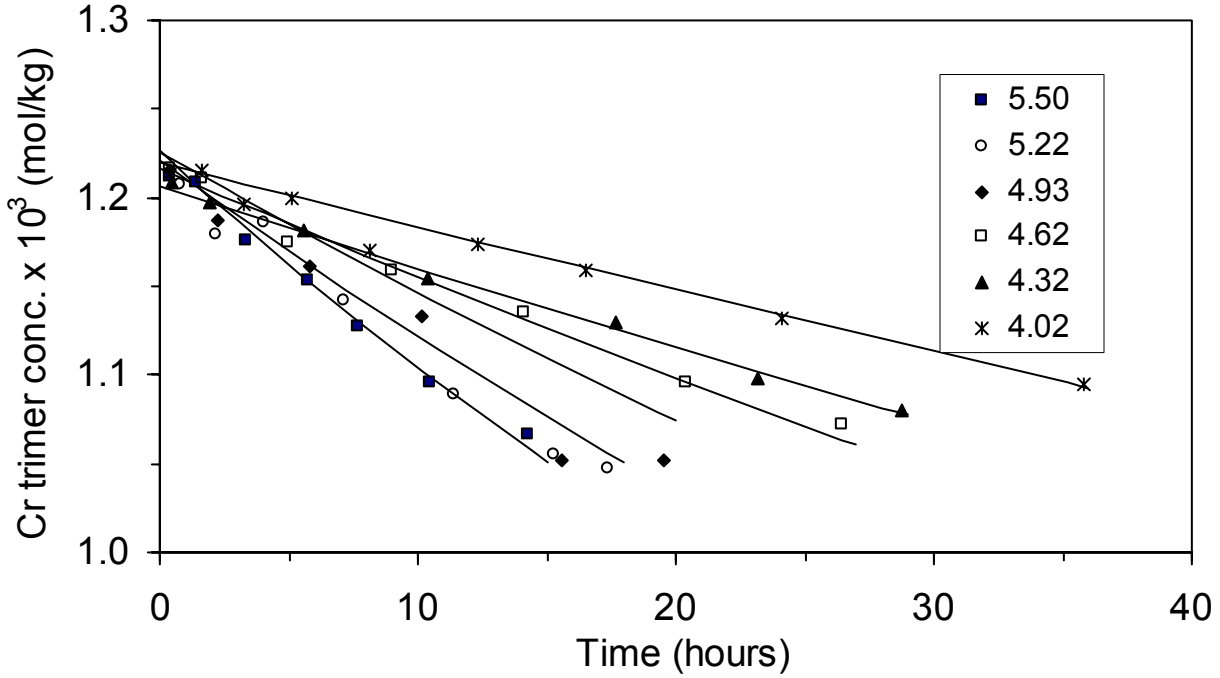

Figure 3.7 – Comparison of the results of the integration of the rate equation with data of the unreacted chromium trimer concentration as a function of time at different initial pH values; ~200 mg/kg chromium conc. and a pH of 4.9.

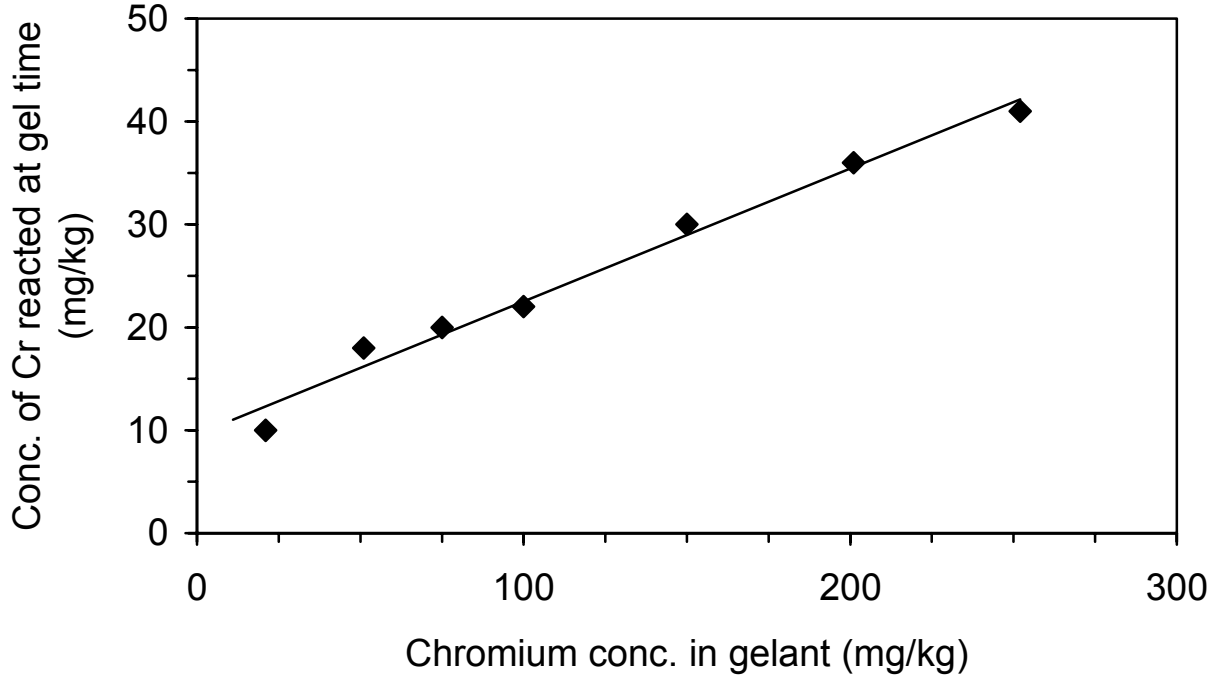

Figure 3.8 – Concentration of reacted chromium at the gel time as a function of the chromium concentration in the gelant; ~5000 mg/kg polymer conc. and a pH of ~4.9.

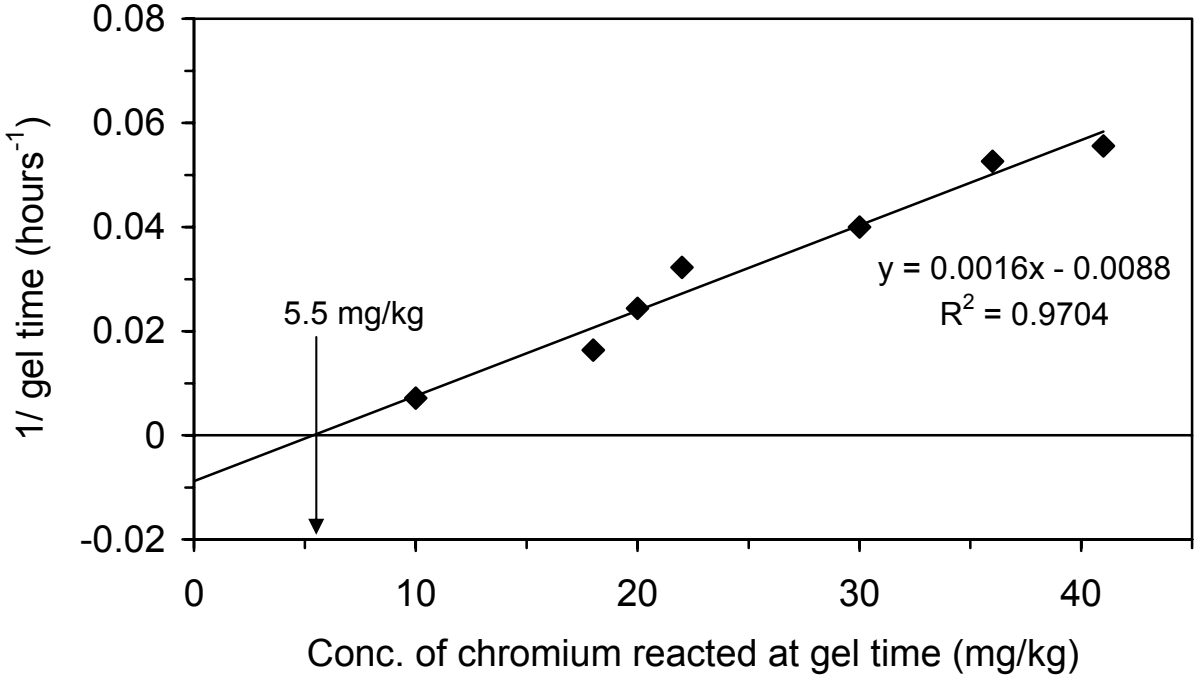

Figure 3.9 – Correlation of the reciprocal of the gel time with concentration of reacted chromium at the gel time; ~5000 mg/kg polymer conc. and a pH of ~4.9.

Conclusions

The following conclusions from this study of the uptake of chromium by HPAM are applicable over the range of conditions that were investigated.

1. The rate of the reaction between chromium acetate and hydrolyzed polyacrylamide was described well by the following empirical equation.

$$r_{Cr3} = -\frac{dC_{Cr3}}{dt} = k\,\frac{C_{Cr3}^{1.01}\;[(C_{carb})_0 - ((C_{Cr3})_0 - C_{Cr3})]^{0.84}}{C_H^{0.39}}$$

   The value of the reaction rate constant, k, was 6.2×10^{-3} h^{-1} $(mol/kg)^{-0.46}$. The above rate expression was regressed for chromium trimer concentrations between 20 mg/kg (1.3×10^{-4} mol/kg) and 250 mg/kg (1.6×10^{-3} mol/kg), HPAM concentrations from 2000 mg/kg to 7500 mg/kg and pH values from 4.0 to 5.5. Conditions used in the development of the rate expression were a temperature of 25°C, 10% degree of hydrolysis of the HPAM, aqueous solvent containing 1% KCl and an acetate-to-Cr(III) mole ratio of 3.0.

2. The order of reactions with respect to Cr(III) and carboxylate group on polymer were comparable to those found in studies of the reaction using inorganic salts of Cr(III). The absolute value of the order of reaction with respect to hydrogen ion concentration was less than that for inorganic chromium salts which indicated the weaker dependence of pH on the reaction rate.

3. The minimum concentration of chromium required to gel a solution containing 5,000 mg/kg HPAM was between 5 and 10 mg/kg.

Nomenclature

C_{Cr3} - Concentration of unreacted chromium trimer, mol/kg,
C_{carb} - Concentration of unreacted carboxylate groups, mol/kg.
C_H - Concentration of hydrogen ion, mol/kg.
k - Reaction rate constant.
a,b,c - Order of reactions with respect to chromium trimer, carboxylate groups and hydrogen ion.
C_{CrS} - Concentration of chromium in sample, mg/kg.
C_{PS} - Concentration of polymer in sample, mg/kg.
f_s - Fraction of chromium(III) reacted in sample.
C_{CrF} - Concentration of chromium in filtrate, mg/kg.
C_{PF} - Concentration of polymer in filtrate, mg/kg.
M_S - Mass of sample, kg.
M_F - Mass of filtrate, kg.
t - Reaction time, h.
r_{Cr3} - Rate of chromium uptake, mol/(kg h).

References

1. Albonico, P., Burrafato, G. and Lockhart, T.P.: "Effective Gelation-Delaying Additives for Cr+3/Polymer Gels," paper SPE 25221 presented at the SPE Intl. Symp. on Oilfield Chemistry, New Orleans, March 2-5, 1993.
2. Banerjea, D. and Chaudhari, S.D.: "Kinetics Studies on the Formation of Metal Chelates-II: Reaction of Hexa-aquo-chromium(III) Ion with Glycine and the Nature of the Product Formed in Weakly Acidic Aqueous Solution", *J. Inorganic Nuclear Chemisty*, **30** (1968), 871-880.
3. Burrafato, G., Carminati, S., Bonaccorsi, F. and Lockhart, T.P.: "Evidence for Molecular Cross-Links in Cr^{3+}/Polyacrylamide Gels", *Macromolecules*, **23** (1990), 2402-2406.
4. Dona, C.L.: "An Experimental Study of the Uptake and Gelation Reactions of CR(III) Oligomers with Polyacrylamide," Doctoral Dissertation, University of Kansas, Lawrence, KS (1993).
5. Hamm, R.E., Johnson, R.L. Perkins, R.H. and Davis, R.E.: "Complex Ions of Chromium. VIII. Mechanism of Reaction of Organic Acid Anions with Chromium(III)", *JACS*, **80** (1958), 4469-4471.
6. Hartley, F.R.: "Studies in Chrome Mordanting: V. Kinetics and Mechanism of the Interaction of Chromium(III) Salts with Wool", *Aust. J. Chem.*, **21** (1970), 275-285.
7. Hunt, J.A.: "An Experimental Study of the Kinetics of the Crosslinking Reaction Between Chromium(III) and Polyacrylamide," Doctoral Dissertation, University of Kansas, Lawrence, KS (1987)
8. Khan, A.K. and Ud-din, K.: "Anation of Hexaaquochromium(III) by Glycine", *J. Inorg. Nucl. Chem.*, **43** (1981), 1082-1085.
9. Lockhart, T.P.: "Chemical and Structural Studies on Cr+3/Polyacrylamide Gels," paper SPE 20998 presented at the SPE Intl. Symp. on Oilfield Chemistry, Anaheim, February 20-22, 1991.
10. Michnick, M.J., Unpublished results, University of Kansas, 2003.
11. Montanari, L., Scotti, R. and Lockhart, T.P.: " Kinetics and Mechanism of the Reaction of Hydrated Chromium(III) with Partially Hydrolyzed Polyacrylamide," *Macromolecules*, **27** (1994), 3341-3348.
12. Rollinson, C.L.: "Olation and Related Chemical Processes", from Bailar, J.C., *Chemistry of the Coordination Compounds*, Chapter 13, New York, Reinhold Publishing Co., (1956).
13. Tackett, J.E.: "Characterization of Chromium(III) Acetate in Aqueous Solution," *Applied Spectroscopy*, **43** (1989) 490-499.
14. Udy, M.J.:*Chromium*, Volume 1, Reinhold Publishing Corp., New York (1956).

Appendix
Determination of Un-Reacted Chromium Concentration using the Centrifugal Filter Device

Small concentrations of polymer passed through the centrifugal filter device. Chromium concentrations measured in the filtrate were corrected for the amount of chromium that was attached or reacted with the polymer in order to determine the concentration of un-reacted chromium in the solvent. Material balances around the centrifugal filter device were made using the following assumptions.

1. Un-reacted chromium concentrations were the same in the sample and filtrate (and retentate).
2. The mass ratio of reacted chromium to polymer is the same in the sample and filtrate (and retentate).

A sample of gelant was placed in the top compartment of the filter device and centrifuged, resulting in a retentate that remained in the top compartment and the filtrate that passed through the filter. The following definitions are used to describe the mass quantities shown in Figure 3.10.

M = mass of solution, kg
C_{Cr} = concentration of chromium, mg/kg
C_P = concentration of polymer, mg/kg
f_S = fraction of Cr(III) reacted in Sample.

Subscripts
Cr = chromium
P = polymer
S = Sample
R = Retentate
F = Filtrate

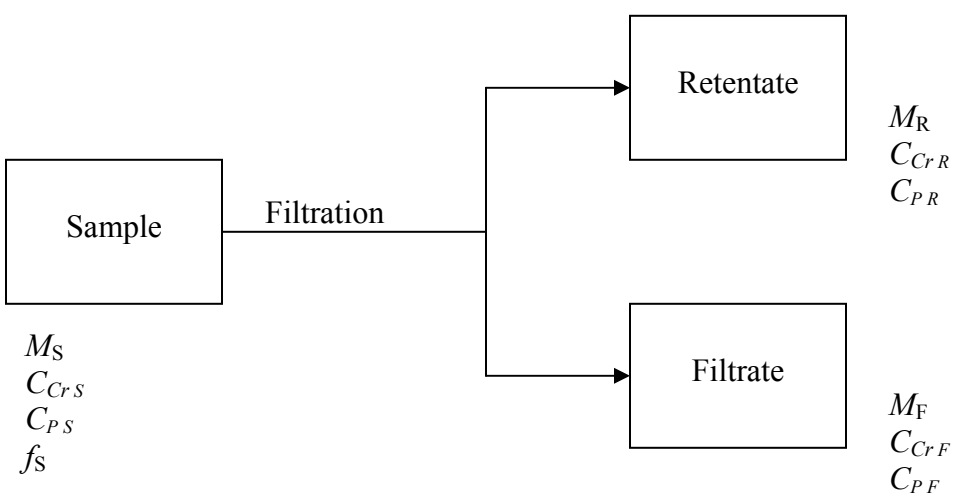

Figure 3.10 – Variables used in mass balances on the centrifugal filter device.

Mass balances on Sample

Mass of chromium reacted in Sample (mg) $= M_S C_{Cr\,S} f_S$

Conc. of un-reacted chromium in Sample (mg/kg) $= \dfrac{M_S\ C_{Cr\,S} - M_S\ C_{Cr\,S}\ f_S}{M_S} = C_{CrS}(1 - f_S)$

$$\frac{\text{Mass of chromium reacted}}{\text{Mass of polymer}} = \frac{M_S\ C_{Cr\,S}\ f_S}{M_S\ C_{P\,S}} = \frac{C_{Cr\,S}}{C_{P\,S}} f_S$$

Mass balances on Filtrate

Un-reacted chromium concentrations were the same in the Sample and Filtrate (Assumption 1).

Conc. of un-reacted chromium in Filtrate (mg/kg) $= C_{Cr\,S}(1 - f_S)$
Mass of un-reacted chromium in Filtrate (mg) $= M_F\ C_{Cr\,S}(1 - f_S)$

The mass ratio of reacted chromium to polymer is the same in the Sample and Filtrate (Assumption 2).

Mass of reacted chromium in Filtrate (mg) $= M_F\ C_{PF} \dfrac{C_{Cr\,S}}{C_{P\,S}} f_S$

Total mass of chromium in Filtrate =
mass of un-reacted chromium in Filtrate + mass of reacted chromium in Filtrate

$$M_F C_{Cr\,F} = M_F\ C_{Cr\,S}(1 - f_S) + M_F\ C_{P\,F} \frac{C_{Cr\,S}}{C_{P\,S}} f_S \qquad \text{Eq. 3.12}$$

Division of Eq. 3.12 by M_F and solving for f_S gives:

$$f_S = \frac{1 - (C_{Cr\,F} / C_{Cr\,S})}{1 - (C_{P\,F} / C_{P\,S})} \qquad \text{Eq. 3.13}$$

The fraction of chromium reacted, f_S, was calculated by Eq. 3.13 by measuring the concentrations of chromium and polymer in the Filtrate and knowing or measuring the concentrations of chromium and polymer in the original Sample (gelant).

The concentration of un-reacted chromium trimer in moles per kg, C_{Cr3}, was calculated by Eq. 3.14.

$C_{Cr3} = C_{Cr\,S}\ (1 - f_S)$ (0.001 g/mg) / (156.0 grams of trimer/mole of trimer) Eq. 3.14

Chapter 4

Effects of Composition of a Polyacrylamide-Chromium Acetate Gel System and the Applied Pressure Gradient on Gel Dehydration and Disproportionate Permeability Reduction in Sandpacks

Graduate research Assistant: Tuan Q. Nguyen

Introduction

High water production is a major concern in mature hydrocarbon reservoirs. Costs of handling and disposing of water produced from oil reservoirs often shortens the life of a production well. Disposal of the water is also an environmental concern. In order to reduce water production, polymer gels have been used to modify the mobility of water and oil in petroleum reservoirs.

When some gels are placed in a petroleum reservoir, permeability reduction occurs to a much greater extent for water than for oil. This phenomenon is known as favorable disproportionate permeability reduction (DPR). Reduced permeability to water leads to decreased production of water, and sometimes increased oil production, thereby prolonging the useful life of the reservoir. Results reported in the literature have shown that the application of several polymer gel systems can result in DPR. Mechanisms for DPR have been debated and the magnitude of the effect has been unpredictable from one application to another. Mechanisms for DPR that have been proposed and studied by several researchers are shown in Table 4.1.

This chapter presents the results of a study on the effects of gel composition, i.e. partially hydrolyzed polyacrylamide (HPAM) and Cr(III) concentrations, and applied pressure gradients on the magnitude of gel dehydration, and on the magnitude of residual resistance factors and DPR during flow through gel-treated sandpacks. Additionally, material balances on the phases and components in the sandpacks during flow experiments were conducted to give insights into mechanisms that are responsible for permeability reductions and DPR.

Experimental Equipment, Materials and Procedures

Flow experiments were conducted in sandpacks. Various compositions of Cr(III)-acetate-polyacrylamide gelant were injected into the sandpacks that contained brine at residual oil saturation of 13-17% and allowed to gel. Oil (n-dodecane) was then injected into the sandpacks at a constant pressure drop to dehydrate the gels. Brine (1% KCl solution) and oil floods were conducted following the dehydration to determine end-point permeabilities, residual resistance factors, and DPR. Figure 4.1 is a schematic of the experimental setup. Pumps were used to inject fluids into the sandpack. The effluent was collected in fractions. Pressure drops across the entire sandpack and each of the sections were monitored and recorded by pressure transducers and a data acquisition system. The experimental system was maintained at 30 ^{o}C. Table 4.2 summarizes the sequence of runs in each sandpack. For those sandpacks where weak gels (<3000 ppm polymer) were placed, Runs 14-18 were omitted. Following is a description of the preparation of the sandpacks and gelant and the experimental procedures. Experimental details can be found elsewhere [Nguyen, 2003].

Table 4.1 - Proposed mechanisms for disproportionate permeability reductions.

1	Gels swell in water but shrink in oil.	Dawe and Zhang, 1994;Gales et al.,1998; Liang et al., 1995; Sparlin and Hagen, 1984.
2	Gravity affects gel locations in pores.	Liang et al., 1995.
3	Lubrication effects.	Sparlin and Hagen, 1984; Zaitoun and Kohler, 1988.
4	Gels constrict water pathways more than oil pathways in a given pore (wall effects).	Liang and Seright, 1997; Liang et al., 1995; Zaitoun et al. 1998.
5	Segregated pathway theory.	Liang and Seright, 1997; Liang et al., 1995; Nilson et al., 1998; White et al., 1973.
6	Effect of capillary forces and gel elasticity on oil and water flow.	Al-Sharji et al., 1999; Liang and Seright, 1997;
7	During brine injection, polymer leaches from the gel and significantly decreases the brine mobility.	Liang and Seright, 1997.
8	Gels alter rock wettability.	Zaitoun et al., 1998.
9	Pore blocking by gel droplets.	Liang and Seright, 2000; Nilson et al., 1998.
10	New pathways for oil and water are created by gel dehydration.	Dawe and Zhang, 1994; Green et al. 1998; Willhite et al. 2000.

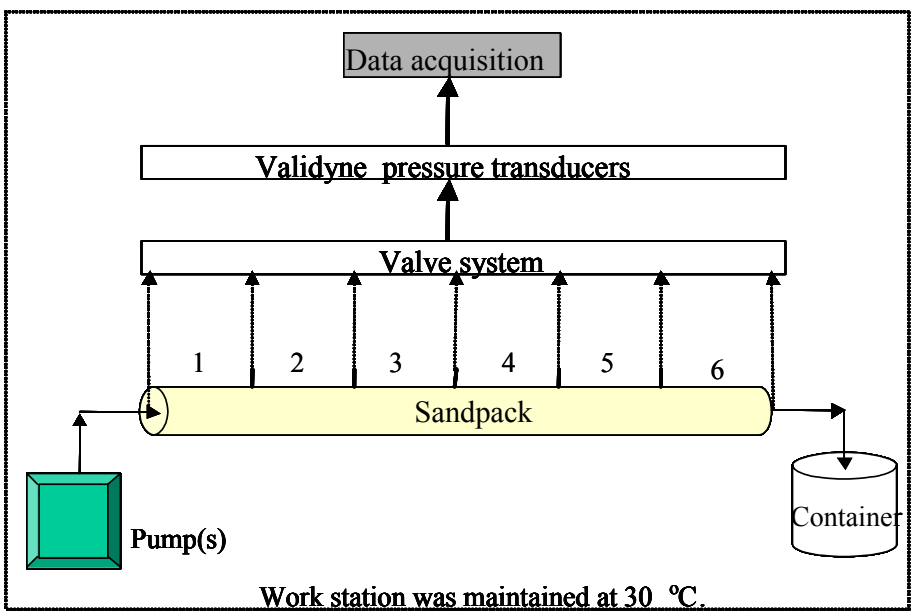

Figure 4. 1 – Schematic of equipment for flow experiments.

Table 4.2 - Sequence of experiments in each sandpack.

Run	Experiment	Description
0	Pack preparation	Packed sand and saturated porosity with water.
1	Base permeability	Water was injected stepwise at 10 different rates.
2	Tracer tests	Verification of pore volume .
3	Brine saturation	Water was displaced by 1.0% KCl brine.
4	Oil flood	Oil was injected until negligible amount of brine was displaced.
5	Brine flood	Brine was injected until negligible amount of oil was displaced.
6	Tracer tests	Verification of S_{or}.
7	Gelant injection	Gelant was injected into the sandpack.
8	Shut-in experiments	Sandpack was shut in to allow gelation.
9	Gel dehydration @ 20 psi/ft	Oil was injected at a nominal pressure gradient of 20 psi/ft until the criterion for termination of the dehydration met.
10	Brine flood @ 20 psi/ft	Brine was injected at a nominal overall pressure gradient of 20 psi/ft until oil displacement was negligible.
11	Rate tests	Brine was injected at various flow rates in a range such that pressure gradients did not exceed 20 psi/ft.
12	Oil flood @ 20 psi/ft	Oil was injected at a nominal overall pressure gradient of 20 psi/ft until brine displacement was negligible.
13	Rate tests	Oil was injected at various flow rates in a range such that pressure gradients did not exceed 20 psi/ft.
14	Gel dehydration @ 50 psi/ft	Oil was injected at a nominal overall pressure gradient of 50 psi/ft until a negligible amount of brine was produced.
15	Brine flood @ 50 psi/ft	Brine was injected at nominal overall pressure gradient of 50 psi/ft until oil displacement was negligible.
16	Rate tests	Brine was injected at various flow rates in a range such that pressure gradients did not exceed 50 psi/ft.
17	Oil flood @ 50 psi/ft	Oil was injected at a nominal overall pressure gradient of 50 psi/ft until brine displacement was negligible.
18	Rate tests	Oil was injected at various flow rates in a range such that pressure gradients did not exceed 50 psi/ft.
19	Tracer Tests	Tracer tests were carried out on oil phase to verify mobile volume (based on material balance).

The sandpacks were made by packing silica sand (F110, US Silica Co.) in one-foot long holders. The sand holders were fabricated from acrylic tubes with an ID of 1.5 inches. End caps were attached to both ends of the holder body and sealed with O-rings. The end caps had fittings at the center to allow fluid to flow in and out. Grooves cut on the inner face of the end caps provided uniform distribution of fluid across the entrance and exit faces of the sandpacks.

The holders were divided into six 2-inch long sections by pressure ports. Pressure drop across each section and the entire sandpack were monitored and recorded. Plastic screens of 215-mesh were placed in pressure ports to prevent sand particles from entering tubing connections to the transducers. Fine, 330-mesh, and coarse, 37-mesh, screens were placed at the end caps to prevent sand from exiting the pack. A 1.5 cm length of course sand was packed adjacent to the screens in Sections 1 and 6. Since both end sections were partially packed with coarse sand, the average values of the internal sections (Sections 2 through 5) were used for values of permeability and quantities derived from permeabilities (residual resistance factors and DPR). Values determined for the entire sandpack volume were used for pore volume, porosity, and saturations.

Fine sand, grain size from 50-270 mesh, underwent a pretreatment process (acid wash, rinse, dry, and screen) before packing. The sand was manually packed using a vibrator. After packing, the sandpack was evacuated to remove air and then filled with carbon dioxide. Porosity was determined by saturating the sandpack with water. Porosity was verified by aqueous tracers. Oil with a 100 ppm stilbene tracer was injected at a constant flow rate of 21 mL/min to achieve and determine an interstitial water saturation (S_{wi}), and the permeability to oil (k_o) at S_{wi}. The stilbene tracer in the oil allowed for the determination of the amount of residual oil that was displaced from the pack during injections after the gel treatment. Brine was then injected at 21 mL/min to achieve and determine the residual oil saturation (S_{or}) and the permeability to water (k_w) at S_{or}. S_{or} was determined both by weight and volume methods and verified by tracer tests. S_{or} determined by tracer tests was used because it was deemed to be the most accurate of the three methods. Table 4.3 summarizes sandpack properties.

Table 4.3 - Summary sandpack properties. Permeability values were determined for the internal 8-inch long section of the sandpack. Porosity and saturations were determined for the entire sandpack.

Sandpack	Pore vol. (mL)	Porosity (%)	k (Darcy)	S_{wi} (%)	S_{or} (%)	k_o (Darcy)	k_w (Darcy)
TN003	112.9	33.3	4.49	14	13	3.73	2.98
TN004	115.4	34.1	4.54	14	16	3.68	2.67
TN006	117.2	33.8	4.36	15	16	3.74	2.73
TN007	111.4	33.5	4.28	15	15	3.69	2.45
TN008	115	33.1	4.37	14	17	3.72	2.64
TN009	120.5	33.7	4.22	14	16	3.49	2.62
TN010	115	33.1	4.37	14	17	3.72	2.64
TN011	117.2	33.4	4.05	13	17	3.54	2.31

The gelants were prepared from partially hydrolyzed polyacrylamide and chromium acetate. The polymer was Alcoflood 935, Lot No. A2247 BOV. The molecular weight of this polymer was around 6 million. Cr(III) stock solution was prepared from a Cr(III) acetate solution that contained 12.4% Cr(III) and 42.2% acetate by weight (McGean Rohco, Lot No. 40086816). The acetate-to-Cr(III) mole ratio was 3:1. Polymer to Cr(III) mass ratio was maintained at 40:1. All gelants contained 1.0% KCl and 10 ppm sodium azide (bactericide).

Bottle tests were conducted at 30 °C to determine bulk gel times and to monitor syneresis of the gels. Small samples were withdrawn at different times for viscosity measurement in a cone-and-plate geometry and at two different shear rates. When the viscosity was less than 103 cp, a shear rate of 22.5 s^{-1} was used and when the viscosity of gelant was greater than 103 cp, the samples were sheared at a rate of 2.25 s^{-1}. Gel time was defined as the time when the viscosity of gelant reached 1000 cp. However, for the gelant with polymer concentration of 2100 ppm, the gel time was taken as 27 days when the viscosity of the gelant reached 300 cp. The viscosity of this weak gelant was still about 300 cp after 7 months.

Gelants were bulk mixed and immediately injected into the sandpacks via a transfer cylinder for flow experiments. Approximately three pore volumes of gelant were injected at a flow rate of 4 mL/min. The sandpack was then shut-in for a time period that was at least twice the bulk gel time to allow the gelant to mature before the injection of oil in the dehydration step.

After the shut-in period, oil was injected (Run 9, Table 4.2) at a constant pressure of 20 psi, which is equivalent to a nominal pressure gradient of 20 psi/ft, to form channels through the gelled sandpack by dehydrating the gel. Effluent samples of brine and oil were collected in fractions. Brine in the samples was analyzed for polymer and Cr(III) concentrations and oil in the samples was analyzed for stilbene. The stilbene tracer allowed for the calculation of the amount of pre-treatment residual oil that was displaced from the pack. Connections between the ports on the sandpack and the pressure transducers were closed during the relatively long dehydration process. This was done to eliminate brine from displacing oil in the tubings so that material balances performed on the sandpacks would be more accurate.

The dehydration process was terminated when the brine production rate was less than 1mL/day for weak gels and 0.5 mL/day for strong gels, except in Sandpacks TN007 and TN010. The brine production rate was 2 mL/day for TN007 and 4 mL/day for TN010 when the dehydration runs were terminated. The exit screens in Sandpack TN004 became partially blocked on the second day of the dehydration process and most of the applied pressure drop was observed in Section 6, leaving a reduced pressure gradient across the most of the pack length. TN004 was then brine flooded at the reduced pressure gradient. The exit screens were replaced after the brine flood and a second dehydration was conducted by an oil flood at a nominal pressure gradient of 20 psi/ft (the average pressure gradient across the internal sections was 22.9 psi/ft).

The pressure transducers were re-connected to the pressure ports after the dehydration run so that pressure gradients in each section and the overall sandpack could be measured. The channels that developed through the gel-treated sandpack during the dehydration process are referred to as the "new" pore space. Permeability to oil in the "new" pore space in the dehydrated gel was

determined using Darcy's law, and the residual resistance factor for oil (F_{rro}) was determined using Eq. 4.1.

$$F_{rro} = \frac{k_{ob}}{k_{oa}} \qquad \text{Eq. 4.1}$$

where

k_{ob} is the permeability to oil at S_{wi} before gel placement.
k_{oa} is the permeability to oil in the "new" pore space after the gel treatment at S_{wi}*.

After the dehydration by the oil at 20 psi/ft, brine was injected at a constant pressure of 20 psi (Run 10, Table 4.2), which is equivalent to nominal pressure gradient of 20 psi/ft, until oil displacement was negligible. Effluent fractions containing oil and brine were collected and analyzed as was done in Run 9. Rate tests (Run 11) were then conducted by injecting brine at various flow rates over a range such that the overall pressure gradient did not exceed the original dehydration pressure gradient of 20 psi/ft. This was done to determine whether permeability and residual resistance factor to water were a function of flow rate or pressure gradient. End-point permeability to water in the "new" pore space was determined by Darcy's law at various pressure gradients, and residual resistance factors for water (F_{rrw}) were determined using Eq. 4.2.

$$F_{rrw} = \frac{k_{wb}}{k_{wa}} \qquad \text{Eq. 4.2}$$

where

k_{wb} is the permeability to water at S_{or} before gel placement.
k_{wa} is the permeability to water at S_{or}* after gel placement.

Oil was then injected at an overall pressure gradient of 20 psi/ft (Run 12) until brine displacement was negligible. Effluent brine and oil samples were collected and analyzed. Rate tests during oil injection (Run 13) at pressure gradients not exceeding 20 psi/ft.. End-point permeability to oil and F_{rro} at various pressure gradients were determined.

The dehydration process was then conducted at a constant pressure gradient of 50 psi/ft (Run 14) in the sandpacks containing strong gels that were prepared with polymer concentrations of 3000 ppm or higher. The procedure for Run 14 was the same as for Run 9, except the dehydration pressure gradient was 50 psi/ft. This was followed by a brine flood at 50 psi/ft (Run 15). Brine was then injected at different rates (Run 16) to determine the effect of flow rate on permeability measurements. An oil flood at 50 psi/ft (Run 17) was conducted followed by oil-rate tests (Run 18). The rate tests were conducted at pressure gradients values of 50 psi/ft or less.

A tracer test during the injection of oil (Run 19) was conducted to determine the volume of displaceable oil contained in the "new" pore volume. Oil containing 10 ppm stilbene was injected and the effluent concentration of stilbene as a function of the volume of oil injected was determined. Integration of these data determined the displaceable oil in the 'new" pore space. This tracer test was conducted after Run 13 for the sandpacks where the weaker gels containing less than 3000 ppm polymer were placed.

Oil and brine effluent samples collected during the dehydration processes and the oil and brine floods were analyzed for stilbene in the oil and were analyzed for polymer and Cr(III)

concentrations in the brine. Stilbene was analyzed with a UV/Vis spectrometer at a wavelength of 296 nm. Polymer concentration in the brine samples were determined by measuring total organic carbon (TOC) using a Shimadzu TOC 5000 A. The TOC data were converted to polymer concentrations, assuming the samples did not contain carbon from the acetate ions. Carbon from the acetate ions corresponded to 7% of the carbon from the polymer in the gelant formulations. Cr(III) in the brine samples were converted to Cr(VI) using 1% H_2O_2 and 1 N KOH and the chromium concentration was then determined by measuring absorbance at a wavelength of 373 nm (UV/Vis Lambda 20 Spectrometer). Detailed procedures are given by Nguyen [2003].

Results and Discussion

Bottle Tests for Bulk Gel Time and Gel Syneresis

Bottle tests were used to determine the bulk gel time and to monitor for gel syneresis. Gel times as a function of polymer concentration and polymer-to-Cr(III) mass ratios are shown in Figure 4.2. The gel time was not a strong function of polymer-to-Cr(III) ratios at the three polymer concentrations that were tested. Gel time was a strong function of polymer concentration. A polymer-to-Cr(III) mass ratio of 40:1 was selected for use in the flow experiments because this ratio is commonly used for field treatments.

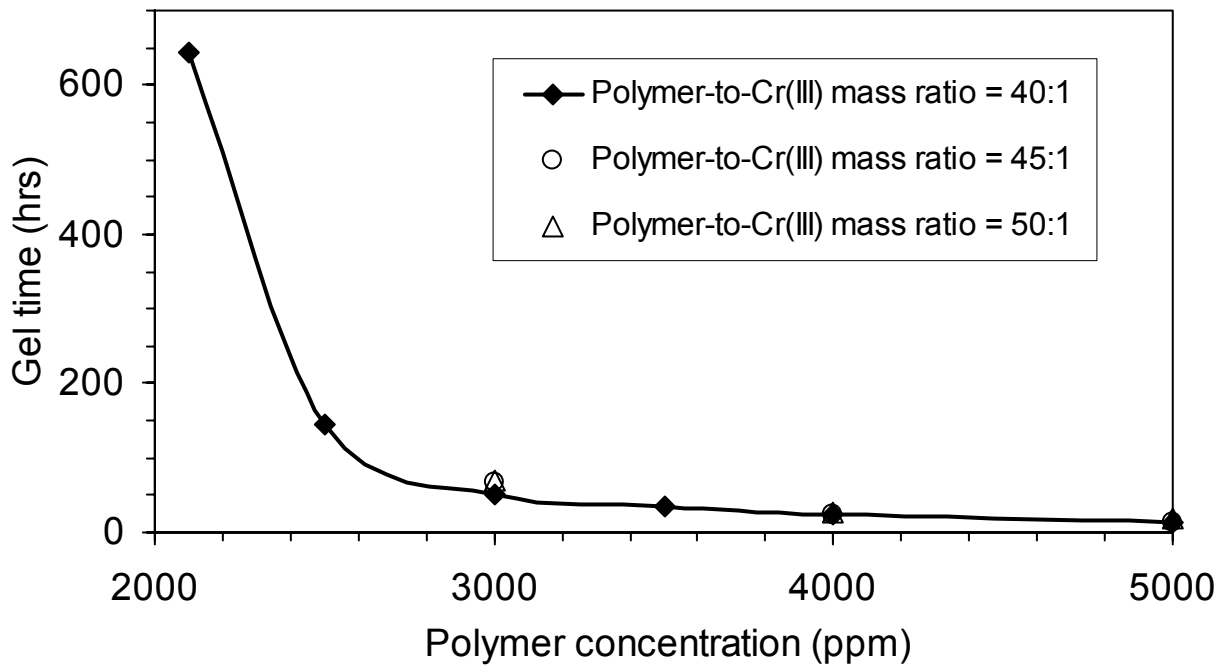

Figure 4.2 – Bulk gel times as a function of polymer concentration and polymer-to-chromium mass ratios.

In bottle tests, gels containing 4000, 3000, and 2500 ppm polymer and a polymer-to-Cr(III) mass ratio of 40:1 underwent slight syneresis after 3.5 months at 30°C. The syneresis volume was less than 1.2% of the gel volume after 4 months. Samples of gel collected during gelant injection for the flow experiments were also monitored. No syneresis was observed during the time required for the dehydration runs and oil and brine displacements (~3-month time period).

Gel Dehydration

After gelant injection, the sandpack was shut in for a period of time at least twice the bulk gel time before oil was injected into the sandpack to dehydrate the gel. Gel dehydration is a process of removing water from the gel by imposing a pressure gradient on the gel. Gel dehydration was thought to be a function of the rigidity or strength of the gel. Results from a study of dehydration on bulk gels by Krishnan [1998] showed that gel dehydration was a function of pressure gradient and dehydrating fluid. In this study, oil was the dehydrating fluid and was injected at a constant pressure of 20 psi, which is equivalent to a nominal pressure gradient of 20 psi/ft, to dehydrate the different gel compositions. In sandpacks containing gels with polymer concentrations of 3000 ppm or higher, oil was injected subsequently at 50 psi/ft to further dehydrate the gels.

Gel composition (polymer and chromium concentrations) affected the rate of gel dehydration. Brine production did not start immediately after bringing oil into contact with the gel at a pressure of 20 psi. Brine production started between 8 and 150 minutes after contact by the oil, depending on polymer concentration as shown in Table 4.4. The stronger the gel, i.e., the higher the polymer concentration, the longer the delay before brine was produced. (Brine production started earlier in TN007 than in TN009 and was thought to be due to a pressure overshoot of 50 psi/ft that occurred for a few minutes at the beginning of the dehydration process in TN007.) After brine was produced for a few minutes, oil breakthrough occurred and a mixture of brine and oil was displaced from the sandpacks.

Table 4.4 - Volume of gel dehydrated and dehydration time of different gel compositions.

Sandpack	Polymer concentration (ppm)**	Elapsed time between start of oil injection and production of brine in the effluent (min)	Total time of oil injection at 20 psi/ft (hrs)	Fraction of gel dehydrated (%)
TN010	2100	8	33	66.5
TN004	2500	10	170	54.8
TN009	2500	13	210	65.7
TN007	3000	10	210	57.2
TN006	3500	30	672	66.0
TN011	3500	75	991	65.3
TN003	4000	150	941	68.5

The volume of the aqueous phase collected in the effluent from the sandpacks during the dehydration process was defined as the volume of gel dehydrated. The rate of gel dehydration was a function of polymer concentration as shown in Figures 4.3 and 4.4 where the volume fraction of gel dehydrated was plotted as a function of time. The weak gels dehydrated faster than the stronger gels. The volume fraction of gel dehydrated was not a strong function of polymer concentration. As shown in Table 4.4 and Figure 4.3, the fractions of gel dehydrated were from 65-69% for the different gel compositions. The volumes of gel dehydrated in TN004 and TN007 were lower than for the other sandpacks since the dehydration process in these two sandpacks was terminated prematurely as described in the previous section.

Sandpacks containing gel with polymer concentrations of 3000 ppm and greater were dehydrated a second time at the higher pressure gradient of 50 pis/ft. An additional 2 to 6% of the original gel volume was dehydrated indicating that the fraction of gel dehydrated was a weak function of pressure gradient.

Experiments in Sandpacks TN009 and TN011 were replications of experiments conducted with Sandpacks TN004 and TN006, respectively. The fraction of gel dehydrated was similar in Sandpacks TN004 and TN009 at early times as shown in Figure 4.4. At later times, the dehydration rate leveled off sooner in TN004 than in TN009. The partially blocked effluent screens in TN004 during the dehydration process was probably responsible for this behavior. After the screens were replaced, an additional of 11.9% of the gel volume was further dehydrated to give a total fraction of gel dehydrated of 66.7%, similar to the value of 65.7% determined for TN009. For Sandpacks TN006 and TN011, the magnitude of gel dehydration was the same but the rate of gel dehydration was different. A longer time period was required to dehydrate the same volume percent of the gel in TN011 (3500 ppm) than in TN006 (3500 ppm). The slower rate of dehydration in TN011 was not in agreement with the trends for all of the sandpacks.

Permeability Reduction Resulting from Gel Dehydration

Permeabilities to oil and water (brine) were determined after the gel treatment at fractional flows of 100%. These end-point permeabilities were determined after dehydration by the injection oil at a pressure of 20 psi over the one-foot long packs and after a subsequent dehydration run at 50 psi. The nominal pressure gradient of the dehydration process that preceded the run (20 or 50 psi/ft) are indicated on the figures. Permeability data that are presented were determined over the 8-inch long internal section (Sections 2 through 5) of the sandpacks to eliminate the influence of the coarse sand and other entrance/exit effects in Sections 1 and 6. Since the permeabilities of Sections 1 and 6 were greater than those of the internal sections, the pressure gradient over the internal sections was somewhat greater than the (nominal) pressure gradient over the entire core length. The end-point permeability data are presented in three forms: (a) permeability, (b) residual resistance factors to oil and water (F_{rro}, F_{rrw}), and (c) selectivity, or the ratio of F_{rrw} to F_{rro}.

Permeability. End-point permeabilities for both oil and water were a strong function of polymer concentration after the gel dehydration at 20 psi/ft as shown in Figures 4.5 and 4.6. End-point permeabilities to both water and oil increased significantly with decreasing polymer concentration. End-point permeabilities to both oil and water (k_o and k_w) were reduced, but

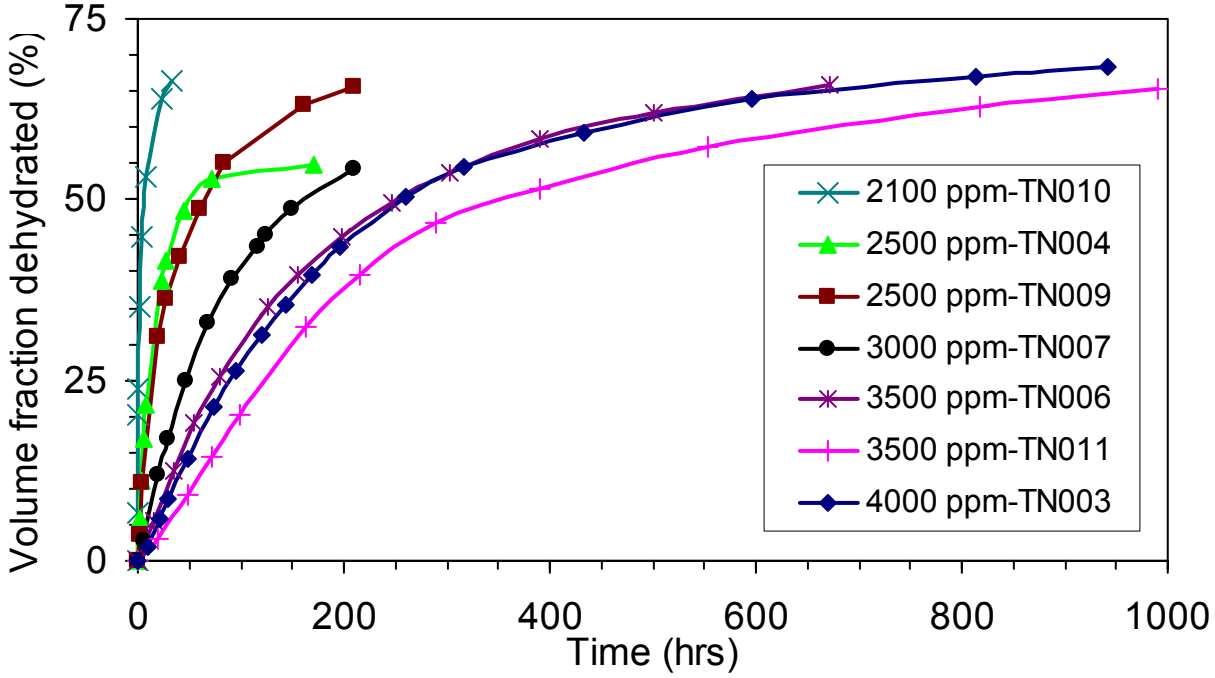

Figure 4.3 – Volume fraction of gel dehydrated as a function of time; oil flood at pressure gradient of 20 psi/ft..

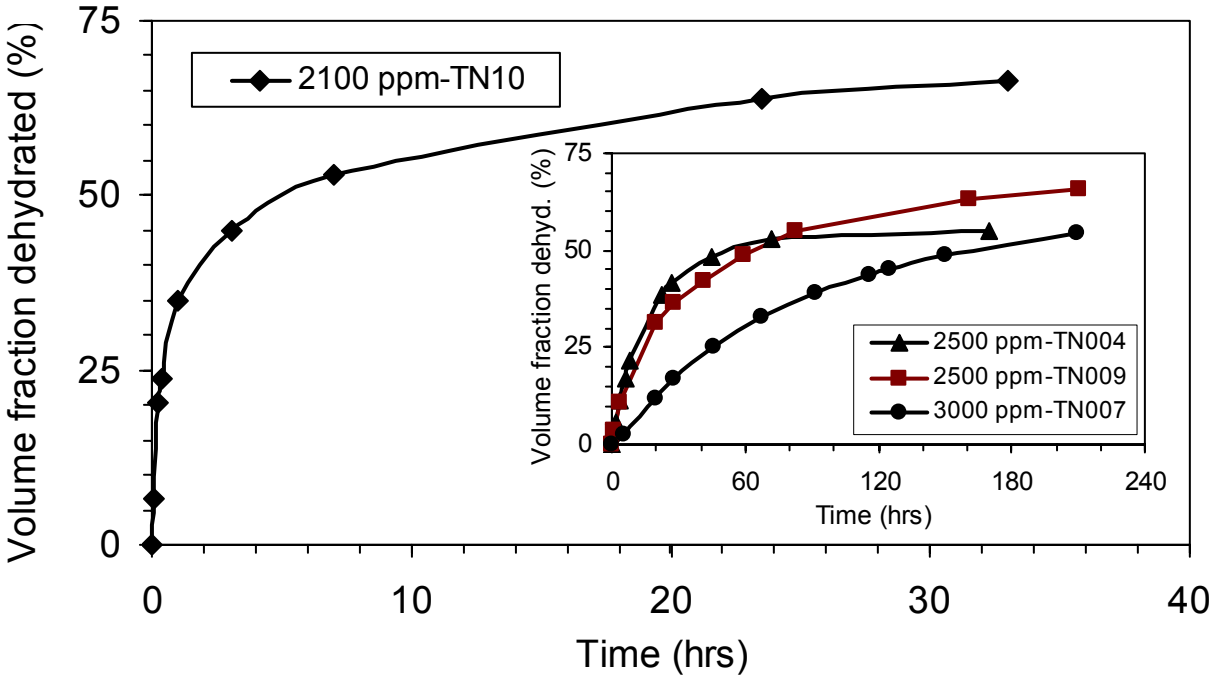

Figure 4.4 – Volume fraction of gel dehydrated as a function of time for weak gels (polymer concentrations of 3000 ppm or less).

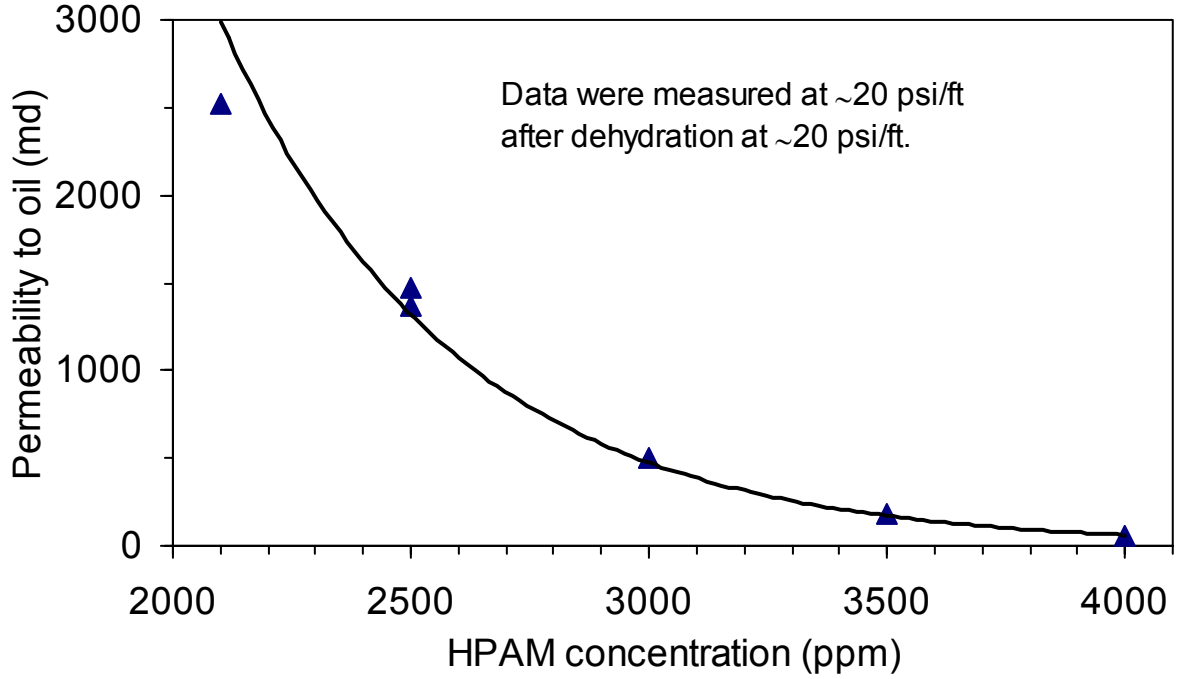

Figure 4.5 – Permeability to oil as a function of polymer concentration after gel dehydration at a pressure gradient of 20 psi/ft.

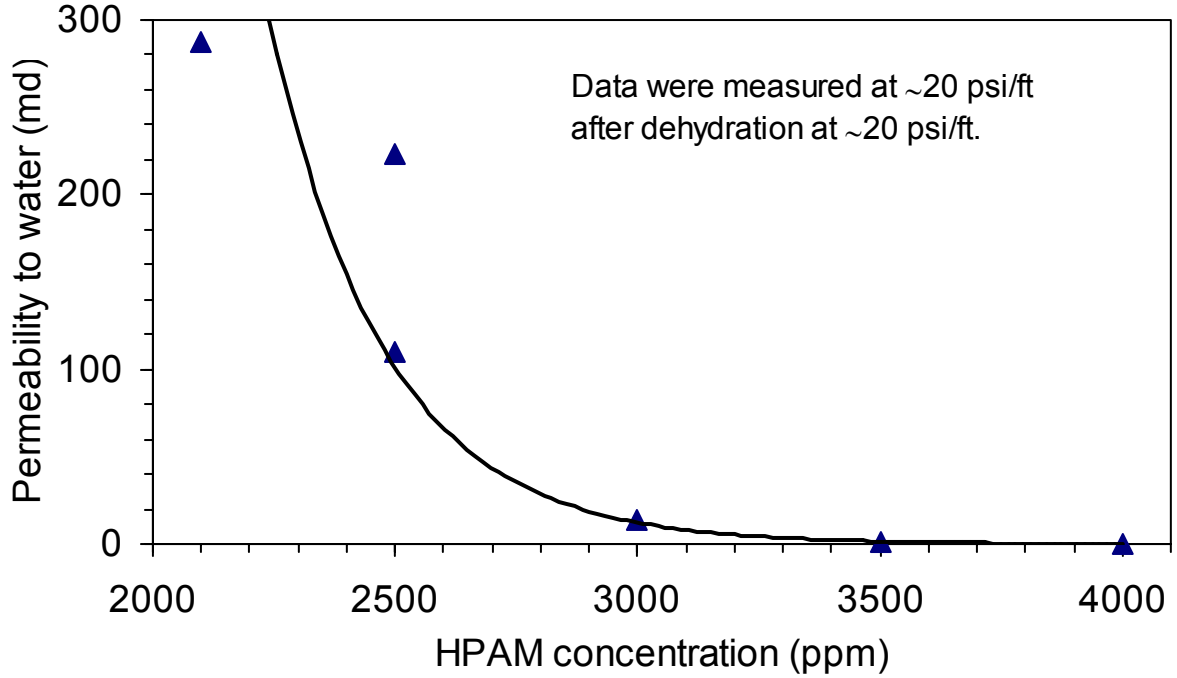

Figure 4.6 – Permeability to water as a function of polymer concentration after gel dehydration at a pressure gradient of 20 psi/ft.

permeability reduction was much greater for water than for oil. Permeability increased from 50 to 2500 md for oil and from 0.2 to 290 md for water as polymer concentration decreased from 4000 to 2100 ppm.

Rate tests were conducted to determine whether end-point permeabilities were a function of applied pressure gradient (or flow rate). Flow rates were varied from high to low and some flow rates were replicated in a random order to determine whether the results were reproducible. End-point permeability to oil at various pressure gradients for both strong and weak gels are shown in Figures 4.7 and 4.8, respectively. k_o was not a function of the pressure gradient except for the weakest gel containing 2100 ppm polymer where k_o decreased slightly with increased pressure gradient. k_w was a function of pressure gradient. As pressure gradient increased, k_w increased for strong gels (positive slope) but decreased for weak gels (negative slope) as shown in Figures 4.9 and 4.10, respectively. k_o and k_w measurements were reproducible and were also not a function of the how the flow rate was varied. The numbers next to data points in the figures indicate the order the flow rates were varied after the initial series of pressures from high to low values.

In summary, end-point permeabilities to both water and oil decreased significantly with increased polymer concentration in the gel, though the fractions of gel dehydrated were about the same. Permeability was a function of pressure gradient for water but not for oil. As pressure gradient increased, k_w increased for a strong gel but decreased for a weak one.

Residual Resistance Factors. Residual resistance factors were used as a relative measure of permeability reduction. Residual resistance factor for oil (F_{rro}) was defined as the ratio of permeability to oil before the gel treatment to permeability to oil after the gel treatment. The corresponding residual resistance factor for water (F_{rrw}) was the ratio of permeability to water before the gel treatment to permeability to water after the gel treatment.

Residual resistance factors for oil and water as a functions of polymer concentration and two pressure gradients are shown in Figures 4.11 and 4.12, respectively. These factors were determined after the dehydration at 20 psi/ft. Both F_{rro} and F_{rrw} increased rapidly with increasing polymer concentration. Permeability reduction was greater for water than for oil.

Residual resistance factors as a function of pressure gradient are shown in Figures 4.13 and 4.14 for oil and in Figures 4.15 and 4.16 for water. These figures present the permeability data of Figures 4.7 through 4.10 in a different form and similar comments apply.

The sandpacks containing gel with polymer concentrations of 3000 ppm and higher were also dehydrated at a pressure gradient of 50 psi/ft. After gel dehydration at 50 psi/ft, rate tests were conducted to determine the effect of pressure gradient on permeability and residual resistance factors. The residual resistance factors for oil and for water as a function of the applied pressure gradient are shown in Figures 4.17 and 4.18, respectively. F_{rro} remained relatively constant with pressure gradient (Figure 4.17) while F_{rrw} decreased with increased pressure gradient (Figure 4.18). Comparison of the values of F_{rro} and F_{rrw} at pressure gradients less than about 20 psi/ft in Figures 4.17 and 4.18 with values in Figures 4.13 and 4.15 (dehydration pressure of 20 psi/ft)

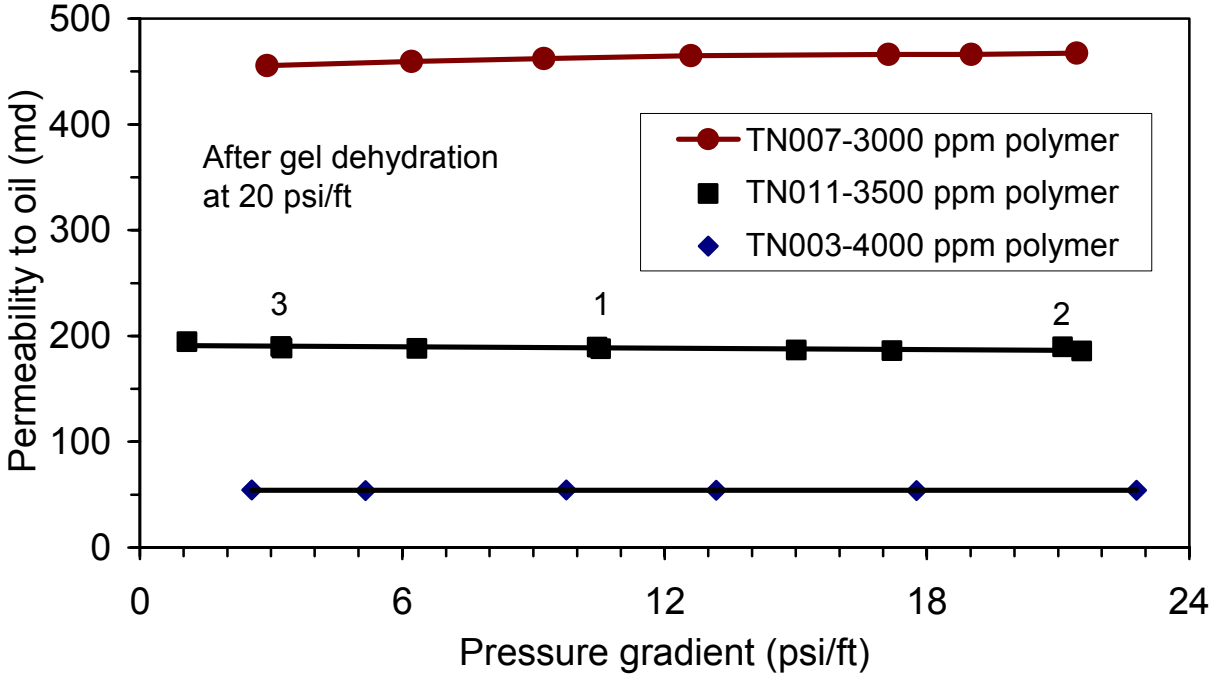

Figure 4.7 - Permeability to oil for strong gels as a function of pressure gradient after gel dehydration at a pressure gradient of 20 psi/ft; polymer concentrations of 3000 ppm and higher.

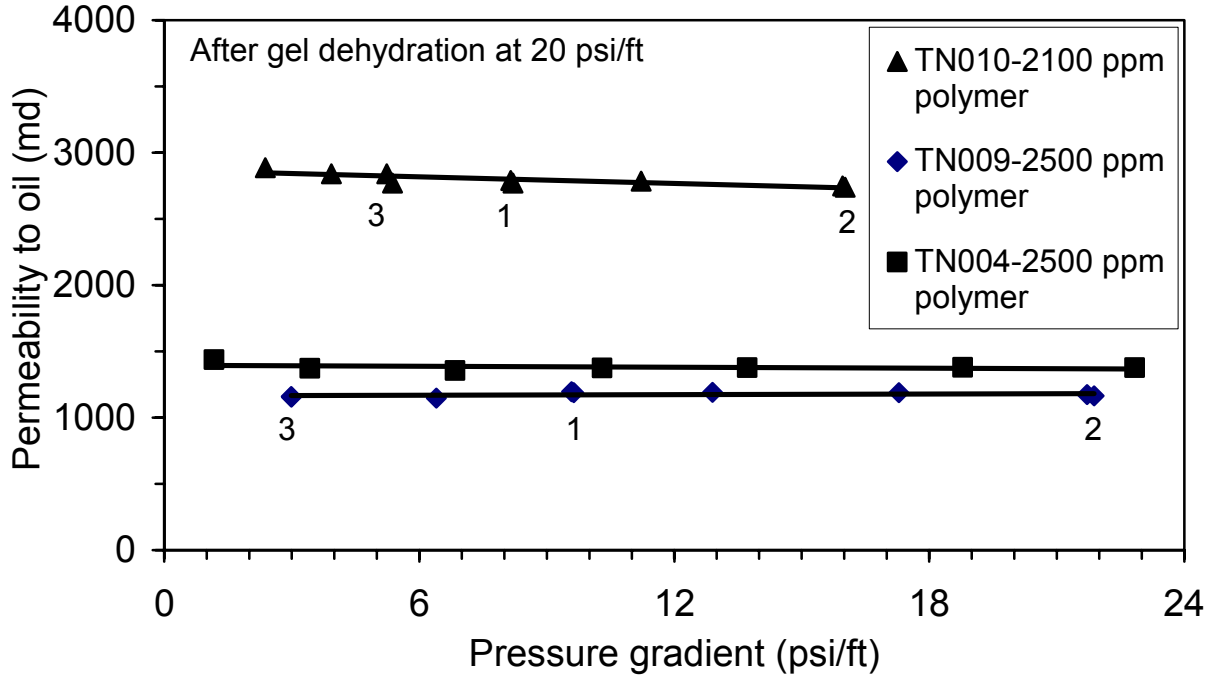

Figure 4.8 - Permeability to oil for weak gels as a function of pressure gradient after gel dehydration at a pressure gradient of 20 psi/ft; polymer concentrations of 2500 ppm and lower.

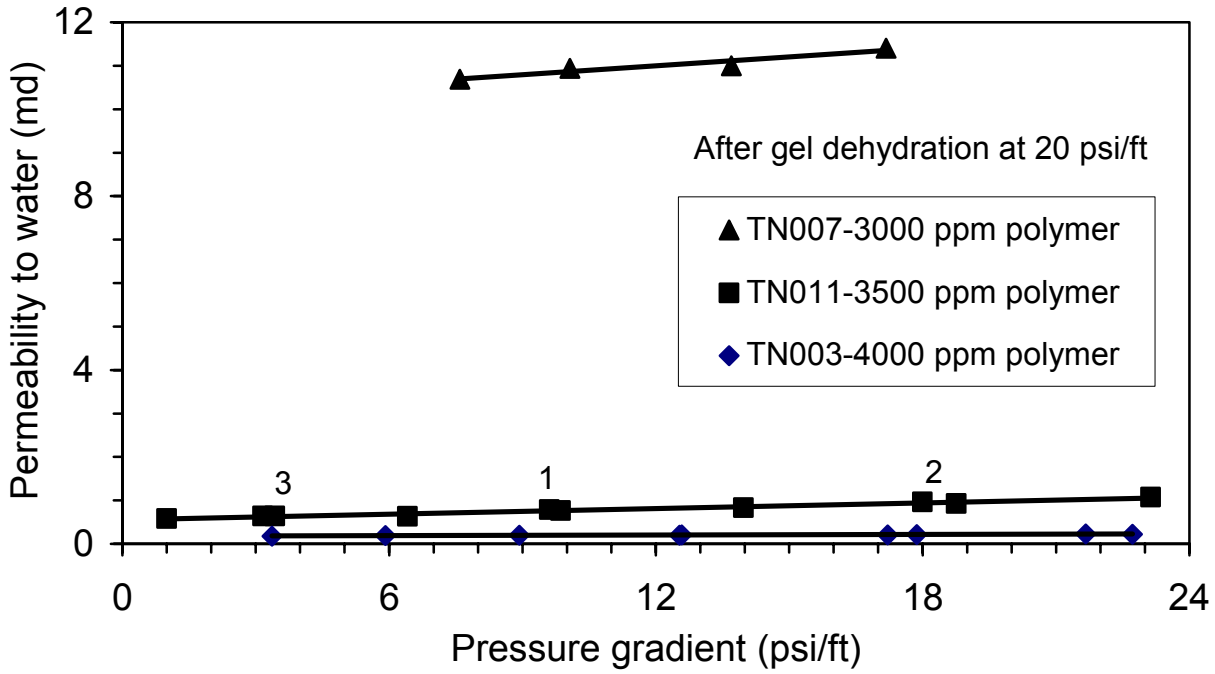

Figure 4.9 - Permeability to water for strong gels as a function of pressure gradient after gel dehydration at a pressure gradient of 20 psi/ft; polymer concentrations of 3000 ppm and higher.

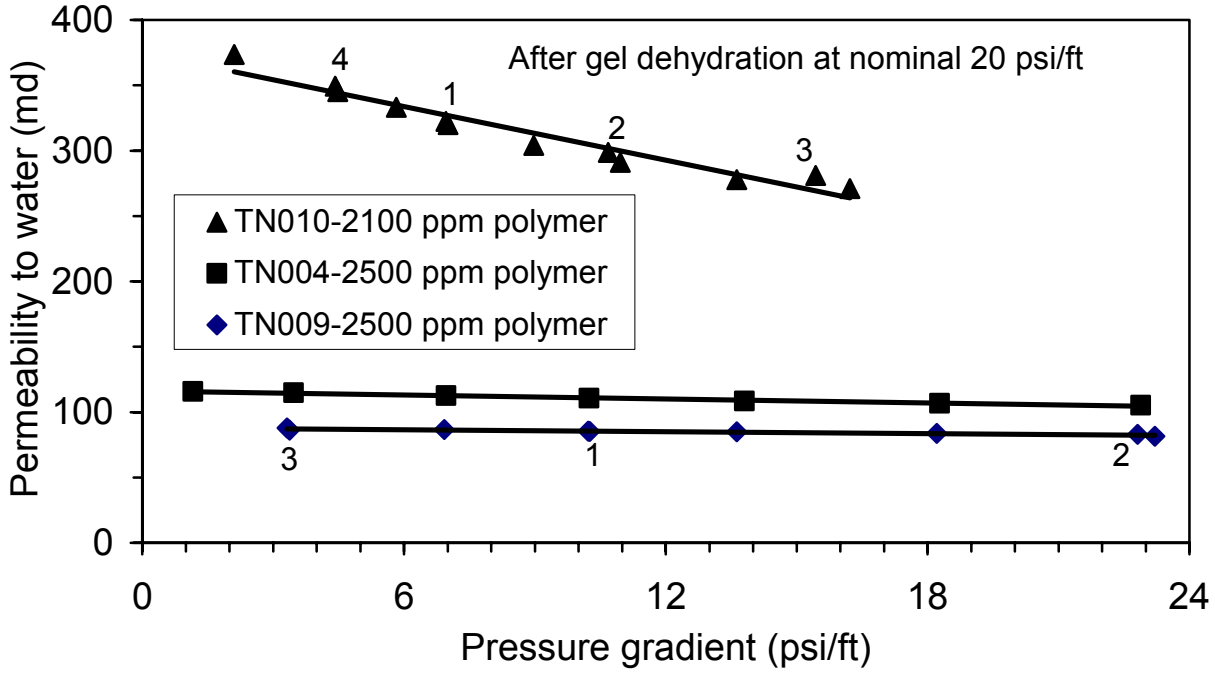

Figure 4.10 - Permeability to water for weak gels as a function of pressure gradient after gel dehydration at a pressure gradient of 20 psi/ft; polymer concentrations of 2500 ppm and lower.

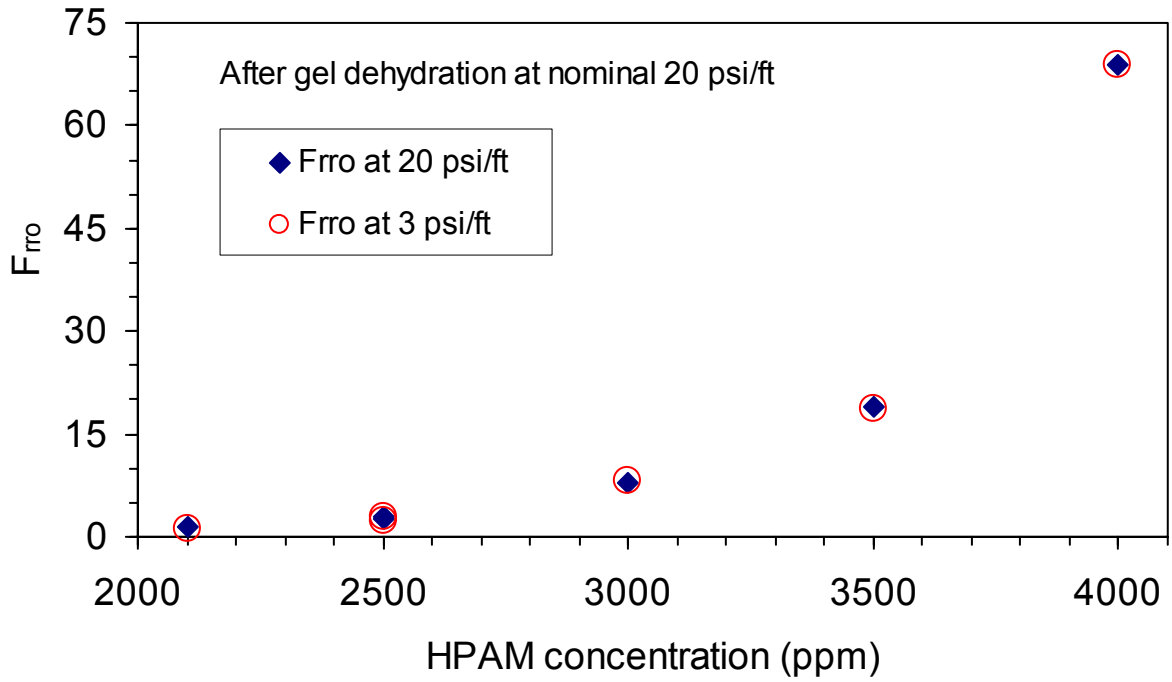

Figure 4.11 – Residual resistance factors for oil as a function of polymer concentration at two applied pressure gradients after dehydration at a pressure gradient of 20 psi/ft.

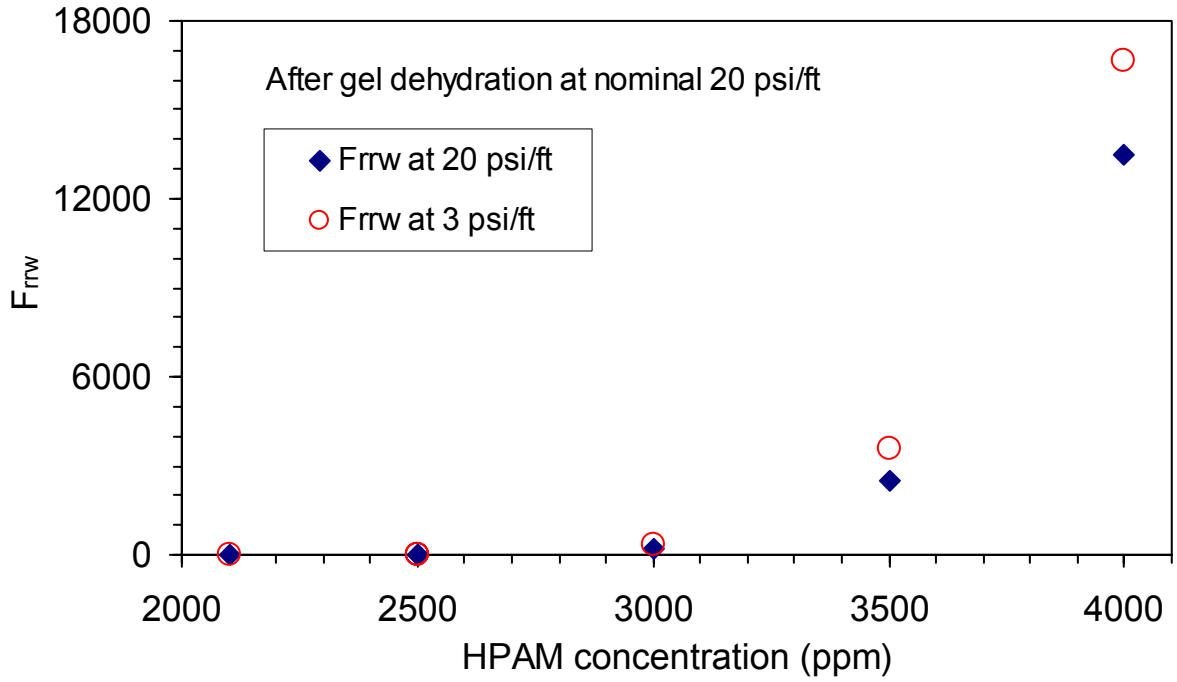

Figure 4.12 – Residual resistance factors for water as a function of polymer concentration at two applied pressure gradients after dehydration at a pressure gradient of 20 psi/ft.

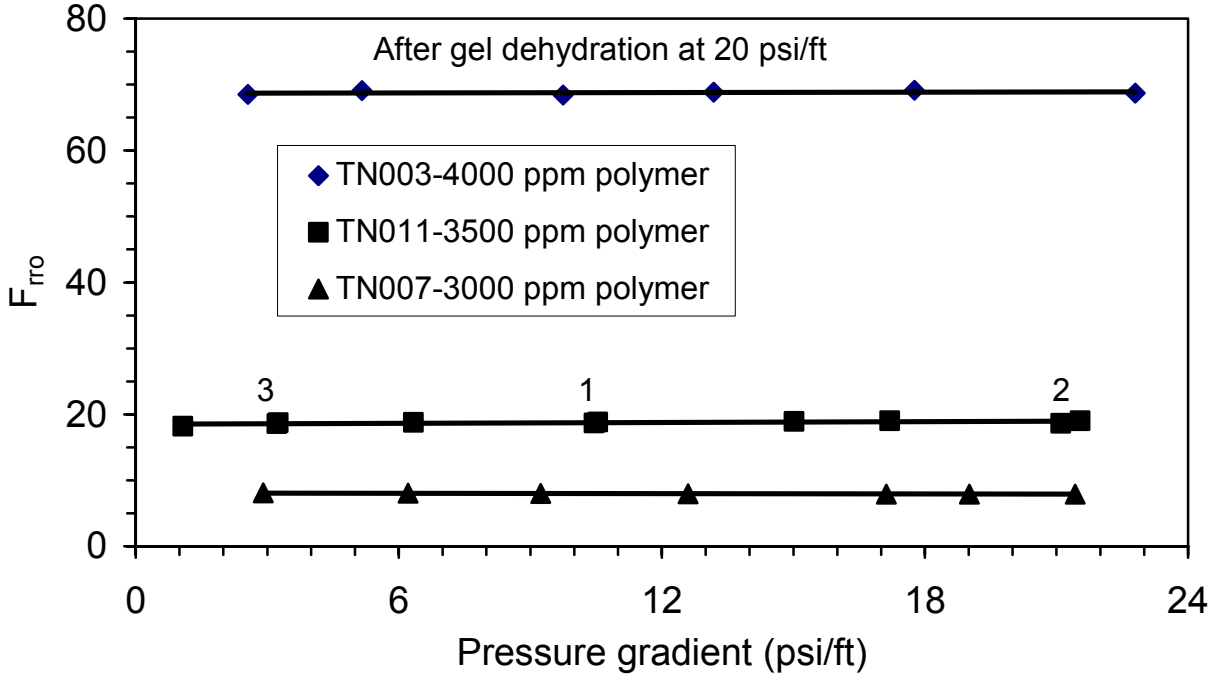

Figure 4.13 – Residual resistance factors for oil as a function of applied pressure gradient for strong gels (polymer concentrations of 3000 ppm or higher) after dehydration at a pressure gradient of 20 psi/ft.

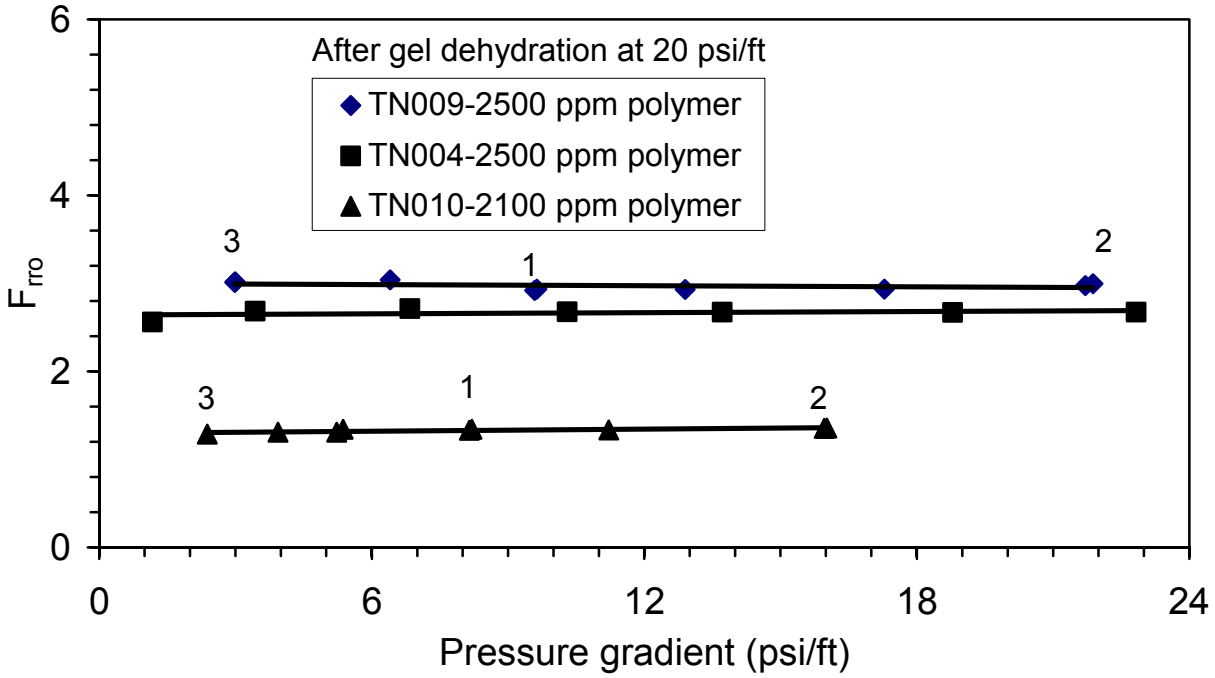

Figure 4.14 – Residual resistance factors for oil as a function of applied pressure gradient for weak gels (polymer concentrations of 2500 ppm or lower) after dehydration at a pressure gradient of 20 psi/ft.

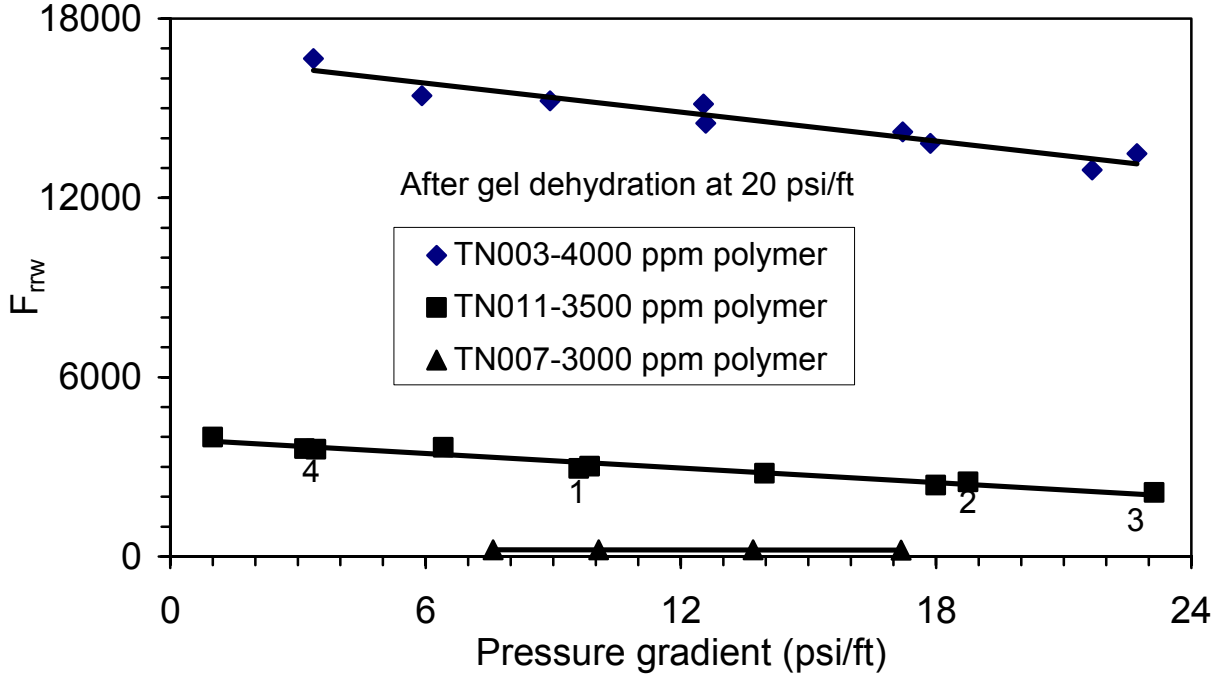

Figure 4.15 – Residual resistance factors for water as a function of applied pressure gradient for strong gels (polymer concentrations of 3000 ppm or higher) after dehydration at a pressure gradient of 20 psi/ft.

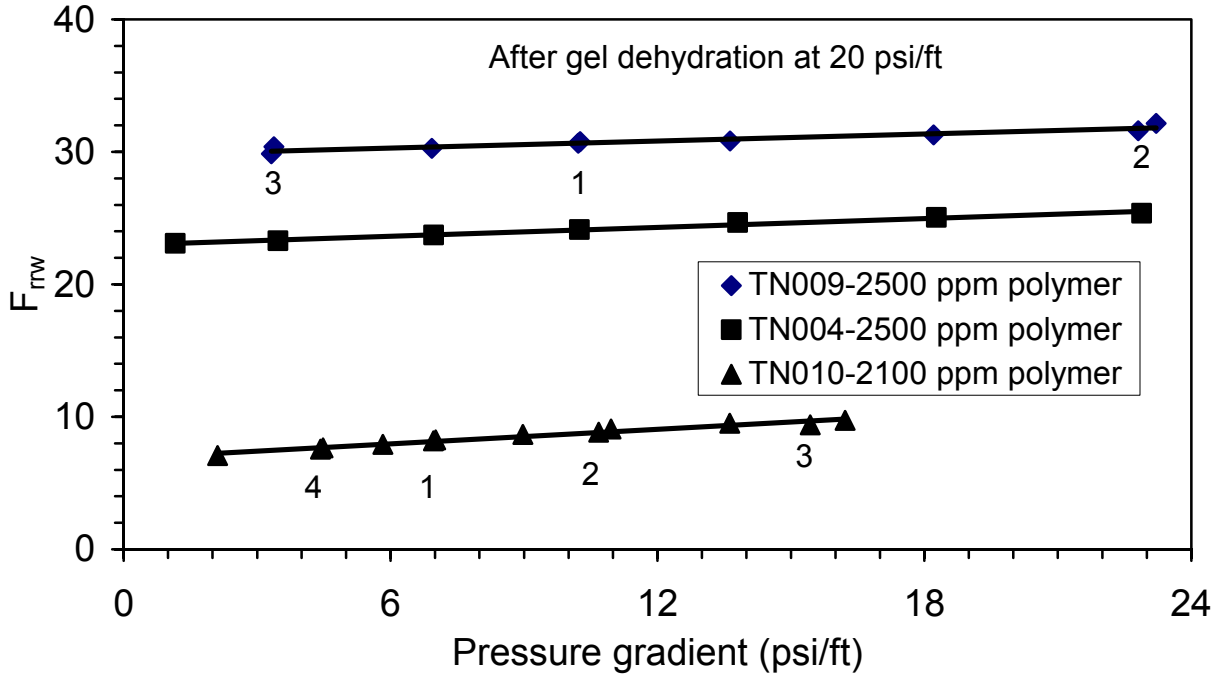

Figure 4.16 – Residual resistance factors for water as a function of applied pressure gradient for weak gels (polymer concentrations of 2500 ppm or lower) after dehydration at a pressure gradient of 20 psi/ft.

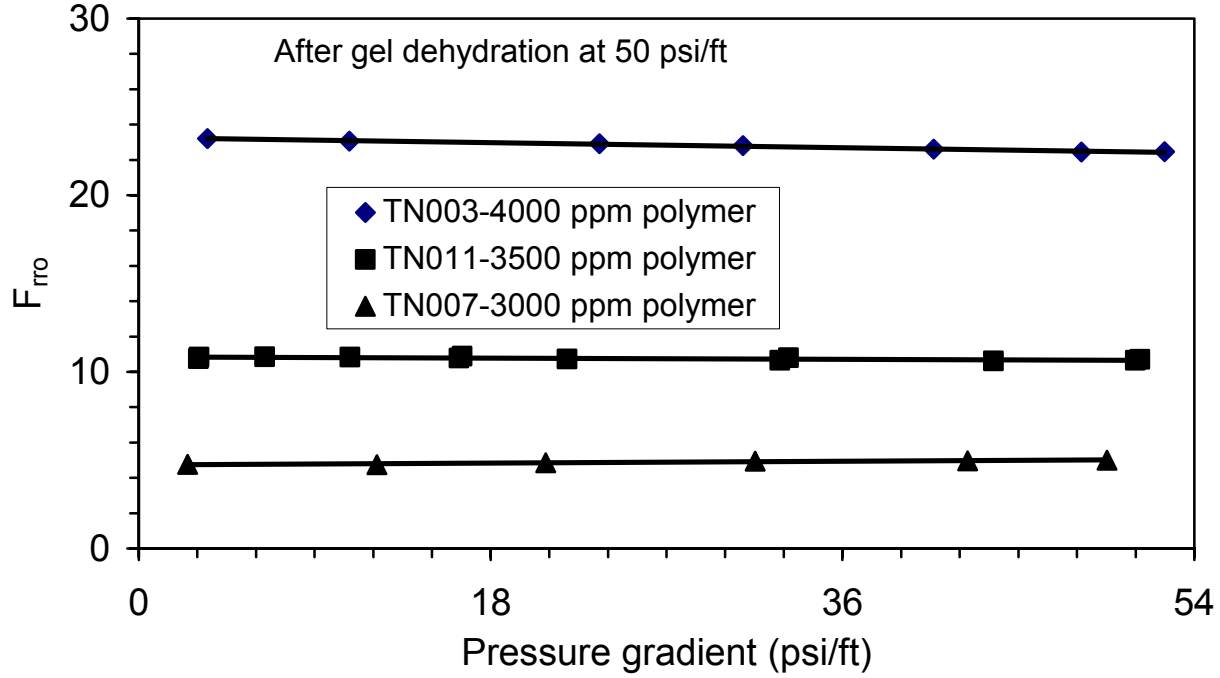

Figure 4.17 – Residual resistance factors for oil as a function of applied pressure gradient for strong gels (polymer concentrations of 3000 ppm or higher) after dehydration at a pressure gradient of 50 psi/ft.

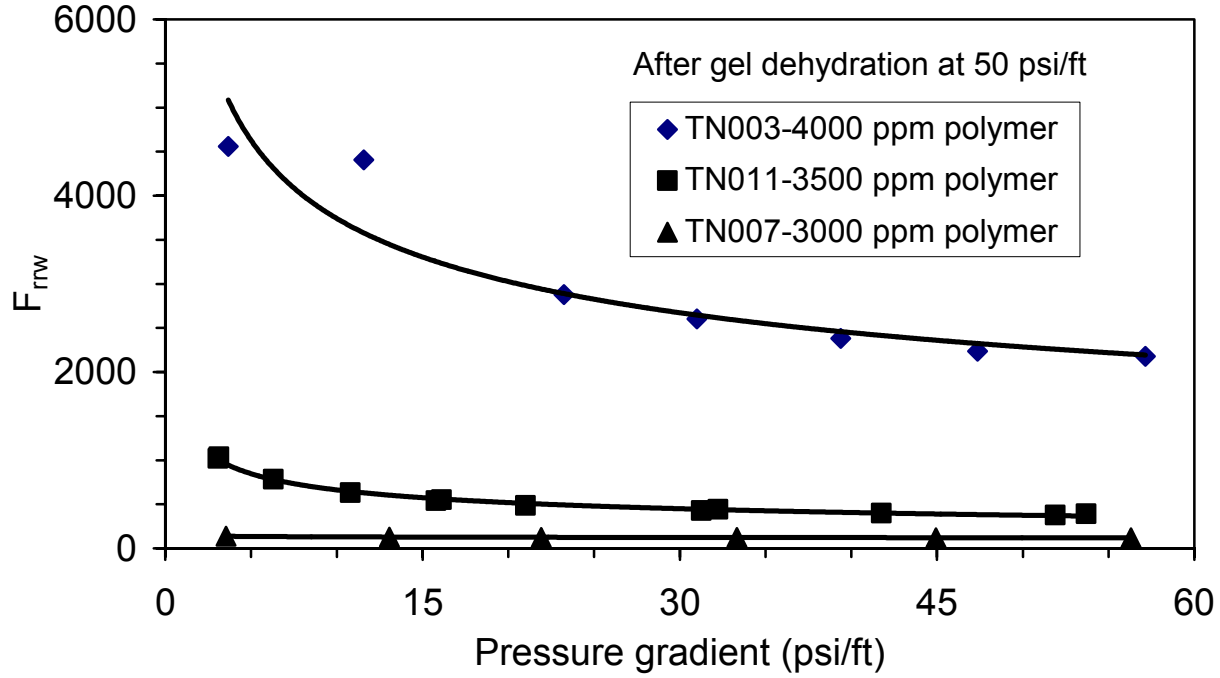

Figure 4.18 – Residual resistance factors for water as a function of applied pressure gradient for strong gels (polymer concentrations of 3000 ppm or higher) after dehydration at a pressure gradient of 50 psi/ft.

show the higher dehydration pressure decreased significantly both residual resistance factors. F_{rrw} decreased to a greater extent than F_{rro}. The additional dehydration of 2-6% of the gel volume during the higher dehydration pressure gradient of 50 psi/ft significantly affected both F_{rro} and F_{rrw}.

Liang et al. [1995] showed that F_{rrw} decreased and that F_{rro} was relatively constant with a decrease in superficial velocity in an experiment with a very strong gel (1.39% HPAM) placed in a strongly water-wet Berea core. Results from flow experiments on a sandstone slab with a strong gel (0.5% HPAM) showed a similar effect of decreased F_{rrw} with increasing pressure gradient [Ganguly et al.; 2003]. In this study in which the sandpacks were treated with various Cr(III)-acetate-HPAM gel compositions, F_{rro} was not a function of pressure gradient or superficial velocity for flow through the dehydrated gels for all gelant compositions. This agrees with the results reported by Liang et al. [1995] and Ganguly et al. [2003]. However in this study, F_{rrw} decreased for a dehydrated strong gel (Figure 4.15) and increased for a dehydrated weak gel (Figure 4.16) with an increase in pressure gradient.

In summary, both F_{rro} and F_{rrw} increased rapidly with increasing polymer concentration. F_{rrw} was a function of pressure gradient but F_{rro} was not. Gel dehydration at the higher pressure gradient of 50 pis/ft strongly reduced both F_{rro} and F_{rrw} from the values determined at the initial dehydration pressure gradient of 20 psi/ft. F_{rrw} was reduced by a greater factor than F_{rro} by the second dehydration.

Selectivity. Gel treatments usually reduce the permeability to water by a greater factor than the oil permeability is reduced. This phenomenon is known as *favorable* disproportionate permeability reduction (DPR). The magnitude of DPR was herein termed selectivity and was defined as the ratio of F_{rrw} to F_{rro}. Higher selectivity values above unity represent more favorable DPR.

Selectivity of the internal section of the sandpack after gel dehydration at 20 psi/ft is shown in Figure 4.19 for two pressure gradients and as a function of the polymer concentration in the gel. Selectivity was always greater than one, illustrating that the permeability reduction for water was much greater than for oil for all of the gel compositions studied. Selectivity increased dramatically with polymer concentration of the gel. Selectivity was larger at a pressure gradient of 3 psi/ft than at 20 psi/ft for a given gel composition, especially for the stronger gels.

Selectivity for the stronger gels at the two dehydration pressure gradients are shown in Figure 4.20 as a function of pressure gradient. Weaker gels were only dehydrated at a nominal pressure gradient of 20 psi/ft and their selectivities as a function of the applied pressure gradient are shown in Figure 4.21.Selectivities generally decreased for the strong gels and increased slightly for the weak gels with increased pressure gradient. Dehydration of the stronger gels at the higher pressure gradient of 50 psi/ft significantly reduced selectivity as shown in Figure 4.20. This occurred even though only a small additional amount of gel volume (2 to 6%) was dehydrated at the higher pressure gradient.

In summary, favorable DPR was observed in all sandpacks that were treated with the different gel compositions. Selectivity increased sharply with increased polymer concentration and

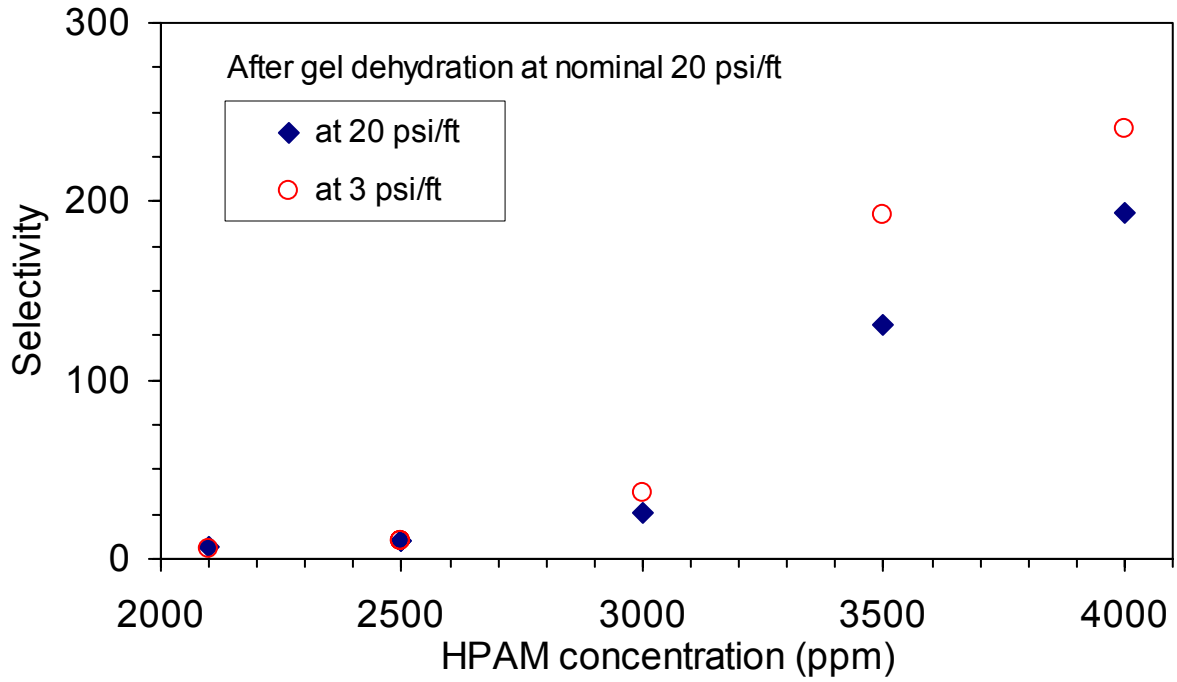

Figure 4.19 – Selectivity as a function of polymer concentration at two applied pressure gradients after dehydration at a pressure gradient of 20 psi/ft.

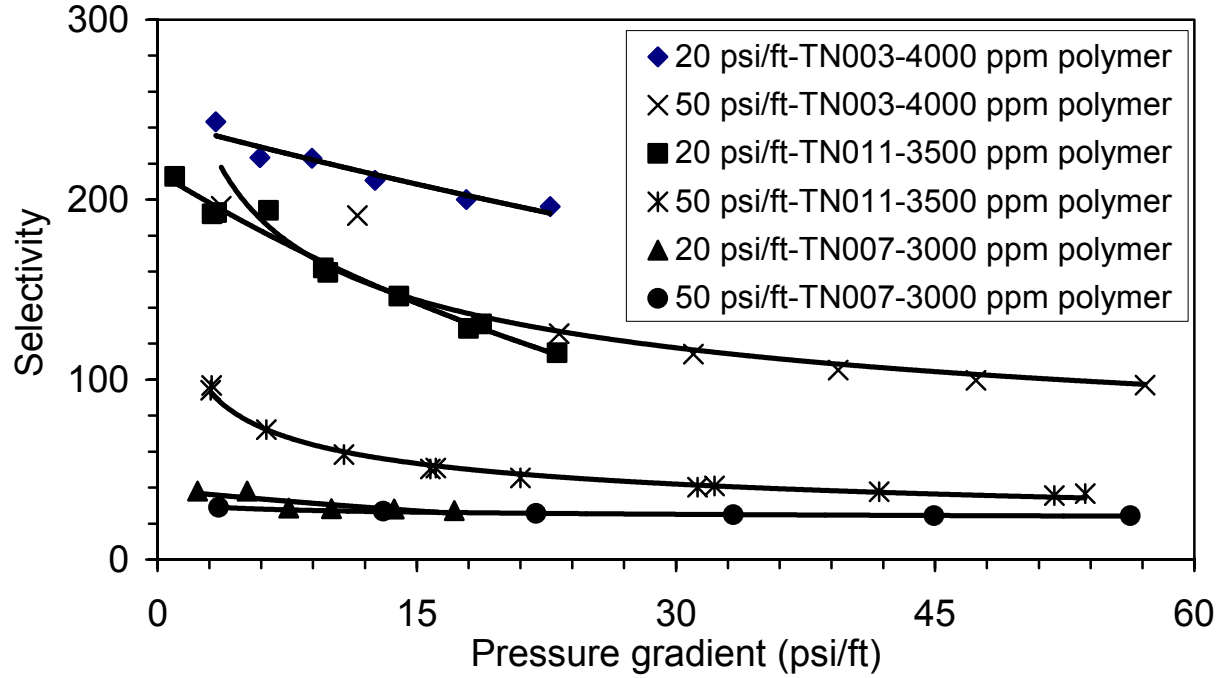

Figure 4.20 – Selectivity as a function of applied pressure gradient for strong gels (polymer concentrations of 3000 ppm or higher) after dehydration at a pressure gradients of 20 and 50 psi/ft.

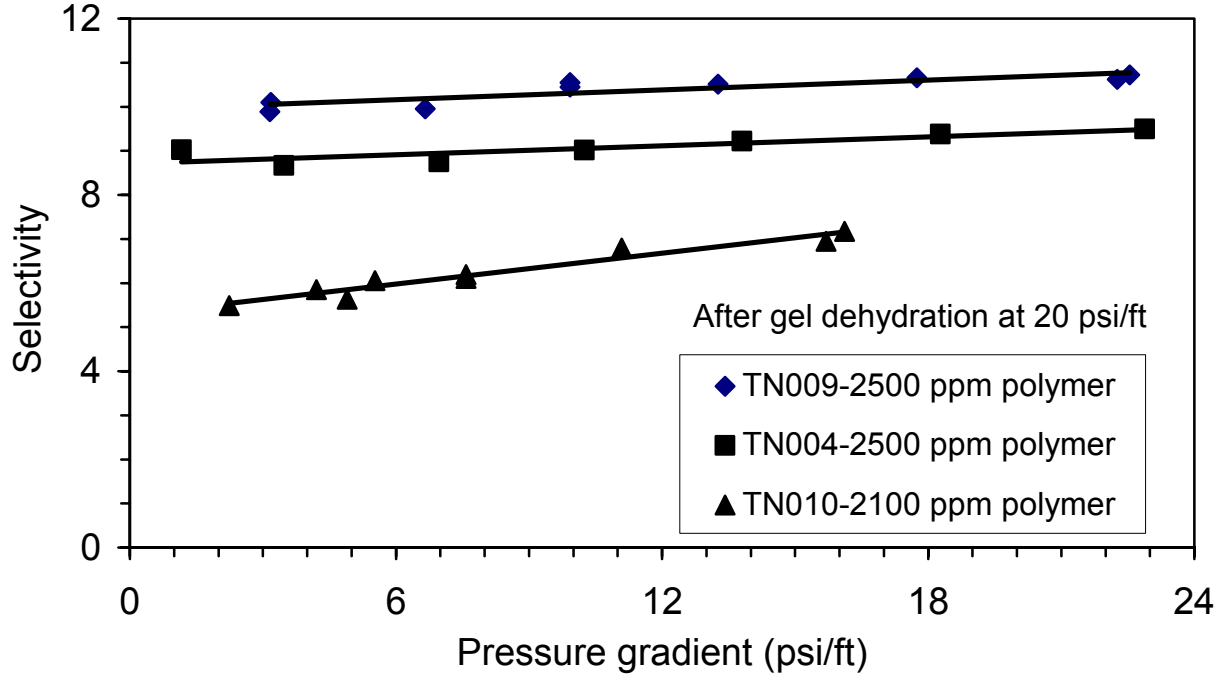

Figure 4.21 – Selectivity as a function of applied pressure gradient for weak gels (polymer concentrations of 2500 ppm or lower) after dehydration at a pressure gradient of 20 and 50 psi/ft.

decreased with the volume of gel dehydrated and/or the applied pressure gradient during the dehydration process. Selectivity decreased with pressure gradient for the stronger gels but increased with pressure gradient for the weaker gels.

Effluent Sample Analyses and Volume Balances

Volume balances on the oil and brine contained in the packs and chemical analyses on the oil and brine effluents from the packs were interpreted to conceptualize the fluid flow behavior that occurred after a gel treatment. The initial oil flood after the gel treatment (pressure gradient of 20 psi/ft) is referred to as a dehydration run. It was assumed at the start of this initial oil flood that the pack was fully saturated with gel and residual oil that was encapsulated by the gel. Aqueous phase displaced from the pack during the initial dehydration run (oil injection @ 20 psi/ft) was fluid and did not contain any gelled fragments. Polymer concentrations in the displaced aqueous phase were appreciably lower than the polymer concentration of the gelant placed in the pack. Comparisons of the polymer concentration in the injected gelant and the highest and the average polymer concentrations in the effluent during the dehydration run at 20 psi/ft are given in Table 4.5. The volume of gel dehydrated was equated to the aqueous volume produced during the initial oil flood (dehydration run). The fraction of polymer recovered during the dehydration was always less than the fraction of gel dehydrated and is indicative of dehydration of the gel left in the pack. Values of the polymer recovered in Table 4.5 were most likely higher than the actual values since the effluent samples probably contained acetate and the measured total organic carbon (TOC) values were attributed solely to polymer content in the calibration for the analysis.

The dehydration process increased the average polymer concentration of the gel remaining in the pack as shown in Table 4.5.

Table 4.5 - Fraction of gel dehydrated and material balances for polymer during and after dehydration at 20 psi/ft.

Sandpack	Polymer conc. in gel (ppm)	During dehyd. at 20 psi/ft		After dehydration at 20 psi/ft		
		Highest polymer conc. in effluent (ppm)	Avg. polymer conc. in effluent (ppm)	Fraction of gel dehyd. (%)	Fraction of polymer recovered (%)	Avg. polymer conc. of gel remaining in sandpack (ppm)
TN010	2100	1600	1400	67	43	3500
TN004*	2500	1700	1300	55	29	3900
TN009	2500	1600	1100	66	28	5300
TN007**	3000	1700	1200	57	23	5400
TN006	3500	1500	1300	66	24	7800
TN011	3500	1200	690	65	13	8900
TN003	4000	3600	2600	68	45	6900

* dehydration conducted at a lower pressure gradient due to partially plugged effluent screen.
** momentary pressure overshoot to 50 psi/ft at start of dehydration.

Additional oil and brine floods were conducted after the initial dehydration run. Values of the fraction of gel dehydrated, the fraction of polymer recovered and the average polymer concentration of the gel remaining in the sandpacks after all the oil and brine displacements were conducted are listed in Table 4.6. The calculated average polymer concentrations in the gel remaining in the sandpacks remained higher than the injected values indicating a dehydration process. Comparison of Tables 4.5 and 4.6 show small increases in the fraction of the gel dehydrated and relatively large increases in the fraction of polymer recovered. Polymer in the pack was solubilized in the brine and removed during brine floods that were conducted after the initial dehydration at a pressure gradient of 20 psi/ft. It was assumed that the polymer was insoluble in the oil phase.

Effluent brine samples in the post-treatment runs were also analyzed for chromium concentration. Chromium concentrations in the first aqueous sample during the initial dehydration run at 20 psi/ft ranged between 54 and 67 % of the chromium concentration in the injected gelant (sample size no doubt affected the concentration value) and decreased with successive samples. The amount of chromium recovered and the average chromium concentration in the gel remaining in the packs after the initial dehydration run at 20 psi/ft and

Table 4.6 - Fraction of gel dehydrated and material balances for polymer after all displacement runs.

Sandpack	Polymer conc. in gel (ppm)	Additional dehyd. at 50 psi/ft (?)	After all oil and water displacements		
			Fraction of gel dehydrated (%)	Fraction of polymer recovered (%)	Avg. polymer conc. of gel remaining in sandpack (ppm)
TN010	2100	no	67	59	2600
TN004	2500	no	67	52	3600
TN009	2500	no	66	33	4500
TN007	3000	yes	59	34	4700
TN006	3500	yes	71	48	6200
TN011	3500	yes	67	54	4800
TN003	4000	yes	73	64	5400

Table 4.7 – Results of material balances on chromium.

Sandpack	Chromium conc. in gel (ppm)	After dehyd. at 20 psi/ft		After all oil and water displacements	
		Chromium recovered (%)	Avg. chromium conc. of gel remaining in sandpack (ppm)	Chromium recovered (%)	Avg. chromium conc. of gel remaining in sandpack (ppm)
TN010	52.5	35	102	43	89
TN004	62.5	29	98	37	119
TN009	62.5	28	132	33	122
TN007	75.0	26	130	36	116
TN006	87.5	21	204	27	220
TN011	87.5	21	200	30	185
TN003	100	21	250	28	267

after all oil and water displacements is given in Table 4.7. Generally more polymer than chromium was recovered from the sandpacks leaving a polymer-to-chromium mass ratio in the packs a bit less than the original value of 40:1.

The volumes of oil, brine, and gel contained in the sandpacks at the end of each of the flow experiments were determined by material balances. A few assumptions were used to perform the volume balances. It was assumed that all of the resident brine was displaced from the pack during the injection of gelant and that, after a shut-in period, the pore space was completely full of gel except for the residual oil. The residual oil was referred to as "encapsulated" oil, that is, encapsulated by the gel. The encapsulated oil contained stilbene tracer and the amount of the encapsulated oil displaced from the sandpack during oil and brine floods was determined by stilbene analysis of the effluent oil samples. It was also assumed that all of the brine that was dehydrated by oil was displaced from the sandpack during the dehydration process. In other words, the interstitial water saturation was assumed to be negligible in the "new" pore space after each dehydration process.

Results of the material balances are given in Tables 4.8 to 4.12 for five of the sandpacks. (Detailed material balances were not performed for TN006 due to possible air injection during post treatment runs and for TN010 due to the absence of stilbene in the residual oil prior to gelant injection.) Saturations of water (S_w), gel (S_{gel}), and oil (S_o) and saturations of oil that was encapsulated (S_{oen}) and not encapsulated (S_{on}) by the gel were determined based on the initial pore volume. The new pore space for oil and brine flow after the gel treatment is described by the effective porosity, ϕ^*. The new pore space was the sum of the space that was occupied by the gel that was dehydrated and the space occupied by the encapsulated (residual) oil that was re-connected. S_w^*, S_o^* are the water and oil saturations in the effective porosity, the new flow channels. The last four columns are the average permeabilities and residual resistance factors of the internal section (Sections 2 to 5) of the packs.

Inspection of the results of the material balances provides insight into the flow behavior of oil and water through a gel-treated porous medium. Porosity of the sandpacks decreased from initial values of 33-34% to values that ranged from 22 to 26% after all the post-treatment floods. Lower porosity in the same rock translates into a lower absolute permeability and, presumably, lower relative permeabilities to oil and brine. The amount of encapsulated oil that was reconnected during the initial dehydration at 20 psi/ft generally decreased with the strength (polymer concentration) of the gelant. Nearly all of the encapsulated oil was reconnected after all of the post-treatment brine and oil floods for all polymer concentrations.

Residual saturations of water and oil (S_w^* and S_o^*) in the "new" pore space were key to our interpretation of how disproportionate permeability reduction (DPR) occurs. The values of S_w^* and S_o^* after the oil and brine floods, respectively, at 20 psi/ft are shown as a function of polymer concentration in Figure 4.22. Water saturations in the new pore space at a 100% fractional flow of oil (S_w^*) were lower than the pre-treatment values at the same condition (13 to 15%) except for the gelant at the highest polymer concentration of 4000 ppm where the values were comparable. Conversely, the residual saturations of oil at 100% fractional flow of water

Table 4.8 – Saturation values and permeability data after each flow experiment in TN003; Gel contained 4000 ppm polyacrylamide.

Experiment	S_w (%)	S_o (%)	S_{gel} (%)	S_{ot} (%)	S_{on} (%)	ϕ^* (%)	S_w^* (%)	S_o^* (%)	k_w (md)	F_{rrw}	k_o (md)	F_{rro}
Brine saturation	100	0.0							4480			
Oil flood	14.3	85.7									3730	
Brine flood	87.6	12.4							2980			
Tracer Sor	87.1	12.9										
Gel placement	0.0	12.9	87.1	12.9								
Dehydration @ 20psi/ft	~0	72.6	27.4	9.7	62.9	23.1	~0	100			52.6	70.9
Brine flood @ 20 psi/ft	32.1	40.5	27.4	2.2	38.3	23.5	45.5	54.5	0.2	13500		
Oil flood @ 20 psi/ft	10.7	61.8	27.4	1.8	60.0	23.6	15.1	84.9			54.3	68.7
Dehydration @ 50psi/ft	~0	76.6	23.4	0.9	75.8	25.3	~0	100			147	25.3
Brine flood @ 50 psi/ft	33.8	42.8	23.4	0.4	42.4	25.4	44.4	55.6	1.4	2180		
Oil flood @ 50 psi/ft	5.1	71.5	23.4	0.0	71.5	25.5	6.7	93.3			166	22.5
Tracer So*					70.5		8.0	92.0				

Original pore volume was 112.9 mL, and bulk volume was 338.8 mL.

Table 4. 9– Saturation values and permeability data after each flow experiment in TN011; Gel contained 3500 ppm polyacrylamide.

Experiment	S_w (%)	S_o (%)	S_{gel} (%)	S_{ot} (%)	S_{on} (%)	ϕ^* (%)	S_w^* (%)	S_o^* (%)	k_w (md)	F_{rrw}	k_o (md)	F_{rro}
Brine saturation	100	0							4050			
Oil flood	12.7	87.3									3540	
Brine flood	83.5	16.5							2310			
Tracer Sor	83.3	16.7										
Gel placement	0.0	16.7	83.3	16.7								
Dehydration @ 20psi/ft	~0	71.1	28.9	5.9	65.2	21.8	~0	100			205	17.2
Brine flood @ 20 psi/ft	38.6	32.5	28.9	4.6	27.9	22.2	58.0	42.0	1.1	2142		
Oil flood @ 20 psi/ft	6.5	64.6	28.9	3.4	61.3	22.6	9.6	90.4			186	19.0
Dehydration @ 50psi/ft	~0	72.6	27.4	0.6	72.0	24.1	~0	100			329	10.7
Brine flood @ 50 psi/ft	35.6	37.0	27.4	0.4	36.5	24.1	49.4	50.6	6.1	379		
Oil flood @ 50 psi/ft	5.9	66.7	27.4	0.2	66.5	24.2	8.1	91.9			332	10.7
Tracer So*					64.1		8.1	91.9				

Original pore volume was 111.8 mL, and bulk volume was 334.0 mL.

Table 4.10 – Saturation values and permeability data after each flow experiment in TN007; Gel contained 3000 ppm polyacrylamide.

Experiment	S_w (%)	S_o (%)	S_{gel} (%)	S_{ot} (%)	S_{on} (%)	ϕ^* (%)	S_w^* (%)	S_o^* (%)	k_w (md)	F_{rrw}	k_o (md)	F_{rro}
Brine saturation	100	0							4280			
Oil flood	15.5	85									3690	
Brine flood	83.1	17							2450			
Tracer Sor	84.8	15										
Gel placement	0.0	15	84.8	15.2								
Dehydration @ 20psi/ft	~ 0	64	36.3	0.2	63.4	21.2	~ 0	100			502	7.4
Brine flood @ 20 psi/ft	38.8	25	36.3	0.0	24.6	21.3	61.0	39.0	12.1	203		
Oil flood @ 20 psi/ft	3.3	60	36.3	0.0	60.4	21.3	5.2	94.8			467	7.9
Tracer So*					59.9							
Dehydration @ 50psi/ft	~ 0	65	35.2	0.0	64.8	21.7	~ 0	100			688	5.4
Brine flood @ 50 psi/ft	39.6	25	35.2	0.0	25.2	21.7	61.1	38.9	20.2	122		
Oil flood @ 50 psi/ft	2.9	62	35.2	0.0	62.0	21.7	4.4	95.6			739	5.0
Tracer So*					62.9		3.0	97.0				

Original pore volume was 111.8 mL, and bulk volume was 334 mL

Table 4.11 Saturation values and permeability data after each flow experiment in TN004; Gel contained 2500 ppm polyacrylamide.

Experiment	S_w (%)	S_o (%)	S_{gel} (%)	S_{ot} (%)	S_{on} (%)	ϕ^* (%)	S_w^* (%)	S_o^* (%)	k_w (md)	F_{rrw}	k_o (md)	F_{rro}
Brine saturation	100	0.0							4540			
Oil flood	14.4	85.6									3680	
Brine flood	84.2	15.8							2670			
Tracer Sor	84.3	15.7										
Gel placement		15.7	84.3	15.7								
Dehydration @ 20psi/ft	~ 0	61.9	38.1	2.3	59.6	20.3	~ 0	100			1040	3.5
Brine flood @ 20 psi/ft	40.6	21.3	38.1	1.5	19.8	20.5	67.2	32.8	19.9	134		
Oil flood @ 20 psi/ft*	~ 0	71.9	28.1	0.5	71.4	24.3	~ 0	100			1450	2.5
Re-brine flood @ 20 psi/ft	50.3	21.6	28.1	0.4	21.2	24.3	70.3	29.7	105	25.4		
Re-oil flood @ 20 psi/ft	0.9	71.1	28.1	0.0	71.1	24.4	1.2	98.8			1380	2.7
S_o^*					71.6		0.5	99.5				

* New screens were replaced and 11.9% volume of gel was further dehydrated.
Original pore volume was 115.5 mL, and bulk volume was 339.9 mL

Table 4.12 - Saturation values and permeability data after each flow experiment in TN009; Gel contained 2500 ppm polyacrylamide.

Experiment	S_w (%)	S_o (%)	S_{gel} (%)	S_{ot} (%)	S_{on} (%)	ϕ^* (%)	S_w^* (%)	S_o^* (%)	k_w (md)	F_{rrw}	k_o (md)	F_{rro}
Brine saturation	100	0.0							4220			
Oil flood	14.1	85.9							0		3490	
Brine flood	84.3	15.7							2620			
Tracer Sor	84.2	15.8										
Gel placement		15.8	84.2	15.8								
Dehydration @ 20psi/ft	~ 0	71.1	28.9	0.7	70.4	23.7	~ 0	100			1220	2.9
Brine flood @ 20 psi/ft	54.8	16.3	28.9	0.4	15.9	23.8	77.5	22.5	83.0	31.6		
Oil flood @ 20 psi/ft	3.2	67.9	28.9	0.0	67.9	23.9	4.5	95.5			1170	3.0
Tracer oil phase					68.0		4.3	95.7				

Original pore volume was 119.1 mL, and bulk volume was 353.6 mL.

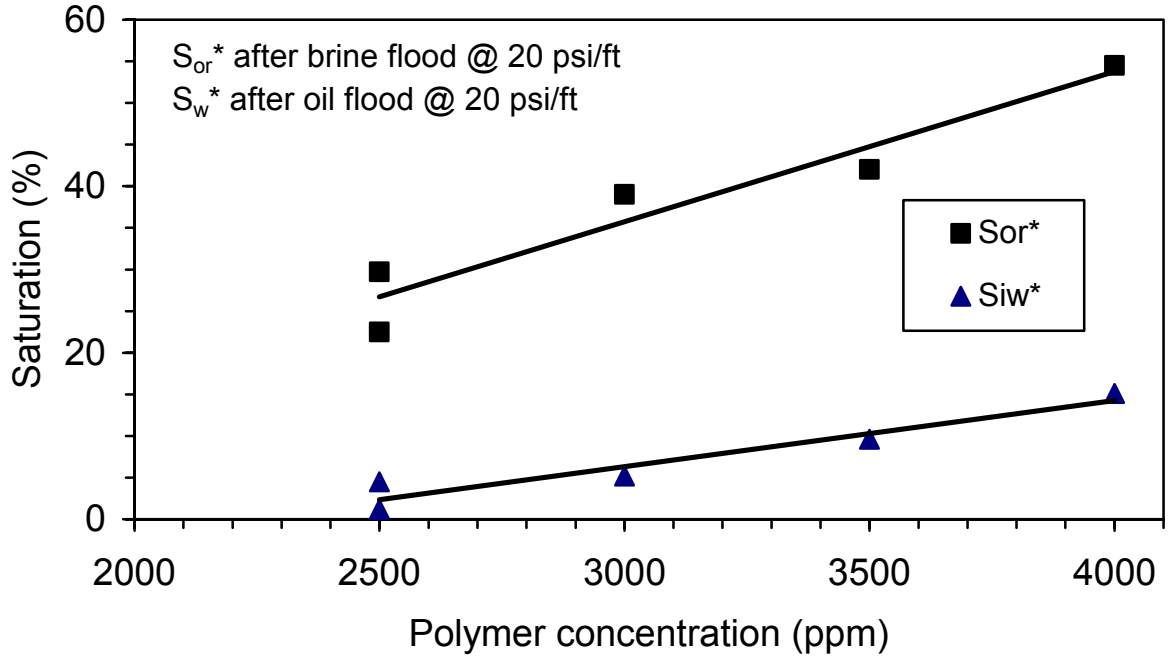

Figure 4.22 – Residual oil and water saturations in the new pore space after brine and oil floods, respectively, at pressure gradients of 20 psi/ft.

(S_o*) were much higher than S_w* and significantly higher than the pre-treatment values that ranged from 12 to 17%. The high residual oil saturations increased the flow resistance to water significantly while oil flow was not as restricted due to the low residual water saturations, resulting in favorable DPR.

The increase with polymer concentration of the residual saturations of oil and water in the new pore space (Figure 4.22) correlated with increased residual resistance factors with polymer concentration as shown in Figures 4.11 and 4.12. It is noted that the residual oil saturations increased faster with polymer concentration (higher slope) than did the residual water saturations with polymer concentration and this correlated with the increased selectivity with polymer concentration as shown in Figure 4.19.

Conclusions

1. The magnitude of gel dehydration was not a strong function of gel composition (polymer concentration) and the pressure gradient imposed during dehydration.
2. The rate of gel dehydration was a function of polymer concentration. Gel was dehydrated faster for a weaker gel than for a stronger gel.
3. End-point permeabilities to both oil and water after a gel treatment decreased from values measured before the treatment. The endpoint permeabilities decreased with increased polymer concentration in the gelant.
4. F_{rro} and F_{rrw} were strong functions of polymer concentration and varied from 1.3-69 and 7.1-16,700, respectively at nominal post dehydration pressure gradient of 3 psi/ft.
5. F_{rrw} was a function of pressure gradient but F_{rro} was not a function of the pressure gradient.
6. Favorable DPR was observed for all gel compositions studied. The magnitude of DPR increased significantly with increasing polymer concentration in the gelant.
7. The magnitude of DPR decreased with increased volume of gel dehydrated and/or applied pressure gradient during the dehydration process.
8. As post dehydration pressure gradient increased, the magnitude of DPR decreased for a strong gel but increased for a weak one.
9. The effective porosities of the porous matrix were reduced from 33-34% to 22-26% after the gel treatment and subsequent oil and brine floods.
10. After gel dehydration and displacement experiments, almost all of encapsulated oil or initial residual oil trapped by the gel was reconnected.
11. After brine and oil floods at 20 psi/ft, S_{wi}* and S_{or}* in the "new" pore space increased with increasing polymer concentration. S_{or}* was 72-97% larger and increased faster than S_{wi}*.
12. Gel dehydration and the re-connection of pre-treatment residual oil provided the channels, or new pore space, for oil and water flow after a gel treatment.
13. The trapping of significant saturations of residual oil in the new pore space restricted brine flow much more than the low saturations of residual water restricted oil flow. The concept is responsible for favorable disproportionate permeability reduction (DPR).

Nomenclature

C - Polymer concentration in ppm (part per million).
F_{rro} - Residual resistance factor to oil.
F_{rrw} - Residual resistance factor to water.
k_b - Base permeability in md.
k_o - Permeability to oil in md.
k_{ob} - Permeability to oil before gel placement in md.
k_{oa} - Permeability to oil after gel placement in md.
k_w - Permeability to water in md.
k_{wb} - Permeability to water before gel placement in md.
k_{wa} - Permeability to water after gel placement in md.
S_{gel} - Gel saturation in the sandpack determined based on the initial PV.
S_{on} - Oil saturation that is not encapsulated by the gel based on the initial PV.
S_{or} - Residual oil saturation.
S_{or}* - Residual oil saturation in the "new" pore space determined based on effective PV.
S_{oen} - Saturation of oil that was encapsulated by the gel and determined based on stilbene recovery and the initial PV.
S_o* - Oil saturation in the "new" pore space determined based on effective PV.
S_w - Water saturation in the sandpack determined based on the initial PV.
S_w* - Water saturation in the "new" pore space determined based on effective PV.
S_{wi} - Interstitial water saturation in the sandpack determined based on the initial PV.
S_{wi}* - Interstitial water saturation in the "new" pore space and based on effective PV.

References

1. Al-Sharji, H.H., Grattoni, C.A., Dawe, R.A., Zimmerman, R.W.: "Pore-Scale Study of the Flow of Oil and Water through Polymer Gels," paper SPE 56738, presented at the SPE Annual Technical Conference and Exhibition, Houston, Texas, October 1999.
2. Al-Sharji, H.H., Grattoni, C.A., Dawe, R.A., Zimmerman, R.W.: "Disproportionate Permeability Reduction Due to Polymer Adsorption Entanglement," paper SPE 68972, presented at the SPE European Formation Damage Conference, The Hague, The Netherlands, May 2001.
3. Dawe, R.A., and Zhang, Y.: "Mechanistic Study of the Selective Action of Oil and Water Penetrating into a Gel Emplaced in a Porous Medium," *Journal of Petroleum Science & Engineering* (1994) **12**, 113-125.
4. Gales, J.R., Young, T.S., Willhite, G.P., and Green, D.W.: "Equilibrium Swelling and Syneresis Properties of Xanthan Gum-Cr(III) Gels," paper SPE/DOE 17328, presented at the SPE/DOE Enhanced Oil Recovery Symposium, Tulsa, Oklahoma, April 1988.
5. Ganguly, S., Willhite, G.P., Green, D.W., and McCool, C.S.: "Effect of Flow Rate on Disproportionate Permeability Reduction," paper SPE 80205 presented at the SPE International Symposium on Oilfield Chemistry, Houston, Texas, February 2003.
6. Green, D.W., Willhite, G.P., McCool, C.S., Heppert, J.A., Vossoughi, and Michnick, M.J.: "In-Situ Permeability Modification Using Gelled Polymer Systems," Final Report for the period June 10, 1996 to July 31, 1998, DOE Contract No. DE-AC22-94PC91008, Subcontract No. G4S60031, Chapter 5, University of Kansas, 1998.

7. Krishnan, P.: "An Experimental Study of Dehydration of Polyacrylamide-Chromium(III)-Acetate Gel System Under a Pressure Gradient," Master Thesis, University of Kansas, 1998.
8. Krishnan, P., Asghari, K., Willhite, G.P., McCool, C.S., Green, D.W., and Vossoughi, S.: "Dehydration and Permeability of Gels Used in In-Situ Permeability Modification Treatments," paper SPE/DOE 59347, presented at the SPE/DOE Improved Oil Recovery Symposium, Tulsa, Oklahoma, April 2000.
9. Liang, J. and Seright, R.S.: "Further Investigations of Gels Reduce k_w MoreThan k_o," paper SPE 37249, presented at the SPE International Symposium on Oilfield Chemistry, Houston, Texas, February 1997.
10. Liang, J. and Seright, R.S.: "Wall-Effect/Gel-Droplet Model of Disproportionate Permeability Reduction," paper SPE 59344, presented at the SPE/DOE Improved Oil Recovery Symposium, Tulsa, Oklahoma, April 2000.
11. Liang, L., Sun, H., and Seright, R.S.: "Why Do Gels Reduce Water Permeability More Than Oil Permeability?" *SPE Reservoir Engineering* (November 1995) 282-286.
12. Nguyen, T.Q.: "Effect of Polyacrylamide-Chromium(III)-Acetate Gel Composition on the Magnitude of Gel Dehydration and Disproportionate Permeability Reduction," Master Thesis, The University of Kansas, 2003.
13. Nilson, S., Stavland, A., and Jonsbraten, H.C.: "Mechanistic Study of Disproportionate Permeability Reduction," paper SPE 39635, presented at the SPE/DOE Improved Oil Recovery Symposium, Tulsa, Oklahoma, April 1998.
14. Seright, R.S.: "Gel Dehydration During Extrusion Through Fractures," paper SPE 39957, presented at the 1998 SPE Rocky Mountain Regional/Low-Permeability Reservoirs Symposium and Exhibition, Denver, April 1998.
15. Seright, R.S.: "Mechanism For Gel Propagation Through Fractures," 21st Annual International Energy Agency Workshop and Symposium, Edinburgh, Scotland, U.K., September 2000.
16. Seright, R.S, Liang, J., Lindquist W.B., and Dunsmuir, J.H.: "Characterizing Disproportionate Permeability Reduction Using Synchrotron X-Ray Computed Microtomography," *SPE Reservoir Evaluation and Engineering* (October 2002) 355-364.
17. Sparlin, D.D. and Hagen, R.W.: "Controlling Water in Producing Operations—Part 5," *World Oil* (July 1984) 137.
18. White, J.L., Goddard, J.E., and Phillips, H.M.: "Use of Polymers to Control Water Production in Oil Wells," *Journal of Petroleum Technology* (February 1973) 143.
19. Willhite, G.P., Zhu, H., Natarajan, D., McCool, C.S., Green, D.W.: "Mechanisms Causing Disproportionate Permeability in Porous Media Treated With Chromium Acetate/HPAM Gels," paper SPE 59345, presented at the SPE/DOE Improved Oil Recovery Symposium, Tulsa, Oklahoma, April 2000.
20. Yan, Z., McCool, C.S., Green, D.W., and Willhite, G.P.: "Modification of Oil and Water Permeabilities in Berea Sandstone by a Gel Treatment," paper SPE 50753 presented at the SPE International Symposium on Oilfield Chemistry, Houston, Texas, February 1999.
21. Zaitoun, A., Bertin, H., and Lasseux, D.: "Two-Phase Flow Property Modifications by Polymer Adsorption," paper SPE 39631, presented at the SPE/DOE Improved Oil Recovery Symposium, Tulsa, Oklahoma, April 1998.

22. Zaitoun, A., and Kohler, N.: "Two-Phase Flow Through Porous Media: Effect of an Adsorbed Polymer Layer," paper SPE 18085 presented at the SPE Annual Technical Conference and Exhibition, Houston, Texas, October 1988.
23. Zaitoun, A., Kohler, N., and Rahbari, R.: "Thin Polyacrylamide Gels for Water Control in High-Permeability Production Wells," paper SPE 22785 presented at the SPE Annual Technical Conference and Exhibition, Dallas, Texas, October 1991.

Chapter 5

Technology Transfer

The following presentations and technical papers were given/published during the time period between July, 2002 and July, 2003. The presentations and papers were based on work conducted under this contract(DE-FC26-02NT15363) and the previous contract (DE-AC26-99BC15209).

Presentations

"Disproportionate Permeability Reduction," presented by G.P. Willhite at the Arbuckle Water Control Program forum, Petroleum Technology Transfer Council, Wichita, KS (4 February 2003).

"Effect of Flow Rate on Disproportionate Permeability Reduction," S. Ganguly, G.P. Willhite, D.W. Green and C.S. McCool, presented by G.P. Willhite at the SPE International Symposium on Oilfield Chemistry, Houston, TX (5-7 February 2003).

"Overview of the Tertiary Oil Recovery Project's Gelled Polymer Research and Field Applications," presented by G.P. Willhite at the *Reducing Water Production Using Gelled Polymers* workshop, Petroleum Technology Transfer Council, Wichita, KS (31 July 2003).

Technical Papers

"The Effect of Fluid Leakoff on Gel Placement and Stability in Fractures," S. Ganguly, G.P. Willhite, D.W. Green and C.S. McCool, *SPE Journal*, **7** (September 2002) 309-315.

"Effect of Flow Rate on Disproportionate Permeability Reduction," S. Ganguly, G.P. Willhite, D.W. Green and C.S. McCool paper No. SPE 80205, SPE International Symposium on Oilfield Chemistry, Houston, TX (5-7 February 2003).

"Propagaton of Chromium(III) Acetate Solutions Through Dolomite Rock," H. Jin, C.S. McCool, G.P. Willhite, D.W. Green and M.J. Michnick, *SPE Journal*, **8** (June 2003) 107-113.

Two technical papers that are based on Chapters 3 and 4 of this report have been accepted for presentation at the SPE/DOE Fourteenth Symposium on Improved Recovery, Tulsa, OK (17-21 April 2004).

> "Reaction Kinetics of the Uptake of Chromium(III) Acetate by Polyacrylamide," R. Jain, C.S. McCool, D.W. Green, G.P. Willhite and M.J. Michnick
>
> "Effect of Composition of a Polyacrylamide-Chromium Acetate Gel on the Magnitude of Gel Dehydration and Disproportionate Permeability Reduction," T. Nguyen, D.W. Green, G.P. Willhite and C.S. McCool.